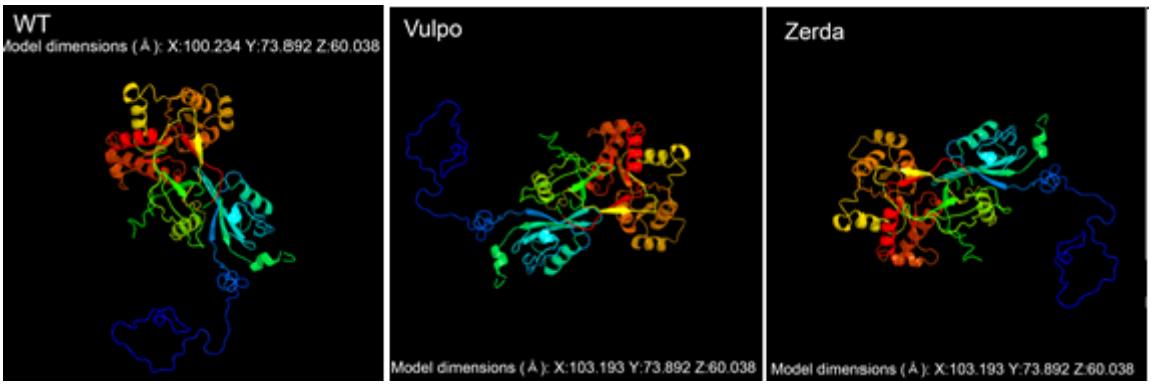
Forward genetic analysis of natural T regulatory cell development

A thesis submitted for the Degree of Doctor of Philosophy

2013



Dr Emma Salisbury

Imperial College London

Department of Medicine

Front cover image: *Predicted 3D protein structures of wild-type CARMA1 versus mutant CARMA1-Vulpo and CARMA1-Zerda.*

(Phyre2 program http://www.sbg.bio.ic.ac.uk/phyre2/html/page.cgi?id=index)

Declaration of Originality

I, Emma Salisbury, confirm that the work presented in this thesis is my own. Where information has been derived from other sources I confirm that this has been indicated in the thesis.

Signed: ***Emma Salisbury***

Copyright Declaration

The copyright of this thesis rests with the author and is made available under a Creative Commons Attribution Non-Commercial No Derivatives licence. Researchers are free to copy, distribute or transmit the thesis on the condition that they attribute it, that they do not use it for commercial purposes and that they do not alter, transform or build upon it. For any reuse or redistribution, researchers must make clear to others the licence terms of this work.

Acknowledgements

I am especially glad to have the opportunity to thank my supervisors, Professor Philip Ashton-Rickardt and Professor Charles Pusey, for their support, encouragement and wisdom.

I would like to thank the *Wellcome Trust* for funding this work through a Clinical Research Fellowship.

I owe a debt of gratitude to my colleagues in the laboratories in which I have worked - especially Drs Sophie Rutschmann, Lihui Wang and Onjee Choi; and to my collaborators, Professor Marina Botto and Dr Francesco Carlucci. I would also like to thank Drs Dean Heathcote and Phillip Mueller, as well as Cherry Alyahya and Tess Boreham for their technical support.

Finally, I thank my family for their support and interest.

For my mother

Abstract

Natural (n) T regulatory (Treg) cells generated in the thymus are essential throughout life for the maintenance of T cell homeostasis and prevention of autoimmunity. T cell receptor (TCR)/CD28-mediated activation of Nuclear Factor Kappa-light-chain-enhancer of activated B cells (NFκB) and Jun N-terminal kinase (JNK) pathways is known to play a key role in nTreg development but many of the predicted molecular interactions are based on extrapolations from non-Treg cell TCR stimulation with non-physiological ligands. For the first time, this work provides strong genetic evidence of a scaffold function for the Caspase Recruitment Domain (CARD) of the TCR signalling protein CARD-MAGUK1 (CARMA1) in nTreg development *in vivo*. I report two, new, N-ethyl-N-nitrosourea (ENU)-derived mutant mice, Vulpo and Zerda, with a profound block in the development of nTregs in the thymus as well as impaired inducible (i) Treg differentiation in the periphery. Despite independent heritage, both mutants harbour different point mutations in the CARD of the CARMA1 protein. *vulpo* and *zerda* mutations do not affect expression levels of CARMA1 but still impair signalling through the TCR due to defective downstream B cell CLL/Lymphoma 10 (Bcl-10) protein recruitment by the mutated CARD of CARMA1. Phenotypic differences observed between Vulpo and Zerda mutants suggest a role for the CARD of CARMA1 independent of Bcl-10 activation of downstream pathways. I conclude that this forward genetic approach demonstrates a critical role for the CARD function of CARMA1 in Treg development *in vivo*.

Publications arising from this work

1. Salisbury E, Game D, Lechler R. Transplantation Tolerance. *Pediatric Nephrology*. (In Press).

2. Salisbury E, Wang L, Choi O, Rutschmann S, Ashton-Rickardt P. ENU mutagenesis in the mouse provides strong genetic and in vivo evidence for the role of the CARD of CARMA1 in T regulatory cell development. *Immunology*. (In Press).

Table of Contents

List of Abbreviations 15

Chapter 1: Introduction 18

1.1 Adaptive Immunity 19

1.1.1 The Clonal Selection Hypothesis 21

1.1.2 The Immunological Synapse 24

1.1.3 T lymphocyte tolerance 26

1.2 T regulatory cells 33

1.3 T regulatory cells in health 38

1.4 T regulatory cells in disease 39

1.4.1 T regulatory cells in autoimmune disease 39

1.4.1.1 T regulatory cells and type-1 diabetes 42

1.4.1.2 T regulatory cells and multiple sclerosis 42

1.4.1.3 T regulatory cells and systemic lupus erythematosus 43

1.4.1.4 T regulatory cells and rheumatoid arthritis 43

1.4.1.5 T regulatory cells and inflammatory bowel disease 44

1.4.2 T regulatory cells and cancer 45

1.4.3 T regulatory cell therapy and transplantation 46

1.5 Natural T regulatory cell development 48

1.6 This study 51

1.6.1 Forward Genetics and *N*-ethyl-*N*-ntrosourea (ENU) mutagenesis 51

1.6.1.1 Past successes using Forward Genetics 58

Chapter 2: Results 59

2.1 Dominant mutations Vulpo and Zerda impair nTreg development 60

2.2 Dominant mutations Vulpo and Zerda impair iTreg development 68

2.3 *vulpo* & *zerda* are point mutations in the *carma1* gene 70

2.4 *vulpo* and *zerda* mutations in the *carma1* gene do not affect CARMA1 protein expression 74

2.5 *Carma1*$^{vul/vul}$ & *Carma1*$^{zer/zer}$ mice do not develop spontaneous autoimmunity 76

2.6 *vulpo* & *zerda* mutations disrupt the CARMA1/Bcl-10 association upon TCR activation 80

Chapter 3: Discussion 84

3.1 Discussion & conclusions 85

3.2 Critique of methods 93

3.3 Future work 95

Chapter 4: Materials and Methods 98

4.1 Materials 99

4.2 Methods 107

4.2.1 Mice 107

4.2.2 *N*-ethyl-*N*-nitrosourea mutagenesis 107

4.2.3 Phenotypic screen 108

4.2.4 Cell preparation and flow cytometry 108

4.2.5 Organ dissection 108

4.2.6 Confirmation of mutation heritability and breeding 111

4.2.7 Genotyping 112

4.2.8 *carma1* sequencing 114

4.2.9 *In vitro* $CD4^+$ T cell activation and iTreg differentiation 115

4.2.10 Immunological assays 115

4.2.10.1 Enzyme-linked immunosorbent assay (ELISA) 115

4.2.10.2 Western blotting 116

4.2.11 Statistical analysis 117

Chapter 5: Appendices 118

Appendix A: *Carma1* primers used to sequence *Carma1* in mutant and WT genomic DNA. 119

Appendix B: DNA isolation 120

Appendix C: List of single nucleotide polymorphisms (SNPs) used for genotyping Vulpo 121

Chapter 6: References 123

Table of Figures

Figure 1.1-1	*Phases of the adaptive immune response.*	20
Figure 1.1-2	*The Clonal Selection Hypothesis.*	23
Figure 1.1-3	*The Immunological Synapse*	25
Figure 1.1-4	*Overall scheme of T-cell development in the thymus*	28
Figure 1.1-5	*T-cell intrinsic mechanisms of peripheral tolerance.*	31
Figure 1.2-1	*T regulatory cells maintain tolerance to self .*	37
Figure 1.5-1	*The two-step model of nTreg cell development.*	50
Figure 1.6-1	*N-ethyl-N-nitrosourea (ENU) mutagenesis*	53
Figure 1.6-2	*The practical steps required for germline mutagenesis.*	57
Figure 2.1-1:	*Identification of Vulpo and Zerda mutants with impaired nTreg cell development.*	61
Figure 2.1-2:	*Vulpo and Zerda mice have reduced nTregs & increased Tconv cells in PBL.*	64
Figure 2.1-3:	*vulpo and zerda mutations affect all stages of thymocyte maturation.*	65
Figure 2.1-4:	*vulpo and zerda mutations affect nTreg precursor cell development in the thymus*	67
Figure 2.2-1:	*vulpo and zerda mutations affect iTreg differentiation in the periphery.*	69
Figure 2.3-1:	*vulpo and zerda are point mutations in the carma1 gene.*	71
Figure 2.3-2:	*vulpo and zerda point mutations translate into single amino acid substitutions in the CARD of the CARMA1 protein.*	73
Figure 2.4-1:	*Carma1$^{vul/vul}$* and *Carma1$^{zer/zer}$ mutants express wild-type levels of CARMA1 protein in the thymus.*	75

Figure 2.5-1:	*Vulpo and Zerda mutant mice do not develop autoimmunity.*	77
Figure 2.5-2:	*Vulpo & Zerda mutant mice harbour non-reactive Tconv cells.*	79
Figure 2.6-1:	*The structures of CARMA1, Bcl-10 and MALT1 proteins.*	81
Figure 2.6-2:	*Impaired interaction of mutant CARMA1 proteins with Bcl-10.*	83
Figure 4.2-1:	*A general picture of the morphological characteristics of every lymph node and its localization in the normal mouse.*	110
Figure 4.2-2:	*Diagram illustrating the classical positional cloning strategy adopted to identify causative mutations.*	113

List of Tables

Table 1.2-1:	*Treg cell signature genes and their cellular localization.*	33
Table 4.1-1:	*List of general stock solutions used for this work*	99
Table 4.1-2:	*List of reagents used for SDS-PAGE gels*	100
Table 4.1-3:	*Composition of reagents used for SDS-PAGE*	101
Table 4.1-4:	*List of primary antibodies used for experiments.*	102
Table 4.1-5:	*List of reagents used for immunoprecipitation experiments.*	103
Table 4.1-6:	*Additional materials used for Western Blotting.*	103
Table 4.1-7:	*List of reagents used for cell culture experiments.*	105
Table 4.1-8:	*List of reagents used for Enzyme-linked immunosorbent assay (ELISA).*	106
Table 4.2-1:	*Thermal Cycler program used for DNA amplification by PCR.*	114

List of Abbreviations

αα	Amino acid
AICD	Activation-induced cell death
APC	Antigen presenting cell
Bcl-10	B cell CLL/lymphoma 10
BBS	Borate buffered saline
CARMA1	CARD-MAGUK1 protein
carma1	CARD-MAGUK1 gene
CBM	CARMA1, Bcl-10, MALT1 complex
CARD	Caspase Recruitment Domain
CNS	Central nervous system
γc	Common gamma chain
Tconv	Conventional $CD4^+$ and $CD8^+$ T effector cells
CTLA4	Cytotoxic T lymphocyte antigen 4
DC	Dendritic cell
ELISA	Enzyme-linked immunosorbent assay
EAE	Experimental autoimmune encephalomyelitis
ENU	*N*-ethyl-*N*-nitrosourea
FOXP3	Forkhead box P3 transcription factor (protein)
foxp3	Forkhead box P3 gene
G	Generation
GITR	Glucocorticoid-induced tumour necrosis factor receptor
GVHD	Graft-versus-host disease
HSE	Herpes simplex virus-1 encephalitis

HSV-1	Herpes simplex virus-1
ICAM1	Intercellular adhesion molecule 1
IKK	IκB kinase
IPEX	Immunodysregulation Polyendocrinopathy and Enteropathy, X-linked syndrome
IBD	Inflammatory bowel disease
IFN-γ	Interferon gamma
IL-2	Interleukin- (IL-) 2
IS	Immunological synapse
iTreg	Inducible T regulatory cell
JNK	c-Jun N-terminal kinase
KO	Knockout
LOD	Logarithm of Odds
LAG3	Lymphocyte activation gene 3
LFA1	Lymphocyte function-associated antigen 1
mAb	Monoclonal antibody
MALT1	Mucosa-associated lymphoid tissue lymphoma translocation protein 1
MHC	Major histocompatibility complex
MS	Multiple sclerosis
NOD	Non-obese diabetic
nTeg	Natural T regulatory cell
NF-κB	Nuclear Factor Kappa-light-chain-enhancer of activated B cells
PBL	Peripheral blood leucocytes
PMA	Phorbol 12-myristate 13-acetate
PBS	Phosphate buffered saline
PCR	Polymerase chain reaction

PKC-δ	Protein kinase C-delta (PKC-δ)
PKC-θ	Protein kinase C-theta (PKC-θ)
RBC	Red Blood Cell
STAT5	Signal Transducer and Activator of Transcription 5 (STAT5)
SD	Standard deviation
SLE	systemic lupus erythematosus
SMAC	supramolecular activation cluster
TCR	T cell receptor
Th17	T helper 17 cell
Treg	T regulatory cell
TAK1	TGFβ Activated Kinase 1
TRAF6	TNF receptor-associated factor 6
TGF-β	Transforming growth factor beta
TNF	Tumour necrosis factor
TNFRSF	Tumour necrosis factor receptor superfamily member
Wt	Wild-type
XLAAD	X-Linked Autoimmunity-Allergic Dysregulation syndrome

Chapter 1: Introduction

1.1 Adaptive Immunity

Defence against microbes is mediated by the early reactions of innate, or natural, immunity and the later responses of adaptive, or acquired, immunity. The principle components of innate immunity are physical and chemical barriers, such as epithelia and antimicrobial substances produced at epithelial surfaces; phagocytic neutrophil and macrophage cells, as well as natural killer cells; blood proteins, including members of the complement system and other mediators of inflammation; and cytokine proteins that regulate and coordinate the activities of the cells of innate immunity. Innate immunity is phylogenetically the oldest system of host defence but many pathogenic microbes evolved to resist innate immunity and so their elimination required the more powerful mechanisms of adaptive immunity. In contrast to innate immunity, adaptive immunity is stimulated by exposure to infectious agents. It is exquisitely specific for distinct molecules, and has the capacity for memory which enables it to increase its magnitude and defensive capabilities with each successive exposure to a particular microbe. Lymphocytes are the only cells capable of specifically recognising antigens and are thus the principle component of the adaptive immune system.

Adaptive immune responses consist of distinct phases, the first three being the recognition of antigen, the activation of lymphocytes, and the elimination of antigen (the effector phase). The response contracts as antigen-stimulated lymphocytes die by apoptosis, restoring homeostasis, and the antigen-specific cells that survive are responsible for memory. These phases are illustrated in ***Figure 1.1-1***.

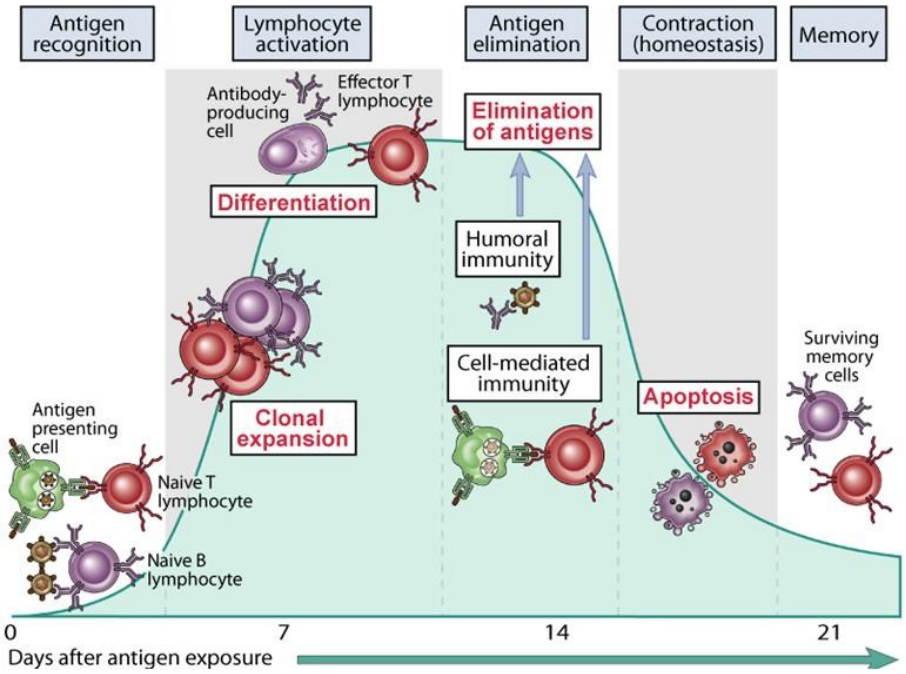


Figure 1.1-1: Phases of the adaptive immune response.

Adaptive immune responses consist of distinct phases, the first three being the recognition of antigen, the activation of lymphocytes, and the elimination of antigen (the effector phase). The response contracts as antigen-stimulated lymphocytes die by apoptosis, restoring homeostasis, and the antigen-specific cells that survive are responsible for memory. The y-axis represents an arbitrary measure of the magnitude of the response.

[Taken from: Cellular and Molecular Immunology, 6th edition. Abbas, Lichtman and Pillai. 2007. Philadelphia: Saunders Elsevier, p. 14.]

The adaptive immune response is itself made up of humoral immunity, mediated by B lymphocytes and secreted antibody products, and cell-mediated immunity which is mediated by T lymphocytes and their products, such as cytokines. In general, humoral immunity functions in defence against extracellular microbes and cell-mediated immunity is important for defence against intracellular microbes. The principle of a phased response to antigenic exposure (***Figure 1.1-1***) applies to both humoral and cell-mediated immunity.

1.1.1 The Clonal Selection Hypothesis

The number of naïve lymphocytes specific for any antigen is very small and the quantity of available foreign antigen may also be very small. As a result, distinct mechanisms are required to capture microbes, concentrate them and deliver their antigens to specific lymphocytes. Dendritic cells, located in epithelia and connective tissues, are the antigen presenting cells (APCs) of the adaptive immune system. They capture antigens, digest their proteins and display these peptides on their surface bound to major histocompatibility complex (MHC) molecules. Dendritic cells carry their antigenic cargo to draining lymph nodes and take up residence in the same region of the nodes through which naïve $CD4^+$ and $CD8^+$ T lymphocytes continuously recirculate. Specialised APCs display antigen to B lymphocytes and intact microbes or microbial antigens that enter lymph nodes or spleen are recognized in unprocessed (native) form by specific B lymphocytes. Antigen recognition provides specificity to the immune response, and the need for co-stimulation ensures that T cells respond to microbes (the inducers of costimulatory molecules) and not to harmless substances.

Antigen-specific clones of lymphocytes develop before and independent of exposure to antigen. When an antigen enters the body, it selects a pre-existing clone of lymphocytes and

activates it (***Figure 1.1-2***). This fundamental concept is called the Clonal Selection Hypothesis and was first described by Niels Jerne in 1955, and then more clearly enunciated by Macfarlane Burnett in 1957 [1], as a hypothesis that could explain how the immune system can respond to a large number and variety of antigens.

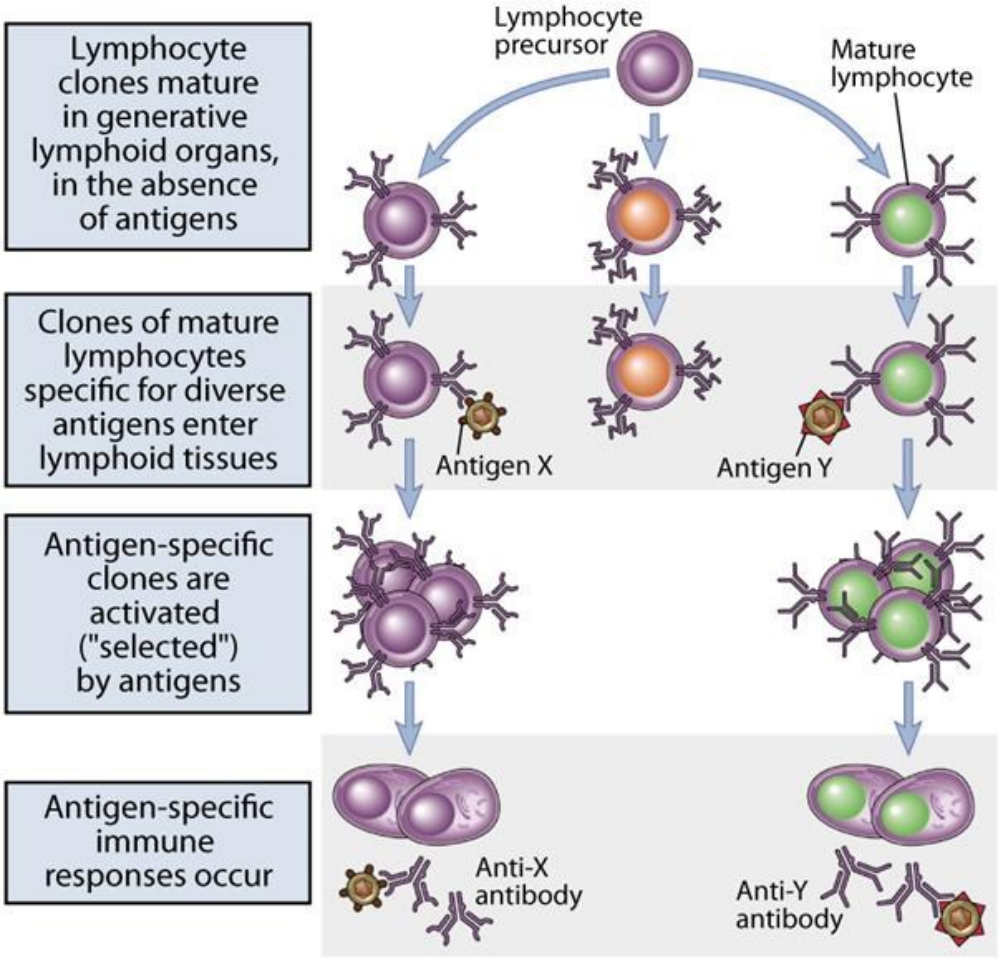


Figure 1.1-2: The Clonal Selection Hypothesis.

Each antigen (X or Y) selects a pre-existing clone of specific lymphocytes and stimulates the proliferation and differentiation of that clone. The diagram shows only B lymphocytes giving rise to antibody-secreting effector cells, but the same principle applies to T lymphocytes.

[Taken from: Cellular and Molecular Immunology, 6th edition. Abbas, Lichtman and Pillai. 2007. Philadelphia: Saunders Elsevier, p. 15.]

1.1.2 The Immunological Synapse

In the case of T cells, the adaptive immune response is initiated by the interaction of T cell antigen receptors (TCR) with MHC-peptide complexes in the nanometer scale gap between a T cell and an APC, referred to as the immunological synapse (IS) (***Figure 1.1-3***). The IS embodies a concept for understanding the high-order temporal and spatial cooperation of multiple biochemical and genetic elements known to be required for T cell activation.

The mature IS has been defined by the bull's eye arrangement of supramolecular activation clusters (SMACs) that form within a few minutes of T cell-APC contact (***Figure 1.1-3b***). The centre of the bull's eye or cSMAC is enriched for TCR and MHC-peptide complexes. It includes the signalling molecules on the T cell cytoplasmic side of the IS, including protein kinase C θ (PKCθ). The ring of the bull's eye or pSMAC contains the integrin Lymphocyte function-associated antigen 1 (LFA-1) and its major counter-receptor Intercellular adhesion molecule 1 (ICAM-1). Physiological T cell activation can be divided into a series of temporal stages: T cell polarization, initial adhesion, IS formation (initial signalling), and IS maturation (sustained signalling) [2]. Recruitment of PKCθ appears to be a marker for attainment of the stable IS [3] and maintenance of the stabilised IS for greater than 1 hour is well correlated with full T cell activation.

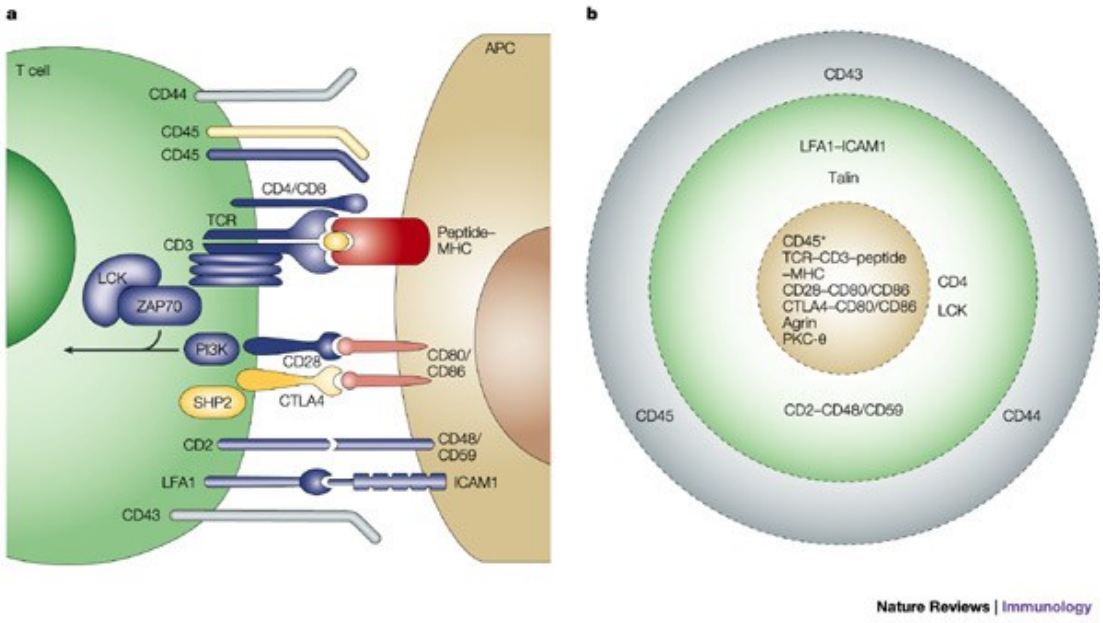


Figure 1.1-3: The Immunological Synapse [4].

a) A profile view showing a selection of the key ligand pairs and signalling molecules that are involved in T-cell recognition. The stimulatory peptide–MHC molecule is shown in red, activating/co-stimulatory molecules are blue, inhibitory molecules are yellow and molecules that are not contributing to signalling are grey. The arrow indicates converging signals that lead to T-cell activation. b)The face on view of the synapse with the characteristic 'bulls-eye' zone pattern, including the central region of the supra-molecular activation complex (cSMAC) (yellow), the peripheral ring surrounding the cSMAC (pSMAC, green) and the region distal to the synapse outside the pSMAC (dSMAC, grey) as well the molecules/ligand pairs that are found enriched within. APC, antigen-presenting cell; CTLA4, cytotoxic T lymphocyte antigen 4; ICAM1, intercellular adhesion molecule 1; LFA1, leukocyte function-associated antigen 1; PI3K, phosphatidylinositol 3-kinase; SHP2, SRC homology 2-domain-containing protein tyrosine phosphatase 2; TCR, T-cell receptor; ZAP70, ζ-chain-associated protein 70. [*]CD45 enters the cSMAC at later stages.

1.1.3 T lymphocyte Tolerance

As I have very briefly discussed, the immune system uses many potent effector mechanisms to clear a broad range of both toxic and allergenic substances. Therefore it is critical that the immune response is able to avoid unleashing these destructive mechanisms against the mammalian host's own tissues. The ability of the immune response to avoid damaging self-tissues is referred to as self-tolerance. Failure of self-tolerance underlies the broad class of autoimmune diseases - a process that has been extensively studied. We now know that antigens may be administered in ways that induce tolerance rather than immunity, and this may be exploited for the prevention and treatment of autoimmune, as well as allergic, disease and transplant rejection.

Immunological tolerance is unresponsiveness to an antigen induced by the exposure of specific lymphocytes to that antigen, and tolerance to self-antigens is a fundamental property of the adaptive immune system. Self-tolerance may be induced in immature self-reactive lymphocytes in generative lymphoid organs (central tolerance), or in mature lymphocytes in peripheral sites (peripheral tolerance). In the late 1980s, the advent of TCR transgenic systems and sensitive flow cytometric technology paved the way for several landmark studies that, by visualising the deletion of autoreactive thymocytes [5, 6], confirmed one of the central predictions of Burnet's clonal selection theory [1]. This 'recessive' mode of tolerance, also known as negative selection, has become a well-accepted paradigm, and more recent findings such as the discovery of 'promiscuous gene expression' [7] and the *autoimmune regulator* (*Aire*) [8-10] gene have been interpreted by many to indicate that central tolerance through negative selection is indeed essential to prevent spontaneous autoimmunity. However, as not foreseen by the clonal selection theory, it later turned out that intrathymic encounter of 'self' by developing T cells does not inevitably lead to their elimination from the repertoire. Instead,

recognition of cognate antigen by particular transgenic TCRs in the thymus was frequently found to increase the proportion and absolute number of natural T regulatory (nTreg) cells among thymocytes of the respective specificity (dominant tolerance) [11]. ***Figure 1.1-4*** provides an overall schematic for T-cell development in the thymus. The role of the avidity of antigen recognition in Treg differentiation versus clonal deletion has been most thoroughly addressed in the TCR-hemagglutinin (TCR-HA) transgenic system [11]. A clear correlation was found between antigen expression levels and the resulting absolute number of specific nTregs, whereby 'low' expression levels favoured the generations of nTregs, whereas 'high' antigen doses favoured clonal deletion [12, 13]. The best defined example of autoimmunity resulting from a defect in negative selection in the thymus is the *autoimmune polyendocrine syndrome* (APS). This group of diseases is caused by mutations in the *Aire* gene, and is characterised by antibody-and lymphocyte-mediated injury to multiple endocrine organs, including the parathyroids, adrenals and pancreatic islets. A mouse model of APS has been developed by knocking out the *Aire* gene. In normal mice, protein antigens thought to be restricted to these endocrine organs are expressed in thymic epithelial cells, and immature T cells specific for these antigens are deleted in the thymus. In *Aire*-knockout (KO) mice, these antigens are not displayed in the thymus and so T cells specific for these self-antigens escape deletion, mature and enter the periphery where they attack the target tissues.

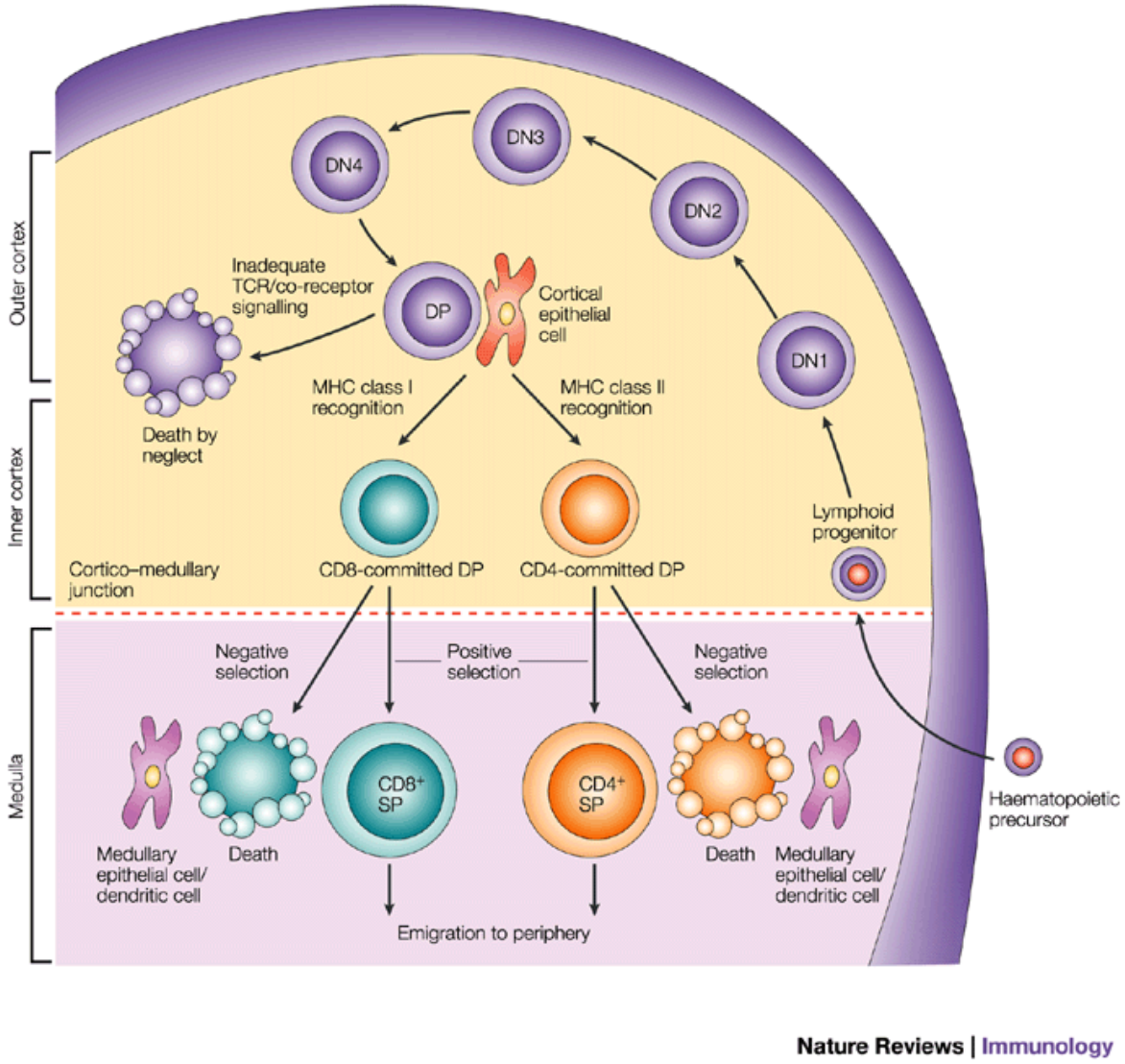


Figure 1.1-4: Overall scheme of T-cell development in the thymus [14].

Committed lymphoid progenitors arise in the bone marrow and migrate to the thymus. Early committed T cells lack expression of T-cell receptor (TCR), CD4 and CD8, and are termed double-negative (DN; no CD4 or CD8) thymocytes. DN thymocytes can be further subdivided into four stages of differentiation (DN1, $CD44^{+}CD25^{-}$; DN2, $CD44^{+}CD25^{+}$; DN3, $CD44^{-}CD25^{+}$; and DN4, $CD44^{-}CD25^{-}$). As cells progress through the DN2 to DN4 stages, they express the pre-TCR, which is composed of the non-rearranging pre-Tα chain and a rearranged TCRβ-chain. Successful pre-TCR expression leads to substantial cell proliferation

during the DN4 to double positive (DP) transition and replacement of the pre-TCR -chain with a newly rearranged TCRα-chain, which yields a complete αβTCR. The αβ-TCR^{+}CD4^{+}CD8^{+} (DP) thymocytes then interact with cortical epithelial cells that express a high density of MHC class I and class II molecules associated with self-peptides. The fate of the DP thymocytes depends on signalling that is mediated by interaction of the TCR with these self-peptide–MHC ligands. Too little signalling results in delayed apoptosis (death by neglect). Too much signalling can promote acute apoptosis (negative selection); this is most common in the medulla on encounter with strongly activating self-ligands on haematopoietic cells, particularly dendritic cells. The appropriate, intermediate level of TCR signalling initiates effective maturation (positive selection). Thymocytes that express TCRs that bind self-peptide–MHC-class-I complexes become CD8^{+} T cells, whereas those that express TCRs that bind self-peptide–MHC-class-II ligands become CD4^{+} T cells; these cells are then ready for export from the medulla to peripheral lymphoid sites. SP, single positive.

However, even with effective negative selection and dominant tolerance mechanisms, central tolerance is incomplete. In order to ensure that a wide repertoire of T cells is available in the periphery to combat foreign antigens, the threshold of clonal deletion is set low enough that T cells with TCRs expressing sub-threshold affinity for self-antigens mature and migrate to the periphery. In addition, T cells which recognise self-antigen derived peptides not expressed or presented in the thymus will also fail to be deleted. Control of these self-reactive T cells is the role of peripheral tolerance.

Peripheral tolerance can act at several levels. The simplest scenario involves T-cell ignorance of self-antigens (***Figure 1.1-5***), either because the latter are sequestered in sites not easily accessible to the blood/lymph-borne immune system [15, 16], or because the amount of antigen does not reach the threshold required to trigger a T-cell response [17]. Alternatively, T-cell encounters with self-antigen might lead to functional inactivation: anergy (***Figure 1.1-5***). Anergy was first shown *in vitro* as a result of TCR ligation in the absence of co-stimulation [18]. However, later work implicated signalling through alternative receptors, rather than just lack of co-stimulation, in the induction of anergy [19]. Even when T cells become fully activated, effective tolerance might still be maintained if the nature of the response is such that pathogenic effects are avoided (***Figure 1.1-5***). Just as certain cytokines and chemokines promote pathogenicity, regulating where self-reactive T cells go and what they make represents another mechanism to prevent autoimmune destruction in the periphery.

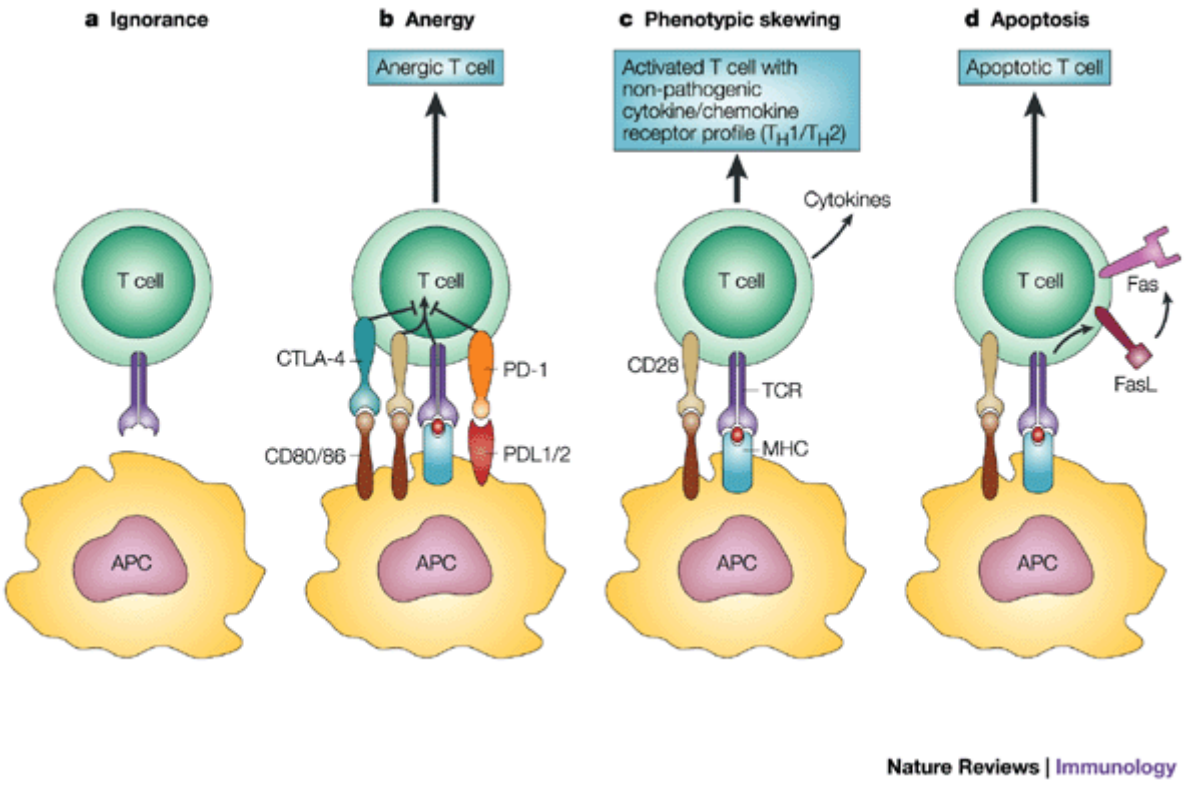


Figure 1.1-5: T-cell intrinsic mechanisms of peripheral tolerance.

Self-reactive T cells might never encounter the self-protein they recognise and therefore exist in a state of ignorance. b) Encounter with self-protein might induce T-cell anergy, possibly involving interaction of the T-cell molecules CTLA-4 or PD-1 with their ligands (CD80/86, PDL1/2). c) T cells interacting with self-protein might undergo full activation, but might develop a non-pathogenic phenotype in terms of which cytokines and chemokine receptors they express. d) Self-reactive T cells might be deleted following contact with self-protein by activation-induced cell death involving upregulation of T-cell Fas ligand and subsequent signalling through the death receptor Fas. APC, antigen presenting cell; CTLA-4, cytotoxic T-lymphocyte-associated antigen 4; FasL, Fas ligand; MHC, major histocompatibility complex; PD-1, programmed cell death 1; PDL, PD-1 ligand; TCR, T cell receptor; T_H cell, T helper cell. ***[Taken from: Walker LS & Abbas AK. Nat Rev Immunol 2002; p.13.]***

However, arguably the most effective way to prevent autoimmune destruction by a given T-cell clone is to delete that specificity from the repertoire by activation-induced cell death (AICD) (***Figure 1.1-5***) [19]. As self-antigens cannot be easily cleared, repetitive TCR engagement might be a feature of T-cell encounters with self-proteins, which perhaps serves as a trigger for AICD [19]. A key mechanism underlying AICD in $CD4^+$ T cells, as well as B cells, is the ligation of the Fas death receptor by its ligand. Interest in this pathway came from the observation that the lymphoproliferative lupus-like syndrome in MRL/*lpr* and *gld* mice was associated with naturally occurring defects in Fas (CD95) and Fas ligand respectively [20-22]. The physiological importance of Fas signalling was underscored by the finding that defects in the Fas pathway in humans are associated with the autoimmune lymphoproliferative syndrome (ALPS) [23]. However, it should be noted that peripheral deletion is rarely complete, and in many models the remaining cells are anergic, which indicates that removal of a T-cell clone from the peripheral repertoire is perhaps an over-representation of events. Instead, deletion might simply serve to decrease the precursor frequency to a level at which anergy can be effectively induced.

Finally, a significant development in the field of tolerance has been the re-emergence of the concept that T-cell reactivity might be controlled extrinsically by a distinct subset of T cells with a regulatory function, and the development of these cells is the subject of my thesis.

1.2 T regulatory cells

Treg cells are a subpopulation of T lymphocytes which modulate the immune system and maintain immune homeostasis. They uphold tolerance to self-antigens, moderate inflammation induced by pathogens and environmental insults, and abrogate autoimmune disease [24-26]. In addition, they can maintain allogeneic transplant tolerance in experimental models [27], but they also facilitate tumour escape from immune monitoring [28]. Given this fundamental importance for immune function and their great potential for therapeutic modulation, it is no surprise that Tregs have attracted extraordinary interest. Despite this, our understanding of their development remains incomplete.

More genome-wide transcriptional profiles have been generated on Treg cells than any other immune cell type [29], which has resulted in the definition of a canonical "Treg signature" that distinguishes Treg cells from conventional T effector (Tconv) cells, at least in their resting states in lymphoid organs [30-35] (***Table 1.2-1***). The Treg signature includes genes over-expressed or repressed in Tregs (in a proportion of 2 to 1), and genes that encode proteins with a wide range of cellular locations and functions: cell surface receptors, signalling kinases and transcription factors [29]. Up to 1500 genes have been found to be differentially expressed in Treg cells [35], but none or very few of these differences are absolute; instead, these variations correspond to quantitative differences between Tregs and Tconv cells [29]. Nor are they specific, as almost all transcripts overexpressed in Treg cells can also be found in non-T cell lineages [29]. Thus, for simplicity, Tregs are generally defined by their expression of the intracellular transcription factor, Forkhead box P3 (FOXP3), in addition to surface phenotypic markers CD4 and CD25 [36].

Gene product cellular localization	**Gene name**	**Gene product putative function**	**Over-/under-expressed in resting Tregs**
Membrane	*Igfbp4*	Protein binding	Under-expressed
	Sh3bgrl2	Receptor	Over-expressed
	Prnp	Receptor	Over-expressed
	Itgae1	Receptor	Over-expressed
	Kirg1	Receptor	Over-expressed
	Ctla4	Receptor	Over-expressed
	Rgs1	Receptor	Over-expressed
	Slc22a2	Receptor	Over-expressed
	Tnfrsf4	Receptor	Over-expressed
	Tnfrsf9	Receptor	Over-expressed
	Il2rb	Receptor	Over-expressed
	Il2ra	Receptor	Over-expressed
	Nrp1	Receptor	Over-expressed
	Gpr83	Receptor	Over-expressed
	Nt5e	Receptor	Over-expressed
	Itgb3	Receptor	Under-expressed
	Vipr1	Receptor	Under-expressed
	Klrd1	Receptor	Under-expressed
	Il1rl2	Receptor	Under-expressed
	Rgmb	Receptor	Under-expressed
	App	Receptor	Under-expressed
	Ptger2	Receptor	Under-expressed
	Tgfbr3	Receptor	Under-expressed
	Sema4f	Receptor	Under-expressed
Cytoplasm	*Rgs16*	GTP or ATP binding	Over-expressed
	Socs2	GTP or ATP binding	Over-expressed
	Tiam1	Receptor	Over-expressed
	Map3k8	Kinase or phosphatase	Over-expressed
	Sgk1	Kinase or phosphatase	Under-expressed
	Appl2	GTP or ATP binding	Under-expressed
	Rapgef4	GTP or ATP binding	Under-expressed
	Myo10	GTP or ATP binding	Under-expressed
	Arhgap29	GTP or ATP binding	Under-expressed
	Sgms1	Transferase or esterase	Under-expressed
	Hs3st3b1	Transferase or esterase	Under-expressed
	St3gal6	Transferase or esterase	Under-expressed
	Pde3b	Transferase or esterase	Under-expressed
Nucleus	*Plagl1*	DNA binding or transcription factor	Over-expressed
	Mdfic	DNA binding or transcription factor	Over-expressed
	Ikzf4	DNA binding or transcription factor	Over-expressed
	Ikzf2	DNA binding or transcription factor	Over-expressed
	Irf4	DNA binding or transcription factor	Over-expressed

	Foxp3	DNA binding or transcription factor	Over-expressed
	Dusp4	Kinase or phosphatase	Over-expressed
	Enc1	Protein binding	Under-expressed
	Pole2	DNA binding or transcription factor	Under-expressed

Table 1.2-1: Treg cell signature genes and their cellular localization [29].

A list of the most differentially expressed genes from a consensus Treg signature [35], either over-expressed or under-expressed in resting Treg cells of spleen or lymph node relative to Tconv cells. Gene products are grouped according to their cellular localization and their putative functions identified.

The majority of Tregs develop naturally in the thymus (nTregs) as a subpopulation of $CD4^+$ T cells. They are positively selected and migrate to the periphery. As I have already alluded to, it is thought that self-peptide - MHC recognition by the TCR is required with an avidity intermediate between that necessary for positive selection of conventional $CD4^+$ and $CD8^+$ T (Tconv) cells and that needed for the deletion of autoreactive T cells [37]. In addition to these naturally-occurring nTregs, transforming growth factor beta (TGF-β) and interleukin- (IL-) 2 are able to promote, in response to TCR/CD28 co-stimulation, the differentiation of peripheral naive $CD4^+$ T cells into $CD4^+CD25^+FOXP3^+$ T cells, otherwise known as inducible (i) Treg cells, that possess T cell suppressive properties akin to those of nTregs [38-40]. nTregs are thought to suppress autoimmunity while iTregs restrain immune responses to foreign antigens, such as those from diet, commensal bacteria and allergens [41].

The importance of Treg cells is underscored by the lymphoproliferative and multi-organ autoimmunity phenotypes of Scurfy mutant mice (***Figure 1.2-1***) and the human conditions *I*mmunodysregulation *P*olyendocrinopathy and *E*nteropathy, *X*-linked (IPEX) syndrome and *X*-*L*inked *A*utoimmunity-*A*llergic *D*ysregulation syndrome (XLAAD), which result from mutations in the *Foxp3* gene and consequent lack of Tregs [42].



Figure 1.2-1: T regulatory cells maintain tolerance to self

Scurfy mutant mice (right) with a genetic FOXP3 (also known as scurfin) deficiency, and consequent lack of Treg cells, develop multi-organ autoimmune disease and die soon after birth. Observable phenotypes include cachexia and runting, flaking, crusty skin on eyelids, ears and tail, dermal thickening and squinted eyes. An age-matched, healthy, wild-type control mouse (left) is shown for comparison.

1.3 T regulatory cells in health

Pregnancy represents a physiological situation where tolerance to paternal *allo*antigens, (antigens from a genetically disparate individual of the same species) is critical for successful reproduction of placental animals and Tregs are thought to facilitate this, based on their increased numbers in pregnant mice and humans [43]. Samstein *et al* recently demonstrated that pregnancy-induced maternal iTregs specifically recognise paternal antigens, indicating that maternal-fetal tolerance to paternal alloantigens is an active process in which iTregs specifically respond to paternal antigens to induce tolerance [44]. These findings are consistent with an increase in the percentage of Tregs during pregnancy and with no such increase in women suffering recurrent pregnancy loss [43]. The authors go on to speculate that these results may provide biological plausibility for the seemingly paradoxical observation that, among women with a history of unexplained recurrent miscarriage, the administration of Filgrastim (granulocyte colony-stimulating factor) in early miscarriage reduces the rate of miscarriage [45].

1.4 T regulatory cells in disease

While Tregs are indispensable for the maintenance of self-tolerance and immune homeostasis, their dysfunction can cause fatal autoimmune disease, immunopathology and allergy.

1.4.1 T regulatory cells in autoimmune disease

To address the question of whether immune suppression by Treg cells is impaired in the setting of human autoimmune disease, it is important to recognise the potential means by which such a defect may occur. Defects in the number and function of Tregs, as well as the resistance of Tconv cells to Treg cell-mediated suppression, could each contribute to failed T cell regulation [46]. The number of Treg cells found in individuals with autoimmune disease is itself influenced by Treg cell development, persistence and proliferation in the periphery, and homing to the site of inflammation [46]. Each of these defects in regulation may contribute, either in isolation or in combination, to the development of human autoimmune disease.

Treg dysfunction in autoimmune disease may be due to a defect in one of the many mechanisms through which Treg cells function [47]. This could occur through inadequate expression of cell surface molecules that are known to be involved in contact-dependent suppression (such as, cytotoxic T lymphocyte antigen 4 (CTLA4), CD39, lymphocyte activation gene 3 (LAG3), granzyme A and CD95 (also known as FAS)), or as a result of a failure to produce the soluble factors (such as TGFβ, IL-10 and IL-35) that are involved in some aspects of suppression [46]. Underlying genetic factors may influence these mechanisms. In addition, the composition of the local milieu, including the types of antigen-presenting cells and cytokines such as tumour necrosis factor (TNF) [48], IL-4 [49], IL-6 [50], IL-12 [51], IL-15 [52] and IL-21 [53], can influence Treg cell function.

Multiple mechanisms by which Tconv cells resist Tregs have been proposed [54]. Cell-intrinsic resistance to suppression has been shown to occur in $CD4^+$ memory T cells and T helper 17 (Th17) cells [55]. The cytokines IL-2, IL-4, IL-7 and IL-15 support the proliferation of Tconv cells in the presence of Tregs, indicating that despite the favourable roles of these cytokines in Treg homeostasis [56], the presence of these cytokines in the short term allows Tconv cells to bypass suppression by Tregs [46]. In addition, several members of the TNF receptor family have been implicated in this process: antibody specific for CD134 (also known as OX40 or Tumour Necrosis Factor Receptor Superfamily Member (TNFRSF) 4) abrogates suppression when bound to Tconv cells [57] and ligation of CD137 (also known as 4-1BB or TNFRSF9) results in suppression-resistant T conv cells [58].

The task of determining the extent and character of these defects in human disease is therefore challenging. Evidence that an inadequate number of Tregs leads to autoimmunity in humans is most clearly shown in patients with IPEX, who completely lack Tregs as a result of a mutation in the *foxp3* gene [42], but most patients with autoimmune disease probably have a more modest reduction in Tregs. The task of enumerating Tregs in human disease is complicated by a number of issues. The lack of a cell surface marker unique to Tregs and the multiplicity of Treg subsets lead to the issue of which cells to count.

With the discovery that expression of FOXP3 has a central role in the differentiation and maintenance of Tregs [59, 60], the use of flow cytometry-based analysis of FOXP3 expression in T cells became the gold standard for defining Tregs. But, FOXP3 is a nuclear protein and so assessment of its expression in T cells requires fixation and permeabilisation of the cells, resulting in an inability to obtain viable cells for further functional analysis [46]. Furthermore, does the peripheral blood reflect the global number of Treg cells in the body and, more

specifically, their number in inflamed tissues? Patients are often on medications which limit their disease but are also likely to interfere with the Treg population and its functions. These reasons alone emphasise the complexities of this subject and limit the conclusions that can be drawn from individual studies.

Identifying defects in the function of Tregs is made difficult both by the multiple mechanisms they use to suppress inflammation [61] and by the manner in which suppression is measured. Assessment of Treg function in humans requires the use of *in vitro* assays that, owing to the rarity of Tregs in the peripheral blood (5-10% of the total peripheral $CD4^+$ T cell population in humans, under basal conditions [24]), must be carried out with low cell numbers limiting the type and quality of assays that can be done. *In vitro* assays provide insight into potential Treg defects but they cannot account for the impact of the local milieu on Treg function [46].

The resistance of Tconv cells to Tregs has been observed in several animal models of autoimmunity. In these models, inflammation and tissue destruction progress despite the presence of functional Tregs at the site of inflammation [46]. Such findings suggest that a resistance of Tconv cells to Tregs may contribute to disease progression and this phenomenon has been described in two mouse models of diabetes: non-obese diabetic mice (NOD) mice [62, 63] and DO11.10 RIP-mOVA mice [53]; experimental autoimmune encephalomyelitis (EAE) [64]and the MRL-lpr model of systemic lupus erythematosus (SLE) [65].

For the reasons described here, delineation of the mechanisms of impaired tolerance in human autoimmune disease has been challenging and slow. Nevertheless, a picture is slowly emerging and with it, a hope is that this knowledge can direct the development of new approaches to the treatment of autoimmunity. A comprehensive review of what is known

about the role of Tregs in individual autoimmune diseases is beyond the scope of this work but I briefly discuss the evidence supporting the involvement of impaired T cell regulation in the context of five of the more common autoimmune and inflammatory diseases below.

1.4.1.1 T regulatory cells and type-1 diabetes

Type-1 diabetes is an immune-mediated disease that results in inflammation and destruction of the pancreatic islet cells, resulting in a lifelong need for insulin. The current evidence does not indicate a global deficiency in Treg numbers in type-1 diabetes [66, 67] but does not rule out a more focal deficiency in the Treg compartment, with respect to either a subset of Tregs [67] or the specificity of Tregs for islet antigens [68]. Multiple studies show that suppression is impaired [69] and indicate that this is, in part, due to the resistance of Tconv cells to suppression by Tregs [70, 71].

1.4.1.2 T regulatory cells and multiple sclerosis

Multiple sclerosis (MS) is an autoimmune disease characterised by inflammatory lesions and degeneration in the central nervous system (CNS). The pathogenic $CD4^+$ T cells in MS target myelin-based antigens [46]. They have the ability to migrate to the CNS as well as unique effector functions [72]. Although the inflammatory components involved in MS are numerous, defects in Tregs are implicated by both the mouse model of MS, experimental autoimmune encephalomyelitis (EAE) and the human disease. Overall, Tregs do not seem to be reduced in number but clear defects in suppression have been identified [73, 74].

1.4.1.3 T regulatory cells and systemic lupus erythematosus

Systemic lupus erythematosus (SLE) is a systemic autoimmune disease characterised by the presence of autoantibodies and immune complexes that target multiple organ systems, including the skin, joints, kidneys and CNS. Unlike the autoimmune diseases discussed above, there are many target tissues in SLE, not just one, and it is thought to be a largely B cell-mediated disease [46]. Defects in the number [75-78] and function of Tregs [75, 79, 80] and in the resistance of effector T conv cells to suppression [75, 81] have been established. The observations of numerous possible regulatory defects may reflect the systemic nature of this disease or a more significant role for Tregs in SLE, compared with their role in other autoimmune conditions [46].

1.4.1.4 T regulatory cells and rheumatoid arthritis

As in other autoimmune diseases, the experimental model of rheumatoid arthritis (collagen-induced arthritis) is exacerbated by the depletion of Tregs [82]. But, unlike the majority of diseases described above, the target tissue – synovium – can be obtained from patients with rheumatoid arthritis which has allowed investigators to analyse the number and function of Tregs in the diseased tissue, as well as the peripheral blood. (Analysis of cerebrospinal fluid offers a similar advantage to the study of MS.) In addition, studies of rheumatoid arthritis benefit from the existence of well-established biological therapies, allowing the impact of these therapies on Treg numbers and function to be studied e.g. the TNF-specific agent infliximab (Remicade®, Merck) [46]. There is a general agreement that the percentage of Tregs is higher in the synovial fluid of patients with rheumatoid arthritis compared to controls [83-85]. Ehrenstein *et al* [86] established a Treg cell-intrinsic defect in interferon gamma (IFN-γ) and TNF production, as well as a defect in CTLA4-mediated inhibition of TCR signalling in patients with rheumatoid arthritis. Resistance of Tconv cells to suppression has not be

exhaustively tested in rheumatoid arthritis and was not the reason for the impaired suppression observed by Ehrenstein *et al* [86].

1.4.1.5 T regulatory cells and inflammatory bowel disease

The term inflammatory bowel disease (IBD) refers to two conditions - Crohn's disease and ulcerative colitis – distinguished by their underlying pathology. Despite these pathological differences, both are thought to be Tconv cell-driven diseases and to result from a loss of immune tolerance in the gut [46]. Tregs have a central role to play in the maintenance of immune tolerance in the gut, which is exemplified by the wasting disease and gastritis that develop in Scurfy mice lacking Treg cells, and by reversal of the disease by adoptive transfer of Tregs [87]. A role for Tregs in human disease is supported by the finding of severe bowel inflammation in IPEX patients [42]. Like rheumatoid arthritis, studies of Tregs in IBD have been aided by the ability to study their role in target organs as well as peripheral blood, but these studies have given mixed and often contradictory results with no clear picture explaining the role of Tregs in IBD currently [88-93].

1.4.2 T regulatory cells and cancer

Under normal circumstances, where Tconv cells accumulate in response to local signals, so do nTregs. The homeostatic balance is maintained and potential tissue damage prevented [94]. In the environment of solid tumours, however, a conversion of Tconv cells into iTregs occurs, creating a poll of highly activated and indiscriminately suppressive iTregs, which interfere with functions of anti-tumour Tconv cells [95, 96]. nTregs control cancer-associated inflammation which is thought to favour tumour progression but it is iTregs that are thought to play the more major role in cancer and cancer therapy [94]. For this reason, it is widely believed that *in vivo* elimination of iTregs may restore or enhance anti-tumour immunity and increase the efficacy of immunotherapy [94].

The division in labour between iTregs and nTregs is not absolute but it is reasonable to assume, albeit simplistically, that Tregs circulating in the peripheral blood of healthy donors largely represent thymus-derived nTregs responsible for maintaining peripheral tolerance, whilst those present in cancer patients are enriched with iTregs, and this allows for a discrimination between Treg subsets in health and disease. Having said that, aggregate results of recent clinical trials using Treg-depleting regimens, such as anti-CD25 dacluzimab and denileukin diftitox (ONTAK®) in cancer patients suggest that the indiscriminate elimination of $CD25^+$ T cells interferes with anti-tumour functions of Tconv cells as well as Tregs [94], and so more specific iTreg therapeutic targets are required. The selective discrimination between nTreg and iTreg to avoid shifting the balance toward autoimmunity and simultaneously achieve robust anti-tumour effects will not be simple and additional knowledge of the molecular mechanisms underlying iTreg and nTreg interactions is required.

1.4.3 T regulatory cell therapy and transplantation*

Transplantation can be defined as the artificial transfer of cells, tissues or organs from one individual to another. Where the graft is syngeneic (genetically identical to the host, e.g. transplantation between identical twins) or autologous (a transplant from one individual to itself, e.g. using stored blood for autotransfusion), there is perfect histocompatibility and no significant immune response is elicited [97]. In this situation, the recipient is fully tolerant to the transplant and accepts it without a rejection phenomenon. Where there is histo*in*compatibility, however, in general an immune response is elicited against the foreign antigens, the magnitude of which determines acceptance or rejection of the transplanted tissues [97].

Since the first human kidney transplant carried out by Dr Joseph Murray in 1954 between identical twins, the regular development of new chemical immunosuppressants, as well as improved surgical and ancillary care, have led to dramatic increases in kidney allograft survival rates and enabled the transplantation of livers, hearts, pancreases and lungs, as well as composite tissues [98]. Nonetheless, substantial problems remain and improvements in short-term (1 year) allograft survival have not been paralleled by gains in long-term graft survival *(US organ procurement and Transplantation network. Annual Data report 2011. Accessed 17th July 2013).* The reasons for graft loss are complex but can, at the risk of oversimplification, be broadly classified into three categories: inflammation-induced reactions against graft tissues, immune–initiated reactions against graft tissues and direct organ toxicity by the immunosuppressive drug. Other side effects of immunosuppression, such as susceptibility to opportunistic infections, malignancy and accelerated cardiovascular disease, contribute substantially to morbidity and mortality amongst transplant recipients. Thus it stands to reason that the ability to induce transplantation tolerance – good allograft function in

the sustained absence of immunosuppressive therapy – could be expected to have an enormous impact on both allograft and patient survival, and that it is a goal worth pursuing.

In recipients of solid-organ transplants, the high frequency of alloantigen-reactive Tconv cells in the immune repertoire of the recipient compared with the relatively small number of Treg cells present at the time of transplantation means that the balance of cells is shifted towards allograft destruction [55]. This crucial balance between graft destruction and regulation can be shifted using strategies to inhibit the activity of Tconv cells and/or increase the relative frequency or functional activity of alloantigen-reactive Treg cells [99-103]. Previous experimental studies using MHC-mismatched combinations in murine skin and heart allo-transplantation have shown that alloantigen-specific Tregs are more effective at inducing indefinite allograft survival than polyclonal Tregs [104-106]. In 2011, Sagoo *et al* translated these observations into a human *in vivo* model [107]. Human Tregs were enriched from peripheral blood donations from healthy volunteers and stimulated with irradiated mature myeloid dendritic cells (DCs). The Tregs were then sorted and expanded if they expressed two activation markers, CD69 and CD71, after allospecific activation with the DCs *in vitro.* Transfer of these customised Tregs into a humanised mouse skin transplant model prevented transplant rejection and skin damage with higher efficacy than that associated with the transfer of nonspecific, polyclonal Tregs. No clinical trials of Treg therapy in solid organ transplantation have been undertaken as yet but promising data are emerging from early trials of Tregs for the prevention of graft-versus-host disease (GVHD) post hematopoietic stem-cell transplantation [108-110] and the ONE Study - a multicentre Phase I/II study funded by the European Union Seventh Framework Programme – has set about investigating the safety of infusing *ex vivo*-expanded Treg cells into kidney transplant recipients (www.onestudy.org).

*Please see: Salisbury E, Game D, Lechler R. Transplantation Tolerance. *Pediatric Nephrology*. (In Press) for a more detailed review.

1.5 Natural T regulatory cell development

Since the description of suppressor T cells in the early 1970s, considerable progress has been made in the characterisation of Treg cells but the signalling events necessary for nTreg development in the thymus are not fully understood. Three main signals have been identified. Firstly, as I suggest earlier, it is thought that self-peptide – MHC recognition by the TCR is required with an avidity intermediate between that necessary for positive selection of Tconv cells and that needed for the deletion of autoreactive T cells [37]. Secondly, costimulatory signals play an important role. We know mice deficient in CD28, its ligands CD80 and CD86, or CD40, or LFA1 all display a marked reduction in nTregs [25, 111-113]. Thirdly, IL-2, in combination with IL-15 or IL-7, is also known to be crucial for nTreg development [36]. Whereas single absence of IL-2 or CD25 (the IL-2Rα-chain) mildly impacts thymic nTreg development [114-116], mice lacking both IL-2 and IL-15, or CD122 (the IL-2βR chain common to both IL-2 and IL-15 receptors), or CD132 (the common γ-chain), or Signal Transducer and Activator of Transcription 5 (STAT5α/β) (the transcription factor downstream of IL-2R) are all devoid of nTregs [116-122]. Conversely, transient or transgenic expression of STAT5 can rescue nTreg numbers in mice deficient in IL-2, CD25, CD122 or CD132 [116, 118, 123, 124], as well as, notably, CD28 [118]. STAT5 is known to have binding sites within the *Foxp3* promoter [116, 121].

Based on these and other data, a two-step model of nTreg development has been projected (***Figure 1.5-1***) in which an initial TCR/CD28-mediated signal is required for activation of the Nuclear Factor Kappa-light-chain-enhancer of activated B cells (NFκB) and c-Jun N-terminal kinase (JNK) pathways, and the consequent induction of common gamma chain (γc) cytokine-responsive $FOXP3^-$ Treg precursor cells from immature thymocytes [25]. Two precursor populations of nTreg cells have been described: $CD4^+CD8^+$ thymocytes that express FOXP3

[30, 125] and a more distal $CD4^+CD8^-CD25^+CD122^+GITR^+FOXP3^-$ thymocyte population [126]. Whether the proximal precursor gives rise to the distal precursor prior to mature nTreg cell generation is not known, but in the second step of nTreg development these distal, now γc cytokine-responsive, $FOXP3^-$ Treg precursor cells are exposed to IL-2 in the absence of new TCR/CD28 ligation, resulting in their differentiation into mature $FOXP3^+$ nTreg cells [118, 126].

Despite this, how the signals arising from multiple receptors are integrated to drive the events necessary for thymic nTreg development *in vivo* is far from resolved and much of what we do know is based on data extrapolated from co-transfection studies in T cell lines [127, 128].

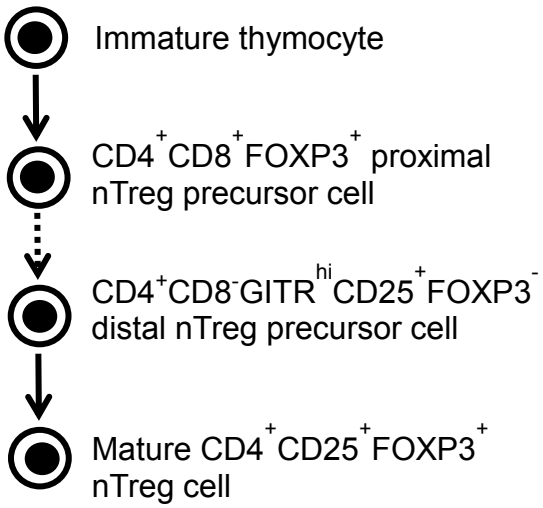


Figure 1.5-1: The two-step model of nTreg cell development.

A schematic diagram illustrating the putative two-step model of nTreg cell development from immature thymocytes.

1.6 This study

Using an unbiased forward genetic approach, I set out to identify dominant genes required for the development of nTregs in the thymus with the aim of enhancing our knowledge in this fundamental area of immunobiology.

1.6.1 Forward genetics and *N*-ethyl-*N*-nitrosourea (ENU) mutagenesis

Genetics originally began with phenotype. The aim was to find the genes responsible for phenotype. This era was interrupted by methods such as the "knock-in/knock-out technology" which permitted the identification of genes irrespective of what they did: "reverse genetics". Reverse genetics requires a hypothesis driven guess on the nature of the molecules of interest and is limited by the lethal nature of complete disruption of genes that control proliferation, cell death or senescence [129]. This project returns to classical genetics. Enlightened by technologies of the modern era, it is now known as "forward genetics" [129]. The strength of forward genetics lies in its unbiased approach and bringing a robust phenotype to the forefront.

Forward genetics requires phenotypes and this is the task of mutagenesis. Powerful germline mutagens exist to increase the rate of naturally-occurring mutations in mammals ~100-fold. The chemical mutagen *N*-ethyl-*N*-nitrosourea (ENU), an alkylating agent, offers an advantage over other compounds by operating at the level of spermatogonia, creating "stable" mutations that are transmitted in the germline for the lifetime of the animal after mutagenesis [129]. It creates chiefly A→G transitions and A→T transversions randomly throughout the genome [129]. ENU has the capacity to generate a range of alleles at any locus, and subtle hypomorphic variations can provide functional insights that binary all-or-nothing gene knockouts often

obscure. Since the mutations are generated randomly, no assumptions are made regarding the nature of the disrupted gene, and the alleles are by definition viable in the adult. ***Figure 1.6-1*** explains the process of ENU mutagenesis.

Analysis of mutation frequency by direct genomic sequencing is now available and the consensus of several groups would indicate that ENU induces a single base-pair change approximately every 0.5 to 1.0 megabase of genomic DNA [130]. This frequency predicts that approximately 1,000 generation (G) 1 animals (or their progeny) need to be screened in order to identify a phenotype caused by a mutation in a single gene [130].

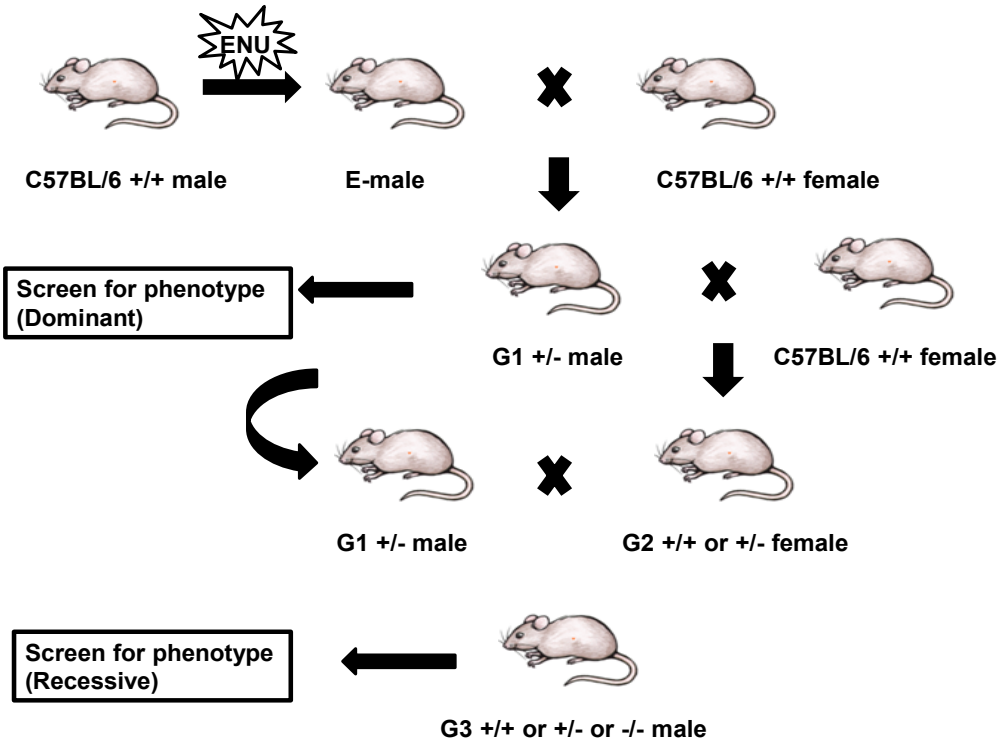


Figure 1.6-1: N-ethyl-N-nitrosourea (ENU) mutagenesis

C57BL/6 male mice are treated with 3 doses of ENU (referred to as "E-male" in diagram) and allowed to recover fertility over a period of 12 weeks. These males are then mated with wild-type (Wt) (+/+) C57BL/6 female animals and the resulting offspring from this cross are referred to as generation (G) 1 mice. They can be screened directly for dominant, heterozygous (+/-) traits or mated with Wt (+/+) animals to produce a G2 population. The G2 animals are heterozygous (+/-) or Wt (+/+) at any given locus. They can then be backcrossed to their G1 heterozygous (+/-) parents to generate G3 animals, some of which will be homozygous (-/-) at various (and random) locations throughout the genome. These G3 animals can be screened for recessive mutations.

Treg cell development cannot be studied *in vitro*. A model organism with an adaptive immune system is required. Invertebrates have no true lymphoid organs. Zebrafish provide a vertebrate model but the mouse model is most closely related to humans. All but a few hundred of our approximately 25,000 expressed genes have direct mouse counterparts [131], and the mouse and human genomes demonstrate extensive synteny. These similarities could be applied to most mammals but use of the mouse model avoids more emotive species, whilst allowing the exploitation of powerful genetic techniques and molecular reagents. Mice are small, easy to maintain in the laboratory and have a short breeding cycle of approximately 8 weeks. They can produce 8-10 offspring per litter and at least one litter per month. This makes them suitable for genetic analysis. In accordance with ethical principles and the requirements of the Secretary of State, reasonable efforts were made to incorporate replacement, reduction and refinement alternatives into the plan of this work.

The random germline mutagenesis strategy has proved paramount to the discovery of previously uncharacterised genes and the identification of new functions of known genes or specific protein domains but, it is only ever as strong as its phenotypic screen. Successful screens need to be reliable (based on strong wild-type phenotypes to reduce the number of false negatives) and the standard deviations for each parameter must be as small as possible so "cut off values" can be defined and isolation of false positives minimised. In addition, the screen should be simple and rapid because it is performed on a large number of mice each week. The combination of mutations required to produce truly revolutionary phenotypic change will never be observed in a panel of ENU mutant mice. True redundancy of function is unusual but overlap of function is exceedingly common and many phenotypic differences prove to be polygenic, limiting the effectiveness of phenotypic screens [25]. For this reason a great deal of ingenuity and screening is required to disclose function, and precisely the correct

molecule must be chosen to reveal the essential nature of a particular gene. One must consider whether the surrogate marker is truly indicative of the process[132].

Understanding whether a phenotype is heritable and, if so, whether it is dominant or recessive, is crucial to the design of subsequent mapping studies. As well as those mice which develop distinct phenotypes as a result of an inherited, spontaneous or ENU-induced mutation, there will always be a small, predictable fraction with phenotypes arising as a result of their position in the tail of a normal distribution curve for a quantitative trait. Others will have outlying phenotypes resulting from environmental factors *in utero* or *post-partum*. Setting up test crosses and examining the phenotype of the resulting progeny can distinguish between these possibilities. Once the isolated mutation is confirmed to affect the germline, a stable mutant stock is established.

Genotyping and phenotyping are usually performed in parallel, until the identity of the affected gene is required for a more thorough in-depth phenotyping [133]. Mutations are identified by a combination of mapping and sequencing. Mapping can be divided into two stages: a low-resolution phase in which the mutation is localised to a large chromosomal interval, and a high-resolution phase in which the size of the interval is reduced to a point at which sequencing can begin [132]. Depending on the resources available, it might be necessary to prioritise the genes in the interval for sequencing. Properties that would influence this include whether mutations in the gene itself or in genes in the same biochemical pathway are known to yield a similar phenotype to the mutation under investigation, whether the gene is expressed in tissues that are known to be affected by the mutation, whether the level of expression and size of transcription differ in affected and unaffected mice; and whether there

is evidence for the existence of a *bona fide* transcript [132]. ***Figure 1.6-2*** summarises the practical steps required for germline mutagenesis.

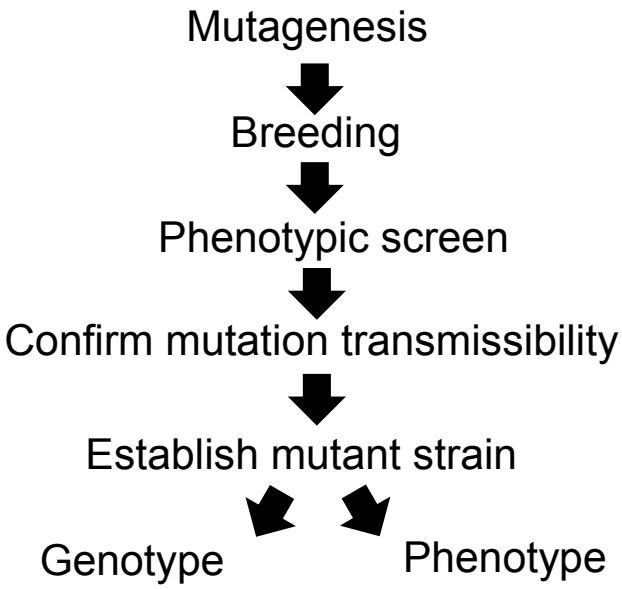


Figure 1.6-2: The practical steps required for germline mutagenesis.

1.6.1.1 Past successes using forward genetics

Early forward genetics projects led to the identification of the adenomatosis *(APC)* gene [134] and the circadian locomotor output cycles kaput (clock) gene [135]. More recently, Beutler's group based at The Scripps Research Institute, La Jolla, USA has had outstanding success in identifying components of toll-like receptor signal transduction pathways, providing invaluable insights into the innate immune system [136]. In fact, together with Jules Hoffmann, Beutler received one-half of the 2011 Nobel Prize in Physiology/Medicine, for "their discoveries concerning the activation of innate immunity". (The other half went to Ralph Steinman for "his discovery of the dendritic cell and its role in adaptive immunity".)

Of course, the ultimate aim of forward genetics is to link a change in phenotype with a defined change in genotype and harness this knowledge to find treatments for disease. In 2006, forward genetics led to the identification of 'triple D' (3d), a mis-sense allele of *Unc93b1*, which encodes the 12-membrane-spanning protein UNC-93B [137]. The mutation caused diminished MHC class II presentation of exogenous antigen and hyper-susceptibility to infection by mouse cytomegalovirus and other microbes. Later that year, Casrouge *et al* went on to elucidate a genetic aetiology for herpes simplex virus-1 (HSV-1) encephalitis (HSE) in two children with autosomal recessive deficiency in the intracellular protein UNC-93B, resulting in impaired cellular interferon-α/β and –λ antiviral responses [138]. They demonstrated that HSE could result from a single-gene immunodeficiency that does not compromise immunity to most pathogens, unlike most known primary immunodeficiency syndromes, raising the possibility that other severe infectious diseases could reflect monogenic disorders of immunity. These results have important therapeutic implications, as at least some HSE patients would benefit from recombinant IFN-α treatment. Where reverse genetics may fail, forward genetics may succeed.

Chapter 2: Results

2.1 Dominant mutations Vulpo and Zerda impair nTreg development

ENU-induced germline G1 mutants (n=766) were screened for dominant mutations that impair nTreg cell development. Abnormal nTreg cell development was defined as a $CD25^{+}FOXP3^{+}CD4^{+}$ cell population out with 2 standard deviations (SD) of the mean. Chronic antigenic exposure represents one of the main sources of iTregs [139] and therefore, it was expected that these non-immunised, 6-week old mice housed under clean, specific pathogen-free conditions had a negligible iTreg contribution. Two ENU mutant mice, Vulpo and Zerda, with >90% reduction in the frequency of $FOXP3^{+}CD25^{+}CD4^{+}$ cells in peripheral blood leucocytes (PBL) by flow cytometry, compared to the mean value for the 766 animals screened ($p<0.001$), were identified (***Figure 2.1-1***). These dominant mutations were confirmed to be heritable in the germline. G2 phenodeviant mutants were inter-crossed and the G3 offspring screened and inter-crossed to establish homozygous strains.

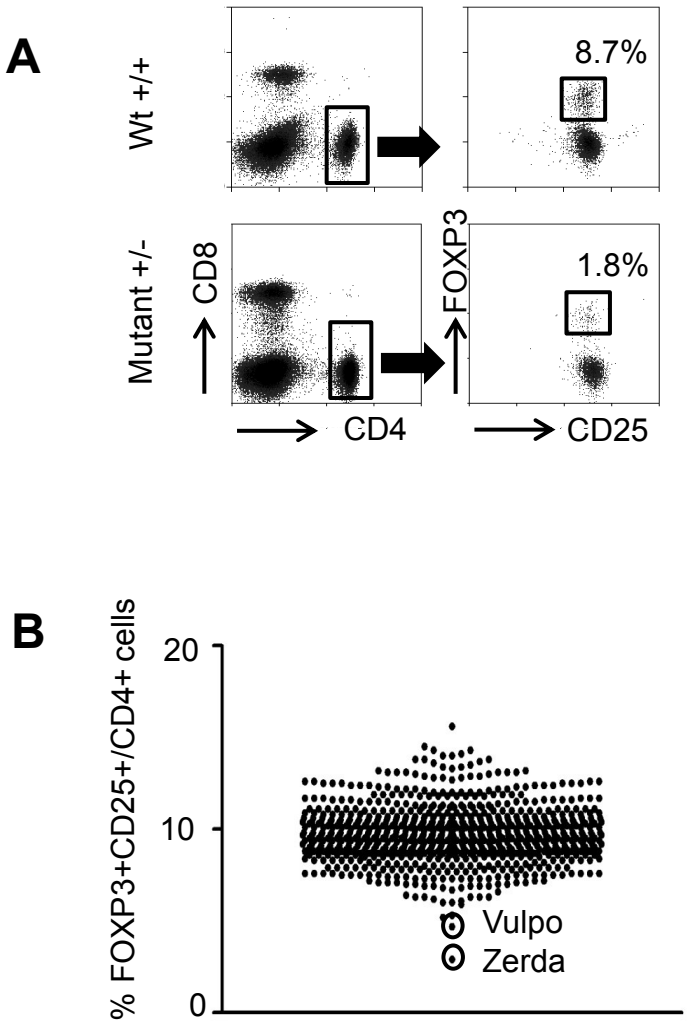


Figure 2.1-1: Identification of Vulpo and Zerda mutants with impaired nTreg cell development.

(A) *A representative dot plot defining the percentage of $FOXP3^+CD25^+$ nTreg cells in the $CD4^+$ T lymphocyte population from PBL in one Wt mouse (top panel) and one heterozygous ENU mutant mouse (Mutant +/-) (bottom panel). Forward scatter plot allowed the exclusion of non-singlet cells and gates were applied to the lymphocyte and $CD4^+$ populations in order to define the $FOXP3^+CD25^+/CD4^+$ population.* ***(B)*** *Two ENU mutant mice, Vulpo and Zerda, with reduced $FOXP3^+CD25^+/CD4^+$ Treg cell frequencies in PBL (values out with 2 SD of the mean). Each symbol represents data from an individual mouse. n=766. The graph is the cumulative result of at least 20 independent experiments.*

The level of nTregs ($CD25^+Foxp3^+/CD4^+$ cells) in the PBL of homozygous mutant Vulpo mice was only 12.8% of Wt (87.2% reduction) ($p<0.0001$) (***Figure 2.1-2A***). The level of nTregs in the PBL of homozygous mutant Zerda mice was only 3.4% of Wt (96.6% reduction) ($p<0.0001$) (***Figure 2.1-2A***). Organ dissection supported these findings (***Figure 2.1-3***). I observed a 57.5% decrease in absolute number of nTregs in the thymus of Vulpo mutants (mean = 4.2×10^5 +/-1SD (8.9×10^4) cells, n=5) and a 92.2% decrease in absolute number of nTreg cells in the thymus of Zerda mutants (mean = 7.8×10^4 +/-1SD (4.9×10^3) cells, n=6) compared to Wt (mean = 1×10^6 +/-1SD (8.7×10^4) cells, n=6) (***Figure 2.1-3***). The absolute number of nTregs in the thymus of Zerda mutants was significantly less than for Vulpo mutants ($p<0.0001$). The Treg lineage remains virtually absent in older mice (1yr) indicating that these were persistent defects and not compensated over time (data not shown).

I also observed a generalised increase in Tconv cells in the PBL of both mutants versus Wt. I recorded a 42.1% increase in the frequency of $CD8^+$ T cells in the PBL of homozygous mutant Vulpo mice compared to Wt ($p=0.0078$) and a 50% increase for homozygous mutant Zerda mice compared to Wt ($p<0.0001$) (***Figure 2.1-2B***). I recorded a 47.9% increase in the frequency of $CD4^+$ T cells in the PBL of homozygous mutant Vulpo mice compared to Wt ($p=0.0037$) and a 75.4% increase for homozygous mutant Zerda mice compared to Wt ($p<0.0001$) (***Figure 2.1-2C***). Organ dissection of spleen (data not shown) and thymus (***Figure 2.1-3***) supported these findings: I observed a significant increase in absolute cell number in Vulpo and Zerda mutants at every stage of thymocyte maturation (see ***Figure 1.1-4*** for an overall schematic of T-cell development in the thymus) compared to Wt. In contrast to the difference observed in frequency of mature nTregs between the two mutants, I observe no significant difference between Vulpo and Zerda mutants at all stages of thymocyte maturation (***Figure 2.1-3***).

Both *vulpo* and *zerda* mutations show incomplete dominance as evidenced by heterozygous (+/-) phenotypes intermediate to the Wt (+/+) and homozygous (-/-) mutant phenotypes (***Figure 2.1-2***). This semi-dominant effect is seen on nTreg cell development and not just FOXP3 expression because no decrease in mean fluorescence intensity (MFI) is observed during flow cytometric analysis (data not shown).

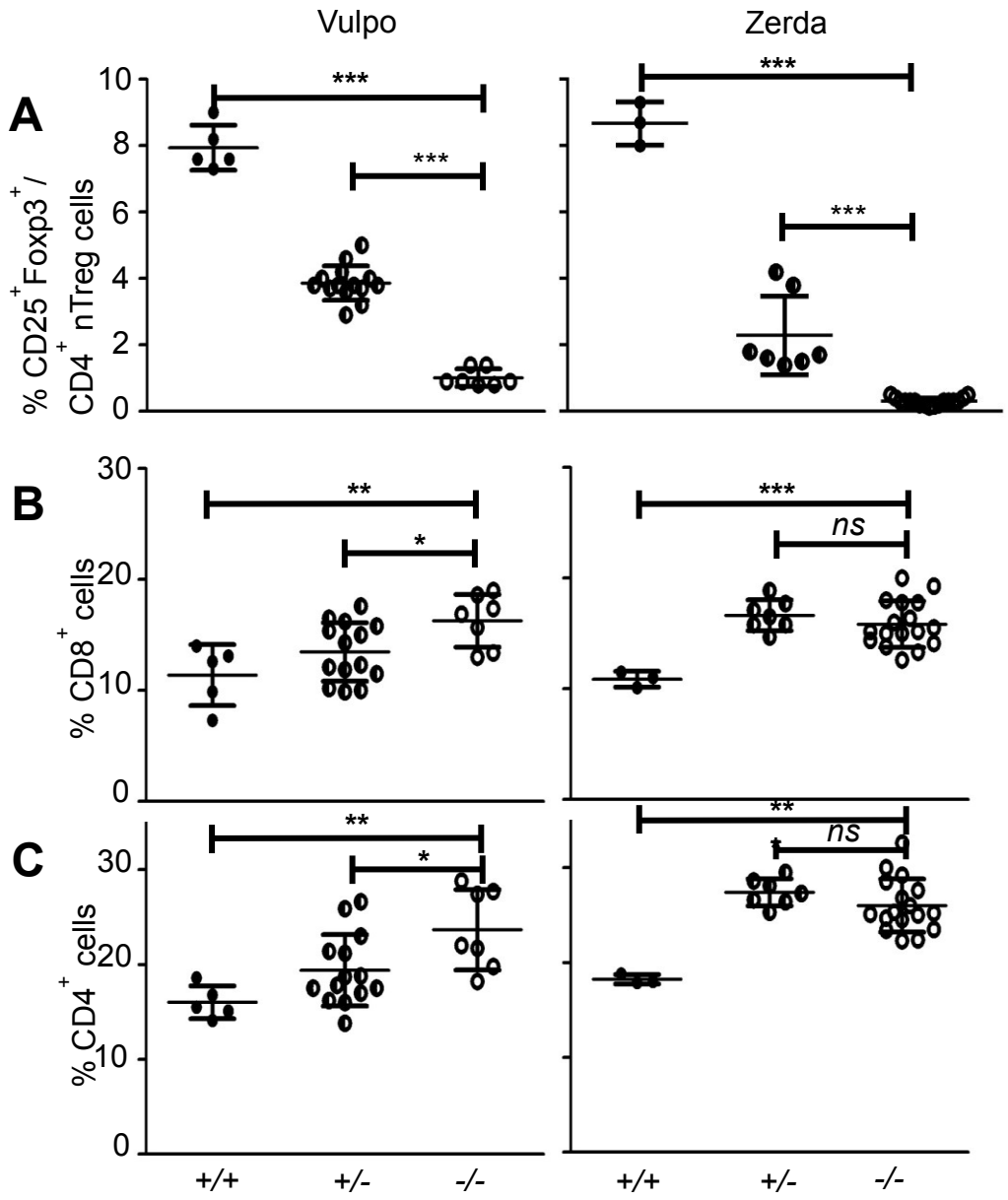


Figure 2.1-2: Vulpo and Zerda mice have reduced nTregs & increased Tconv in PBL.

(A) *Percentage of nTregs in PBL.* ***(B)*** *Percentage of $CD8^+CD4^-$ cells in PBL.* ***(C)*** *Percentage of $CD8^-CD4^+$ cells in PBL.* ***(A-C)*** *Each symbol represents data from an individual mouse. n = 5 for Wt (+/+), 14 for heterozygotes (+/-) and 8 for homozygous (-/-) Vulpo mutants (left column). n = 3 for wt, 7 for heterozygotes and 17 for homozygous Zerda mutants (right column). Error bars represent mean ±1 SD. A nonparametric unpaired t test (two-tailed) was applied: *** $p < 0.001$, ** $p < 0.01$, * $p < 0.05$, ns=not significant. Graphs are representative of at least 2 independent experiments.*

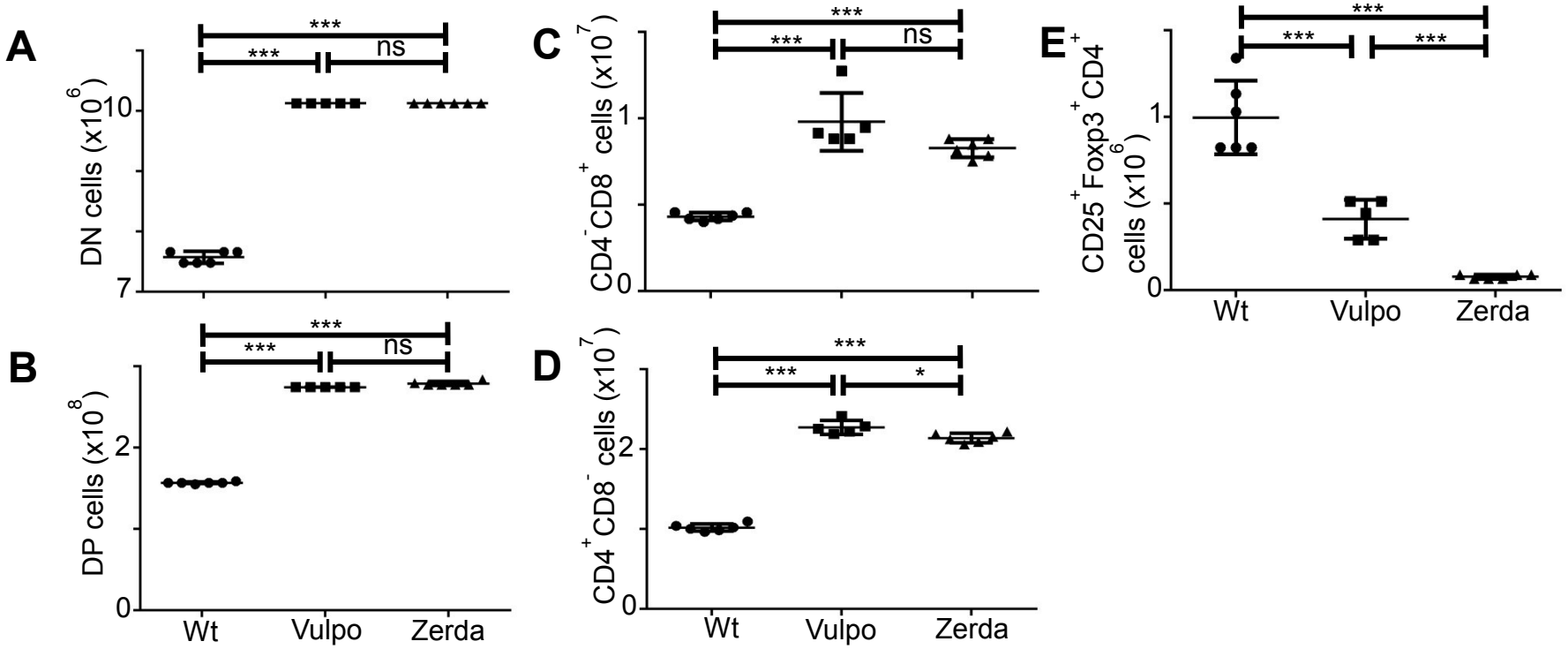


Figure 2.1-3: vulpo and zerda mutations affect all stages of thymocyte maturation.

Thymus dissection was performed in Wt, Vulpo and Zerda mutants. Graphs show absolute numbers for (A) $CD4^-CD8^-$ (DN), (B) $CD4^+CD8^+$ (DP), (C) $CD4^-CD8^+$, (D) $CD4^+CD8^-$ and (E) $CD25^+Foxp3^+CD4^+CD8^-$ thymocytes. Each symbol represents data from an individual homozygous mouse thymus: Wt (n=6), Vulpo (n=5) and Zerda (n=6). A non-parametric unpaired t test was applied to compare data sets.

**** $p < 0.001$, * $p < 0.05$, ns=not significant. Graphs are representative of 2 independent experiments.*

In the two-step model of nTreg cell development [25, 118, 126] (***Figure 1.5-1***), *vulpo* and *zerda* mutations affect both Treg precursor populations (***Figure 2.1-4***). Both mutations result in >70% reduction in frequency of proximal $CD4^+CD8^+FOXP3^+$ thymocytes compared to Wt ($p<0.01$) (***Figure 2.1-4A***) and >40% reduction in frequency of more distal $CD4^+CD25^+GITR^+FOXP3^-$ thymocytes compared to Wt ($p<0.05$) (***Figure 2.1-4B***). No significant difference is observed between the two mutants. *vulpo* & *zerda* mutations therefore block the initial TCR/CD28-mediated induction of ɣc-cytokine-responsive $FOXP3^-$ Treg precursor cells from immature thymocytes.

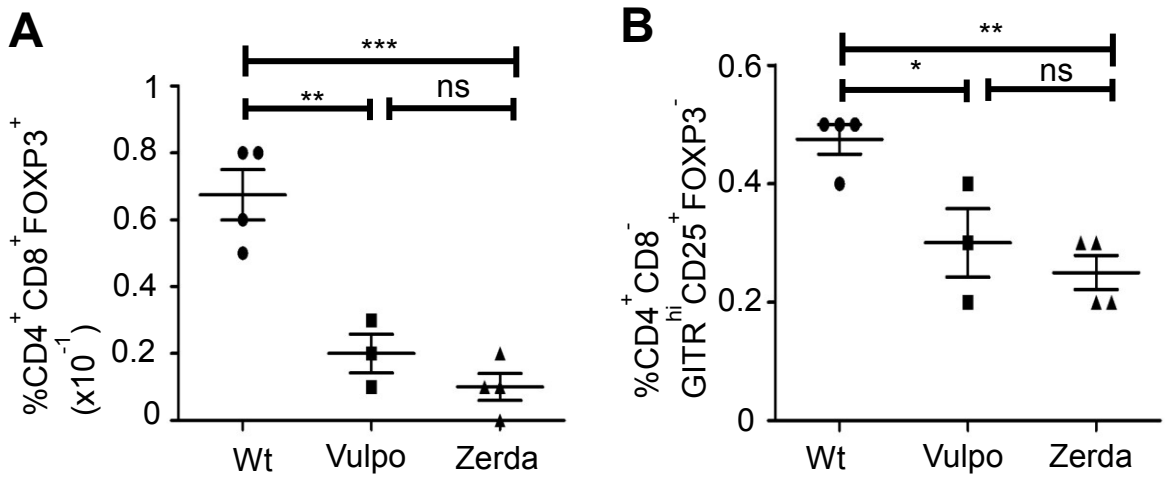


Figure 2.1-4: vulpo and zerda mutations affect nTreg precursor cell development in the thymus

(A) *Percentage of $CD4^+CD8^+$ $FOXP3^+$ precursor cells.* ***(B)*** *Percentage of $CD4^+CD25^+GITR^+$ $FOXP3^-$ precursor cells. Each symbol represents data from an individual mouse. Thymocytes from Wt (n=4), Vulpo (n=3) and Zerda (n=4) homozygous mutants were analysed. An unpaired parametric t test (two-tailed) was applied: *** $p < 0.001$, ** $p < 0.01$, * $p < 0.05$. Each graph is representative of 2 independent experiments.*

2.2 Dominant mutations Vulpo and Zerda impair iTreg development

Next I examined the effects of *vulpo* and *zerda* mutations on iTreg differentiation *in vitro*. Naive $CD4^+$ T cells were stimulated with increasing concentrations of plate-bound anti-CD3 and anti-CD28 monoclonal antibodies (mAb) for 3 days in the presence of IL-2 and TGF-β to generate iTreg ($FOXP3^+CD8^-CD4^+$) cells [140]. The upregulation of FOXP3 in Wt naive $CD4^+$T cells correlates positively with anti-CD3 dose up to 0.5μg/ml but is reduced in Vulpo ($p<0.05$) and Zerda ($p<0.05$) cells (***Figure 2.2-1***). At higher TCR stimulation (doses of anti-CD3 >0.5μg/ml), I observe progressive impairment of iTreg differentiation in Wt cells, as previously reported [141], as well as Vulpo and Zerda cells (***Figure 2.2-1***). I conclude that *vulpo* and *zerda* mutations impede iTreg differentiation. No difference was observed between Vulpo and Zerda iTreg differentiation ($p=0.3$).

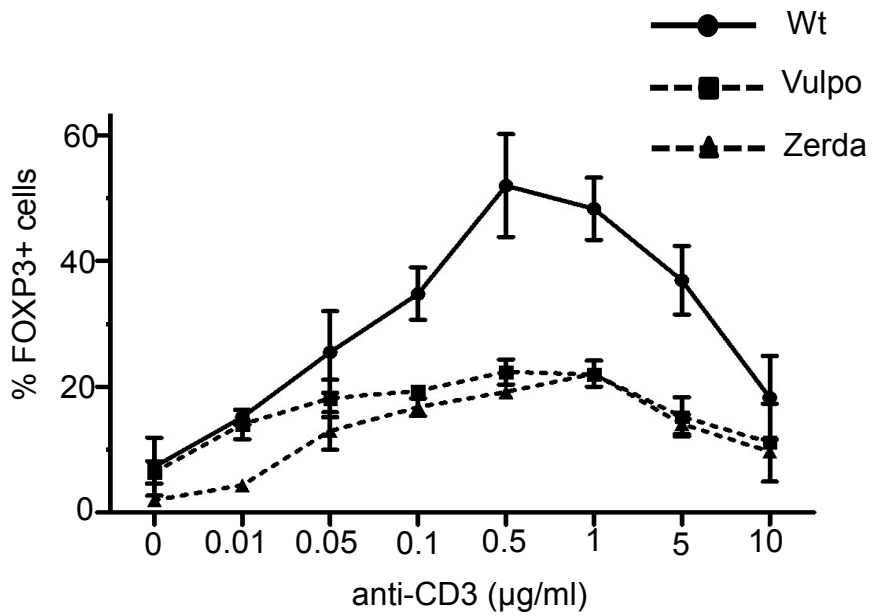


Figure 2.2-1: vulpo and zerda mutations affect iTreg differentiation in the periphery.

FACS-sorted, naive $CD4^+$ splenocytes were stimulated with plate-bound anti-CD3 mAb (0-10µg/ml) and anti-CD28 mAb (1µg/ml) for 3 days in the presence of IL-2 and TGF-β. The percentage of $FOXP3^+$ iTreg cells was then measured for Wt, Vulpo or Zerda by intracellular flow cytometry. Shown are mean values ± 1SD from 3 replicates in 2 independent experiments. A parametric unpaired t test was applied to compare data sets: Wt versus Vulpo p=0.04; Wt versus Zerda p=0.02; Vulpo versus Zerda p=0.3, not significant.

2.3 *vulpo* & *zerda* are point mutations in the *carma1* gene

Given the similar nature of both mutant phenotypes, initial genotyping work was performed on Vulpo. Using a meiotic positional cloning strategy [133], the *vulpo* mutation was mapped to a 20 mega-base pair (Mbp) region on chromosome 5, bounded by markers 128944450 and 149044358, with a Logarithm of Odds (LOD) score of 7.2 ($p<0.001$) (***Figure 2.3-1***).

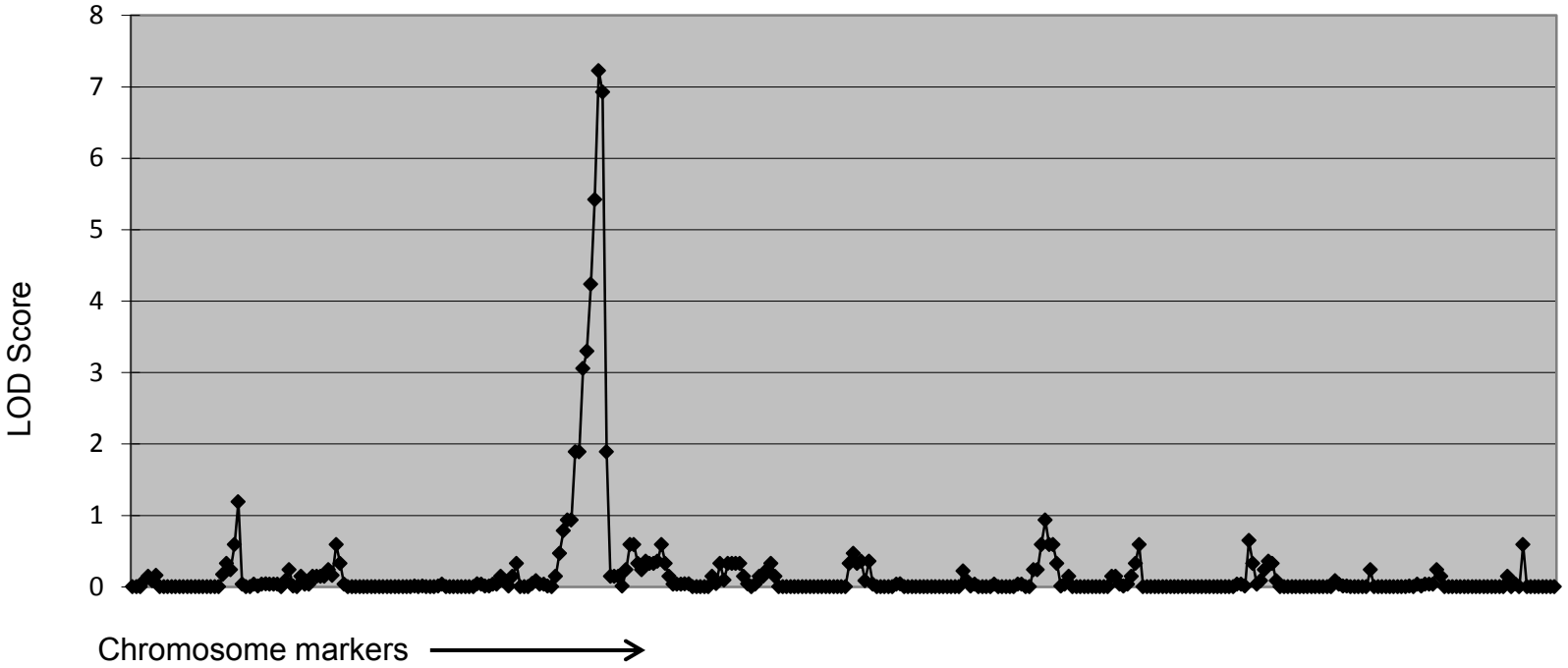


Figure 2.3-1: vulpo and zerda are point mutations in the carma1 gene.

The vulpo mutation was mapped to a 20Mbp region on chromosome 5, bound by markers 128944450 and 149044358, with a LOD score of 7.2 ($p<0.001$).

A search of the corresponding published gene list (Ensembl.org) revealed 317 candidate genes including *caspase recruitment domain family, member 11 (card11)* - more commonly known as *carma1* - which maps to chromosome 5, base pairs 141348953-141476550. Using previously identified *carma1* primers (***Appendix 1***), DNA prepared from both Vulpo and Zerda mutants was amplified by polymerase chain reaction (PCR) and sequenced. The resulting sequences were compared to the reference *carma1* sequence and point mutations identified in exon 4 of the *carma1* gene for both *vulpo* (C→G at base 92061) and *zerda* (T →A at base 92108) mutations. These mutations translate into the substitution of Wt hydrophobic Isoleucine for mutant hydrophobic Methionine at αα79 (I79M) for *vulpo* and the substitution of Wt hydrophobic Leucine for positively-charged Glutamine at αα95 (L95Q) for *zerda* (***Figure 2.3-2A***). Both mutations affect the Caspase Recruitment Domain (CARD) (αα15-105) of the CARD-MAGUK1 (CARMA1) protein (***Figure 2.3-2B***): an αα sequence conserved across mouse and human species [127].

As newly identified alleles of a known gene, homozygous mutants are hereafter referred to as *Carma1*$^{vul/vul}$ and *Carma1*$^{zer/zer}$.

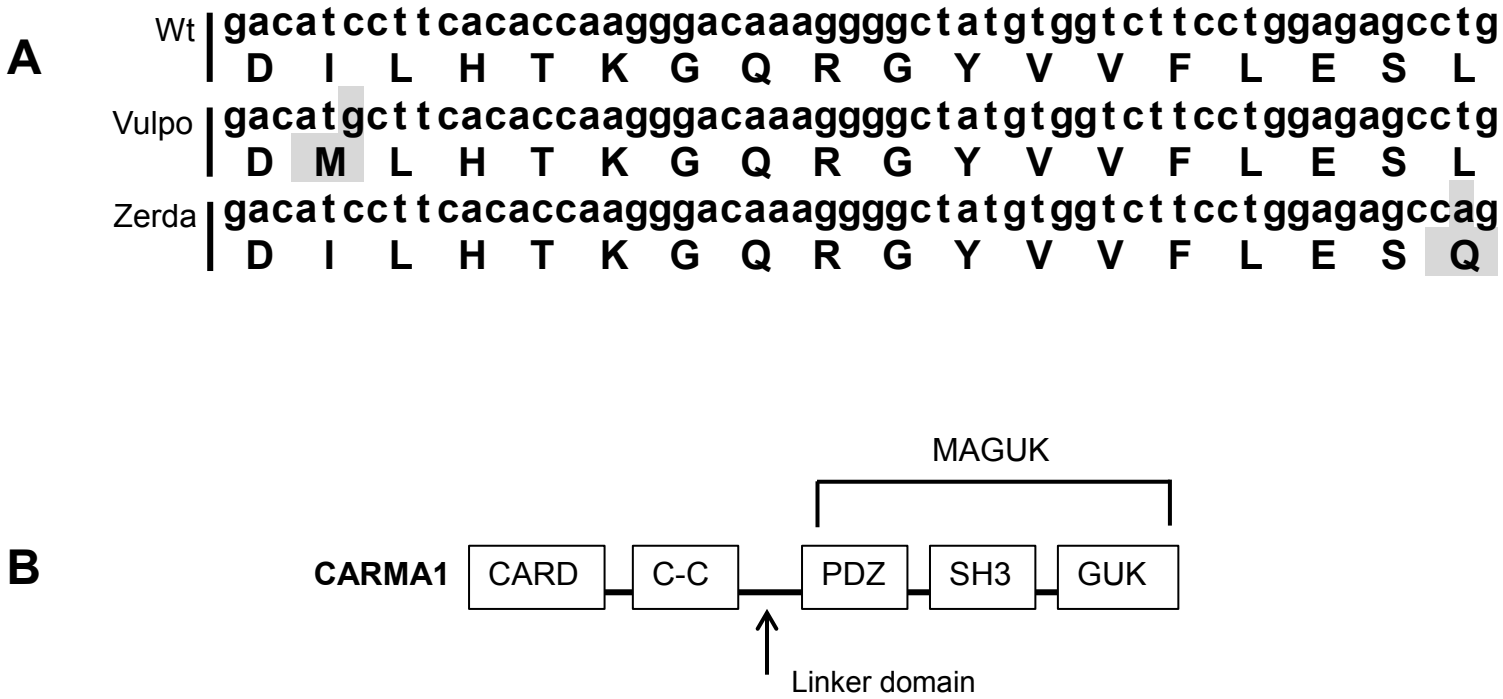


Figure 2.3-2: vulpo and zerda point mutations translate into single amino acid substitutions in the CARD of the CARMA1 protein.

(A) *Point mutations in exon 4 of the carma1 gene from vulpo (C→G at base 92061) and zerda (T→A at base 92108) mutant mice, and corresponding αα substitutions at position 79 (I79M) for vulpo and position 95 (L95Q) for zerda.* ***(B)*** *The structure of the CARMA1 protein. Functional domains: CARD, caspase recruitment domain (residues 15-105); C-C, coiled-coil domain (residues 116-439); MAGUK, membrane-associated guanylate kinase (GuK)-like domain made up of a PDZ domain (residues 660-742), a Src homology 3 (SH3) domain (residues 766-834), and a guanylate kinase (GuK)-like domain (residues 954-1142). The C-C domain and MAGUK region are connected by a region of 232 amino acids designated the linker domain (residues 440-671). vulpo and zerda mutations are located in the CARD of the CARMA1 protein.* [40, 142].

2.4 *vulpo* and *zerda* mutations in the *carma1* gene do not affect CARMA1 protein expression

Western blotting revealed Wt levels of CARMA1 protein expression in the thymi of both *Carma1*$^{vul/vul}$ and *Carma1*$^{zer/zer}$ mutant mice. Thus, neither CARD mutation affects CARMA1 protein stability (***Figure 2.4-1***).

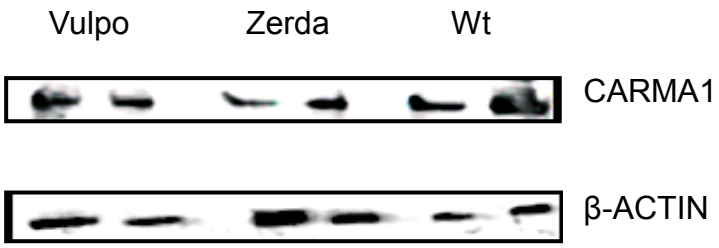


***Figure 2.4-1: Carma1$^{vul/vul}$* and *Carma1$^{zer/zer}$* mutants express wild-type levels of CARMA1 protein in the thymus.**

Western blot analysis of protein expression in homozygous Vulpo, Zerda and Wt thymus lysates using anti-CARMA mAb (top panel) and anti-ACTIN mAb (lower panel). Two independent samples are shown for each phenotype. This figure is representative of 3 independent experiments.

2.5 *Carma1*$^{vul/vul}$ & *Carma1*$^{zer/zer}$ mice do not develop spontaneous autoimmunity

Given the significantly reduced nTreg and increased Tconv cell populations in the periphery (***Figure 2.1-2***), it was initially surprising that *Carma1*$^{vul/vul}$ and *Carma1*$^{zer/zer}$ mice remained healthy at 1 year and showed no macroscopic signs of spontaneous autoimmune disease upon examination e.g. weight loss, red eyes, dermatitis, spontaneous abortion, or splenomegaly. Both homozygous mutants demonstrated Wt levels of circulating anti single-stranded (ss) DNA IgG antibodies, 90% less than MRL/Mp.*lpr/lpr* positive-control mice at 1 year ($p<0.005$) (***Figure 2.5-1***). These results are consistent with published findings in CARMA1-knockout (KO) mice, which demonstrate no overt autoimmunity despite the complete absence of nTregs and normal development of Tconv cells [36, 143, 144].

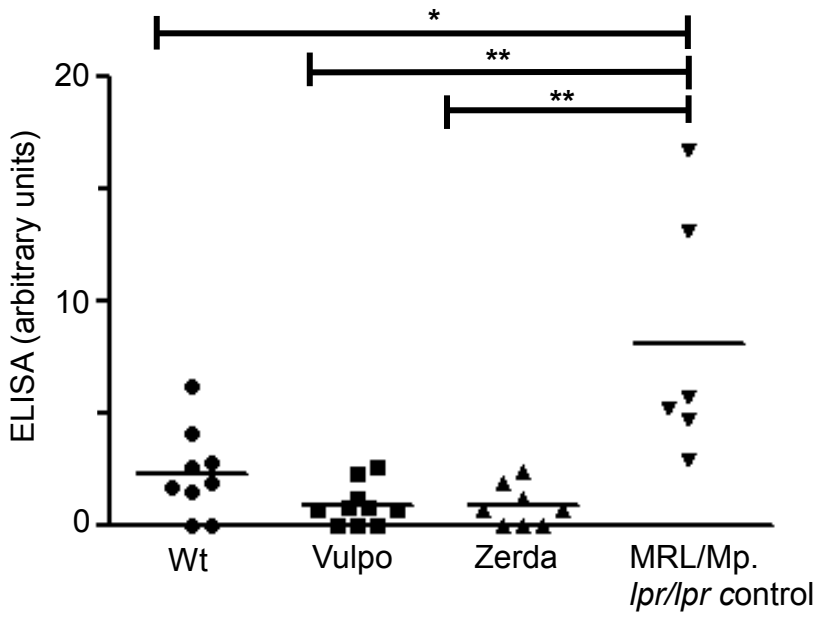


Figure 2.5-1: Vulpo and Zerda mutant mice do not develop autoimmunity.

*Enzyme-linked immunosorbent assay (ELISA) for serum anti-ssDNA IgG auto-antibodies in 1 yr-old Wt (n=8), Vulpo (n=10), Zerda (n=8) and MRL/Mp.lpr/lpr positive control (n=6) female mice. The Ab levels are expressed in arbitrary ELISA units related to a standard positive sample, which was assigned a value of 10 arbitrary units. Serum samples were screened at 1/80 and positive samples titrated to endpoint. Each symbol represents data from 1 mouse. Horizontal bars indicate the mean. Data were analysed using a nonparametric unpaired t test (two-tailed): ** $p < 0.01$, * $p < 0.05$. This graph is representative of 2 independent experiments.*

Failure to develop autoimmunity in CARMA1-KO mice was found to be due to impaired activation of Tconv cells as a result of intrinsic signalling defects [36]. I measured the activation of Tconv cells from *Carma1*$^{vul/vul}$ and *Carma1*$^{zer/zer}$ mice. The percentage of *Carma1*$^{vul/vul}$ CD4^{+} T cells expressing an activated phenotype (CD69^{+}CD44^{+}CD25^{+}CD62L^{low}), increased 1.5-fold in response to anti-CD3/CD28 stimulation, (p=0.03) compared to a 2.3-fold increase in the percentage of activated Wt CD4^{+} T cells (p=0.00004) (***Figure 2.5-2***). The activation of CD4^{+} T cells from *Carma1*$^{zer/zer}$ mutants was even more impaired, as evidenced by the complete absence of activation following TCR stimulation (p<0.0001) (***Figure 2.5-2***). A similar effect was observed in mutant CD8^{+} T cells from both *Carma1*$^{vul/vul}$ and *Carma1*$^{zer/zer}$ mice (data not shown). These findings suggest that *Carma1*$^{vul/vul}$ and *Carma1*$^{zer/zer}$ mice, like CARMA1-KO mice, harbour a generalised TCR/CD28 activation defect in their peripheral Tconv cells, which would explain their lack of autoimmunity despite minimal nTregs. The blockade in mature nTreg development was more pronounced in *Carma1*$^{zer/zer}$ compared to *Carma1*$^{vul/vul}$ mutants (***Figure 2.1-3***) and we also observe a corresponding increase in the degree of impairment of TCR activation in Tconv cells from *Carma1*$^{zer/zer}$ compared to *Carma1*$^{vul/vul}$ mutants (***Figure 2.5-2***).

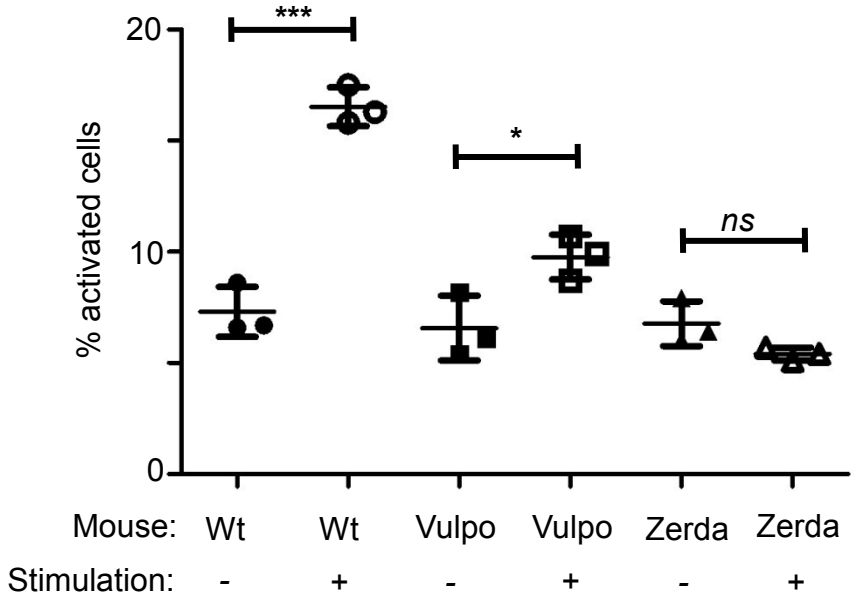


Figure 2.5-2: Vulpo and Zerda mutant mice harbour non-reactive Tconv cells.

*Percentage of activated ($CD69^+CD44^+CD25^+CD62L^{low}$) $CD4^+$ T cells before (-) and after (+) stimulation with plate-bound anti-CD3 and anti-CD28 mAbs for 2 days in Wt, Vulpo and Zerda mutant mice. Data were analysed using a nonparametric unpaired t test (two-tailed): *** $p < 0.001$, * $p < 0.05$, ns = not significant. This graph is representative of four independent experiments in which $CD4^+$ T cell activation was analysed in triplicate with samples pooled from 5 mice per genotype. Black error bars represent mean ±1 SD. Similar results are achieved upon stimulation of mutant peripheral $CD8^+$ T cells (data not shown).*

2.6 *vulpo* & *zerda* mutations disrupt the CARMA1/Bcl-10 association upon TCR activation

Upon TCR activation, CARMA1 recruits the preformed Bcl-10 – mucosa-associated lymphoid tissue lymphoma translocation protein 1 (MALT1) complex to the immunological synapse and, based on extrapolated findings from non-Treg cell studies *in vitro*, CARMA1 is thought to bind with Bcl-10 via the CARD [127, 128] (***Figure 2.6-1***). The C-terminal caspase-like domain of MALT1 then interacts directly with the coiled-coil (C-C) domain of CARMA1 [145] (***Figure 2.6-1***). No other proteins are known to interact with the CARD of CARMA1.

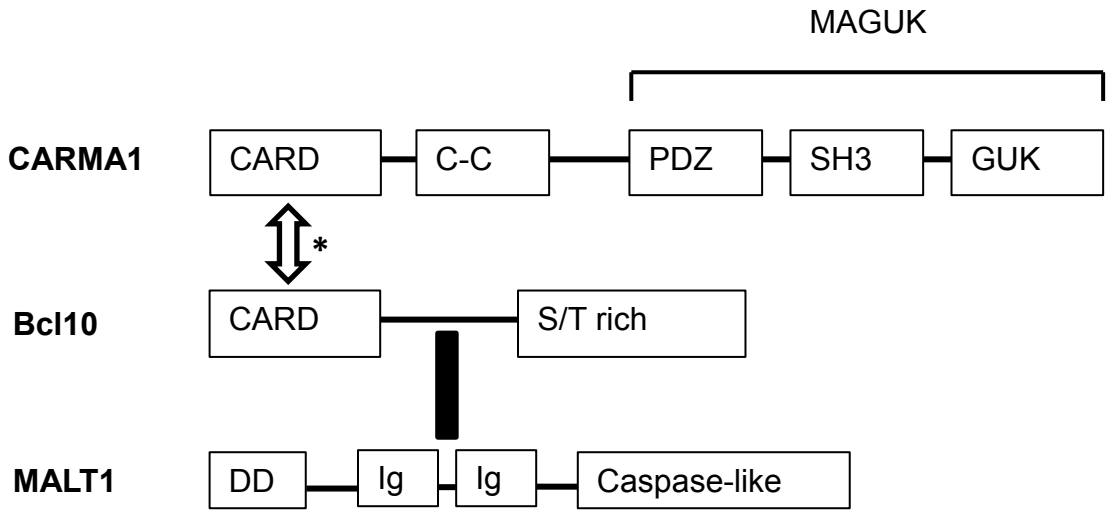


Figure 2.6-1: The structures of CARMA1, Bcl-10 and MALT1 proteins.

Upon TCR activation, CARMA1 recruits the preformed Bcl-10-MALT1 complex to the immunological synapse. ******* *Based on extrapolated findings from non-Treg cell studies in vitro, this is thought to be via a CARMA1-CARD: Bcl-10-CARD interaction* [127, 128]*. MALT1 contains two immunoglobulin (Ig)-like domains that mediate binding to Bcl-10 by means of a motif comprising a short stretch of amino acids following the CARD* [146]*. The C-terminal caspase-like domain of MALT1 is then thought to interact directly with the coiled-coil (C-C) domain of CARMA1* [145]*. DD, Death domain; S/T rich, Ser/Thr-rich domain.*

To examine the effects of *vulpo* and *zerda* CARD mutations on the ability of CARMA1 to recruit Bcl-10 after TCR/CD28 activation, I used immunoprecipitation studies. Using phorbol 12-myristate 13-acetate (PMA)/ionomycin-activated splenic $CD4^+$ T cells, I quantified the amount of CARMA1 protein co-immunoprecipitating with anti-Bcl-10 antibody by western blot, in $Carma1^{vul/vul}$ and $Carma1^{zer/zer}$ versus Wt cells (***Figure 2.6-2***). As expected, Bcl-10 interacts with CARMA1 in Wt but not $Carma1^{vul/vul}$ and $Carma1^{zer/zer}$ activated $CD4^+$ T cells (***Figure 2.6-2***). These results suggest that the mutations in the CARD of both CARMA1-*vulpo* and CARMA1-*zerda* proteins prevent association with Bcl-10 after TCR stimulation.

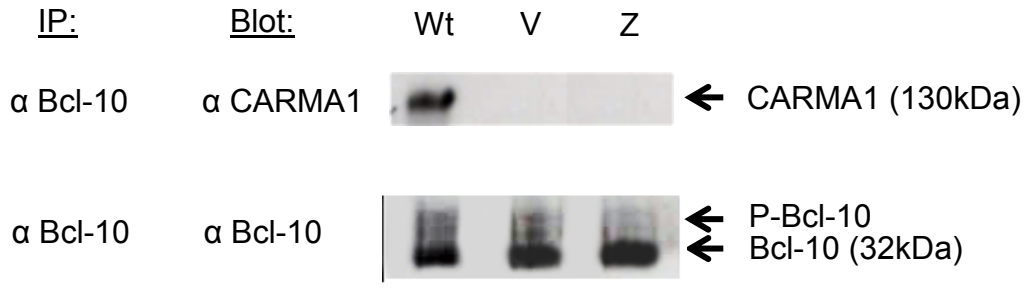


Figure 2.6-2: Impaired interaction of mutant CARMA1 proteins with Bcl-10.

Bcl-10 protein was immunoprecipitated from PMA/ionomycin-activated $CD4^+$ T cells then resolved by SDS-PAGE, electrophorectically transferred and blotted with antibodies specific for CARMA1 (top panel) or Bcl-10 (lower panel). Shown are lanes for Wt, $Carma1^{vul/vul}$ (V) and $Carma1^{zer/zer}$ (Z) cells. CARMA1 runs at 130kDa. Bcl-10 runs at 32kDa. Two additional, fainter bands are seen above Bcl-10 in each lane. Bcl-10 is known to be mono- and bi-phosphorylated upon lymphocyte activation [147]. These phosphorylated Bcl-10 species (P-Bcl10) migrate slightly slower than Bcl-10 itself and are commonly observed immediately above the 32kDa Bcl-10 band [148].

Chapter 3: Discussion

3.1 Discussion and conclusions

The balance of Treg cells and Tconv cells is key to immune homeostasis. This study emphasises the role of CARMA1 at the fulcrum. I report two new mutant mice, Vulpo and Zerda, with a profound block in the development of nTregs in the thymus, as well as impaired iTreg differentiation in the periphery. Despite being independently derived, the mutants harbour different point mutations in the CARD motif of the crucial scaffold protein, CARMA1. The level of CARMA1 is not affected in *Carma1*$^{vul/vul}$ or *Carma1*$^{zer/zer}$ mice but rather the mutant CARMA1 proteins are impaired in their ability to recruit Bcl-10 after TCR stimulation. For the first time, these findings provide genetic and *in vivo* evidence of a critical role for the CARD of the CARMA1 protein in nTreg development in the thymus, as well as *in vitro* evidence to augment our understanding of its role in iTreg differentiation in the periphery.

CARMA1 (also known as CARD11) belongs to the MAGUK family of proteins that function as molecular scaffolds to assist recruitment and assembly of signalling molecules in the cytoplasmic membrane [149]. Scaffold proteins have no enzymatic activity [150]. In addition to the N-terminal CARD motif, CARMA1 contains several protein-protein interaction domains including a coiled-coil (C-C) domain, a PDZ domain, a SH3 domain, and a GuK-like domain ***(Figure 2.6-1)*** [40, 142]. The structural arrangement of PDZ, SH3, and GUK domains is also called the MAGUK domain. The C-C domain and MAGUK region are connected by a region of 232 amino acids designated the linker domain. Two other mammalian homologs exist: CARMA2 (also known as CARD14 or Bimp2) and CARMA3 (also known as CARD10 and Bimp1). They share a high degree of sequence and structural homology with CARMA1 [142, 151, 152]. All three CARMA proteins exhibit a distinct tissue distribution pattern with CARMA1 being predominantly expressed in hematopoietic tissues such as spleen, thymus and PBLs [142];

CARMA2 is expressed only in placenta; and CARMA3 is expressed in a broad range of tissues but not in hematopoietic cells [151, 152]. This distinct tissue distribution suggests that CARMA family members may have the same function and play similar roles in different tissues [153]. Consistent with this hypothesis, ectopic expression of CARMA3 in CARMA1-deficient T cells effectively rescues the defect in TCR-induced NF-κB activation [154].

nTreg development is known to require an intricate set of signalling events, most notably engagement of the TCR and stimulation by IL-2 [25]. The TCR and IL-2 signals regulate the generation of nTreg precursors and their subsequent maturation, respectively [118, 126]. Activation of the transcription factor NF-κB pathway is known to be particularly important in nTreg development, more so than for Tconv cells, as deficits in elements linking the TCR to NF-κB have proven deleterious for Treg development [29]. Mice with conditional knockout of protein kinase C theta (PKC-θ), Bcl-10, CARMA1 or IKK2 are deficient in nTregs [36, 144, 155] and prior to my work, CARMA1 was already thought to play a Treg cell-intrinsic role in both the initial TCR/CD28 activation step and the subsequent IL-2 receptor signalling maturation step of nTreg development [36, 156].

In brief, TCR/CD28 stimulation of immature thymocytes by MHC class II-peptide complexes on APCs induces the formation of the immunological synapse (IS). It is hypothesised that inactive CARMA1 exists in an autorepressed conformation [157]. The linker region between the C-C and MAGUK domains blocks the homotypic interaction of the CARD motifs by binding to the N-terminus of CARMA1 [158]. Upon ligation of the TCR and CD28 co-receptor, CARMA1 is recruited to the IS together with PKC-θ which mediates a series of phosphorylation events in the linker region of CARMA1 between the C-C and PDZ domains, reducing intramolecular affinity for the CARD domain [144]. This liberates the CARD and

coiled-coiled domains, enabling B cell CLL/lymphoma 10 (Bcl-10) and mucosa associated lymphoid tissue lymphoma translocation gene 1 (MALT1) recruitment, and CARMA1-Bcl10-MALT1 (CBM) signalling complex formation [154, 159]. The CC domain of CARMA1 is thought to mediate oligomerisation and association with the preformed Bcl10-MALT1 complex, which appears to be constitutively expressed in the cytoplasm [160]. The C-terminal caspase-like domain of MALT1 also binds directly to the C-C domain of CARMA1 in a Bcl-10 independent manner and so, MALT1, Bcl-10 and CARMA1 form a tri-molecular complex [145]. The function of the MAGUK domain remains unclear; however, mutation studies suggest that the SH3 domain regulates the membrane localisation of CARMA1 [161].

The CBM complex recruits TNF receptor-associated factor 6 (TRAF6) that catalyses the ubiquitination of itself and MALT1, and these ubiquitin chains provide the docking sites for TGF-β activated kinase 1 (TAK1) and the inhibitor of NF-κB (IκB) kinase (IKK) complex recruitment [162]. The NF-κB inhibitor, IκBα, is then degraded, unmasking the nuclear localisation sequence of NF-κB which can then be rapidly translocated into the nucleus to begin transcription of its target genes [153]. The NF-κB subunit c-Rel has been shown to bind to enhancer sequences located in the promoter and third intron of the Foxp3 gene, and plays a direct role in Foxp3 expression during Treg cell development [39, 163-165]. In addition to phosphorylating IKKβ leading to the activation of NF-κB, TAK1 also phosphorylates mitogen-activated protein kinase kinase (MAP2K) which in turn activates the JNK signalling pathway [166]. c-Jun is the main target of the JNK signalling pathway [167], and forms a heterodimer with activating transcription factor (ATF) 2 to activate transcription of FOXP3 [168].

As I mention earlier in this thesis, two precursor populations of thymic Tregs have been described. The most proximal $CD4^+CD8^+Foxp3^+$ thymocyte population can develop into mature nTreg cells if transferred into recipient hosts [125]. The more distal $CD4^+CD25^+CD122^+GITR^+$ precursor cell population lacks FoxP3 expression until exposed to IL-2 without further TCR stimulation [126]. Whether the proximal precursor gives rise to the distal one prior to mature Treg cell generation is not known. In 2009, Molinero *et al* published their observations that the CARMA1 protein is required for the development of both these known Treg precursor cell populations via the TCR-CBM-NF-κB axis, and therefore suggested that CARMA1 was unlikely to also play a role in the second IL-2 -dependent step of $Foxp3^-$ nTreg precursor cell maturation in to mature nTreg cells [36]. But, later that year Lee *et al* revealed a critical role for CARMA1 in regulating the IL-2-stimulated maturation of $CD4^+CD25^+CD122^+GITR^+Foxp3^-$ nTreg precursor cells [156], and showed that IL-2 stimulates strong tyrosine phosphorylation of STAT5 in Wt thymocytes but not $CARMA1^{-/-}$ thymocytes [156]. STAT5 is known to have binding sites within the *Foxp3* promoter [116, 121]. They showed that this signalling defect was unlikely due to the blockade of typical NF-κB activation because competent IL-2 receptor signalling was detected in IκBαΔN transgenic thymocytes despite their lack of NF-κB activation [156].

To-date, it has always been assumed that in the process of nTreg development, CARMA1 and Bcl-10 interact via their CARD motifs. This assumption is based on results from co-transfection studies in unstimulated, non-Treg cell lines [127, 128, 151, 152, 161, 169] and TCR stimulation with non-physiological ligands in murine Tconv cells [148]. In 2003, Newton & Dixit generated knock-in mice expressing a CARD-less form of CARMA1 but the impact of this mutation on the specific Bcl-10: CARMA1 interaction was never reported [170]. In addition to CARMA1-KO mice [36, 143, 171, 172], two other CARMA1 mutant mice have been described:

Unmodulated mice which have a L298Q substitution in the C-C domain [173] and *Carma1*$^{king/king}$ mice which have a L525G substitution in the linker domain [144]. The CARMA1-*king* protein is degraded due to instability [144] and *Unmodulated* mice develop intense dermatitis and atopy by 10 weeks of age [173]. By definition, not one of these mutants is able to provide *in vivo* evidence of CARD-CARD binding of CARMA1 and Bcl-10 in nTreg cell development. For the first time, I show that the CARD of CARMA1 is required for TCR-mediated signals triggered by physiological self-MHC ligands in thymic nTreg development.

I present two new, *in vivo* models, Vulpo and Zerda, both expressing Wt levels of mutant CARMA1 protein. These mutants remain healthy at 1 year, do not develop spontaneous autoimmune disease and have allowed the identification of critical residues in the CARD that mediate CARMA1 function in T cell activation and Treg development. Using co-immunoprecipitation studies to examine the CARMA1: Bcl-10 interaction in activated $CD4^+$ T cells from Vulpo and Zerda mutant mice, I demonstrate complete impairment of CARMA1: Bcl-10 binding in both mutants. I believe that this experiment in which I resolve by SDS-PAGE and electrophorectically transfer a range of Bcl-10 protein concentrations up to a maximum of 500μg/ml total protein, probe with maximum concentration anti-CARMA1 mAb [1:1000] and then incubate with protein A-HRP in place of secondary Ab for improved protein detection avoiding heavy and light chain signals [174], prior to film exposure for up to 3 hours, gave me the best opportunity to detect any difference in CARMA1: Bcl-10 binding between Vulpo and Zerda mutants. I found none. I did not repeat the experiments using heterozygote mice because this would not affect the affinity of mutant CARMA1 for a binding partner but would rather just increase the amount of Wt CARMA1 protein binding. Therefore, I conclude that, as far as I can observe, the *vulpo* and *zerda* CARD mutations both completely impair the association of Bcl-10 with CARMA1.

Given that downstream NF-κB and JNK signalling is completely dependent on CARMA1: Bcl-10 binding in thymic nTreg development, I use CARMA1: Bcl-10 binding as an analogue for NF-κB and JNK signalling after TCR stimulation and conclude that *carma1-vulpo* and -*zerda* mutations, like *Bcl-10*$^{-/-}$ *and carma1*$^{-/-}$ mutations [36, 144, 155], result in complete downstream impairment of NF-κB and JNK signalling in nTreg cell development. In the two-step model of nTreg cell development, I demonstrate a role for the CARD of CARMA1 in the TCR/CD28-mediated induction of γc-cytokine-responsive FOXP3$^-$ nTreg precursor cells from immature thymocytes.

I observe significant differences in the frequency of mature FOXP3$^+$ nTregs (***Figure 2.1-3***), and also in Tconv cell activation (***Figure 2.5-2***), between Vulpo and Zerda mutants. In both cases, the *zerda* mutation results in a more profound phenotype. Despite this, both mutations result in complete impairment of Bcl-10: CARMA1 binding and presumed downstream NF-κB and JNK signalling during nTreg cell development. Therefore, I conclude that my findings suggest a Bcl-10-independent role for the CARD of CARMA1 in TCR signalling during nTreg development. CARD motifs are characterized by their conserved structures containing six helices [158]. They possess acid and basic patches on different sides and the interaction of CARDs requires amino acids with opposite charges [158]. Unlike the I79M *vulpo* mutation, the L95Q *zerda* mutation results in an amino acid charge change from hydrophobic Leucine to positively-charged Glutamine in the CARD and it is likely that this charge change is responsible for the more severe phenotype observed in Zerda compared to Vulpo mutant mice, through as yet unknown alterations in protein: protein interactions. In addition to its role in the NF-κB and JNK pathway-mediated generation of FOXP3$^-$ nTreg precursor cells from immature thymocytes, CARMA1 has recently been shown to play a critical role in the IL-2R signalling pathway-mediated maturation of these precursor cells into mature FOXP3$^+$ nTregs

[156]. How the CARMA1 protein is integrated into this pathway to drive these events is yet to be defined. I suggest that the CARD of CARMA1 facilitates this IL-2R-mediated maturation stage of nTreg development, and that it is the different effects of *vulpo* and *zerda* mutations on this role that accounts for the differences observed between their phenotypes.

To the best of my knowledge, *vulpo* and *zerda* mutations only affect the amino acid sequence of the CARD of CARMA1. Since the CARD motifs are protein interaction modules, their surface features dictate their mode of interactions with their binding partners and my results suggest that *vulpo* and *zerda* mutations impair CARMA1's CARD interaction with its binding partner. However, I recognise that it is a formal possibility that the mutations that affect CARD function may also alter the conformation of non-CARD domains in CARMA1.

In contrast to the high dependency on TCR-CARMA1-NFκB activity for thymic development of nTregs and their precursors, TCR-CARMA1-NFκB activity is thought to be dispensable for iTreg induction in the periphery [144]. In agreement with published findings in CARMA1-KO cells [36, 144, 155], Vulpo and Zerda CARMA1 mutants retain some differentiation of naive $CD4^+$ T cells into iTregs at low dose TCR stimulation, supporting a role for the CARMA1-independent TGFβ-TAK1-JNK signalling pathway in iTreg differentiation. TGFβ does not play a role in the thymic selection of nTregs and so, we assume nTreg precursors are dependent on CBM-TRAF6 for TAK1 activation [29]. However, as observed in CARMA1-KO cells [140], *Carma1*$^{vul/vul}$ and *Carma1*$^{zer/zer}$ $CD4^+$ T cells are less sensitive to increasing concentrations of anti-CD3 and upregulate FOXP3 less rapidly when compared to Wt naive $CD4^+$ T cells. I suggest that despite adequate CARMA1-independent TGFβ-TAK1-JNK signalling, the increased sensitivity offered by the anti-CD3 dose-dependent induction of TCR-CARMA1-NFκB/JNK activity in Wt $CD4^+$ T cells is absent in *Carma1*$^{vul/vul}$ and

Carma1$^{zer/zer}$ CD4^{+} T cells, as well as CARMA1-KO cells. I propose that TCR-CARMA1-NFκB activity is only partially dispensable for iTreg induction at low dose TCR stimulation in the periphery.

Strong TCR stimulation prevents conversion of naive T cells into iTregs and overrules the ability of TGFβ/IL-2 to drive FOXP3 expression[141], although the molecular mechanisms by which FOXP3 expression is inhibited are not well understood. Of note, TAK1 overexpression has recently been shown to restrain CARMA1-dependent activation of NF-κB by reducing Bcl-10 levels which may be relevant [166]. CARMA1-KO CD4^{+} T cells are partially resistant to this high-dose TCR-mediated inhibition of iTreg differentiation suggesting that NF-κB abrogates FOXP3 induction upon high TCR stimulation[140]. In contrast *Carma1*$^{vul/vul}$ and *Carma1*$^{zer/zer}$ CD4^{+}T cells retain sensitivity to this high TCR-induced abrogation of iTreg differentiation. These data support the view of Molinero *et al* [140] that high-dose TCR-mediated inhibition of iTreg differentiation is at least in part NF-κB dependent, but I propose that this negative regulation is not via the conventional CARD-dependent TCR-CBM-NFκB axis but via a novel MAGUK region-dependent TCR-protein kinase C-delta (PKCδ)-CARMA1 signalling pathway [175]. Endogenous PKCδ has recently been shown to be recruited to the MAGUK region of CARMA1 after CD3/CD28 costimulation in a dose-dependent manner where it inhibits the interaction between MALT1 and TRAF6, but not the association of CARMA1 with PKCθ, Bcl-10 or MALT1 [175]. Unlike CARMA1-KO cells, the MAGUK region of CARMA1 is preserved in CARMA1-*vulpo* and CARMA1-*zerda* proteins and so I predict that PKCδ-mediated inhibition of TCR signalling remains intact in Vulpo and Zerda CARD mutants.

Therapeutic targeting of the conserved canonical NF-κB signalosome is difficult due to its ubiquitous functions and multiple inputs. By contrast, due to its non-redundant role in antigen-receptor activation and its specificity to signals from the antigen-receptors, CARMA1 is a unique and appealing target for the design of therapeutic interventions that promote immune tolerance. For the first time, this work provides two healthy *in vivo* models, Vulpo and Zerda, in which to further study the interactions of the CARMA1 protein with its binding partners and contribute to the goal of expounding the essential pathways required for Treg cell development.

3.2 Critique of Methods

Technological advances have changed how biological systems are studied and created scenarios where entire genomes can be sequenced in relatively short time frames. However, progress in understanding complex networks, and the functionality of their components has been far slower. Forward genetics is an extremely powerful tool because of its exploratory nature; with no bias or *a priori* knowledge required about the pathways involved in a process. In addition, ENU mutagenesis causes point mutations that can lead to amorphic, hypomorphic, hypermorphic, neomorphic, as well as conditional mutations; potentially obviating the pitfall of genetic redundancy or lethality. This variety of mutations far exceeds what is possible with biological mutagens, like T-DNA or transposons, which typically lead to amorphic alleles. Point mutations can also be informative with respect to the domain structure of the affected gene product, as is the case in this project.

However, this work also highlights some of the limitations of a forward genetic approach to gene identification. Seen by some as an expensive, labour- and animal- intensive, "scattergun" approach, the strength of forward genetics lies in the phenotypic screen which must be simple,

rapid (the process is often slow and laborious), reliable (based on strong wild-type phenotypes to reduce the number of false negatives) and the standard deviations for each parameter must be as small as possible so "cut off values" can be defined and the isolation of false positives minimised. Nevertheless, overlap of function is exceedingly common and many phenotypic differences prove to be polygenic, limiting the effectiveness of phenotypic screens [25]. When an isolated phenotypic mutation has been identified and confirmed to affect the germline, a stable mutant stock must be established and the job of genotyping commenced. The traditional positional cloning approach I used to genotype the Vulpo mutant phenotype can be criticised for being tedious and time-consuming and indeed, had this approach not worked, whole genome sequencing could have been performed in less time but at significant additional cost.

When I describe the forward genetic approach in my Introduction, I state "…genotyping and phenotyping are usually performed in parallel, until the identity of the affected gene is required for a more thorough in-depth phenotyping [133]." This is theoretically true but leads me to highlight the greatest hazard of forward genetics: the exploratory, unbiased nature of this approach will identify known, as well as novel, genes that are responsible for a given phenotype. Thus, extensive characterisation of a mutant phenotype prior to identification of the affected gene could prove to be an inefficient use of research funds. Although this project may be the first demonstration that mutations in the CARD of CARMA1 affect nTreg development *in vivo*, it could be argued that my findings are predictable based on prior studies of CARMA1-KO mice and *in vitro* assays of CARMA1 mutations. This detracts significantly from the novelty of my work.

Based upon my experience, I would suggest that the forward genetic approach to gene identification may be better suited to large scale operations and two such ENU mutagenesis centres are currently in operation at the Institute of Human Genetics in Munich, Germany and MRC Harwell, UK. These mutagenesis programmes generate and characterise a large and functionally diverse set of mouse mutant lines that go into multi-parameter phenotypic screening programmes looking for different dominant and recessive mutations on behalf of different research groups. Whilst this approach may be less "targeted", it generates a higher result yield with decreased outlay of labour, time and research funds.

3.3 Future work

In the two-step model of nTreg cell development, I demonstrate a critical role for the CARD of CARMA1 in the TCR/CD28-mediated induction of γc-cytokine-responsive $FOXP3^-$ Treg precursor cells from immature thymocytes, and I propose a new Bcl-10/JNK/NF-κB-independent role for the CARD of CARMA1 in the IL-2R-mediated maturation of $FOXP3^-$ Treg precursor cells into mature $FOXP3^+$ nTreg cells. Future characterisation of the IL-2R signalling pathway in the context of nTreg maturation, and confirmation of the proposed role for CARMA1 therein, are required in order to substantiate my hypothesis. Vulpo and Zerda mutant CARMA1 mice will allow determination of how CARD function influences IL-2R signalling in nTreg development.

To the best of my knowledge, *vulpo* and *zerda* mutations only affect the amino acid sequence of the CARD of CARMA1. Since the CARD motifs are protein interaction modules, their surface features dictate their mode of interactions with their binding partners and my results suggest that *vulpo* and *zerda* mutations impair CARMA1's CARD interactions with its binding partners. However, in my discussion, I recognise that it is a formal possibility that the

mutations that affect CARD function may also alter the conformation of non-CARD domains in CARMA1. To that end, in collaboration with experts from the Division of Molecular Biosciences, it would be pertinent to establish the effects of *vulpo* and *zerda* point mutations on the overall structure of CARMA1-Vulpo and CARMA1-Zerda mutant proteins in both activate and inactive states. Several online protein structure prediction tools exist e.g. "Phyre2" (http://www.sbg.bio.ic.ac.uk/phyre2/html/page.cgi?id=index) but obtaining and purifying CARD motifs *in vitro* for molecular analysis is known to be notoriously difficult due to their self-aggregation under physiological conditions and sensitivity to pH and salt concentration [176]. Aside from Bcl-10, no other proteins are known to interact with the CARD of CARMA1. For this reason, I did not study the effects of *vulpo* and *zerda* mutations on CARMA1's interactions with its other known binding partners such as MALT1 and TRAF6. However, insights into the overall effects of *vulpo* and *zerda* mutations on CARMA1 protein structure may prompt me to revisit this.

The supreme aim of this work was to identify novel genes responsible for the development of nTreg cells in the thymus. To that end, I did not study the effects of Vulpo and Zerda mutants on other cell lineages. However, CARMA1 is known to be expressed in all lymphoid cells [150, 170] and to play a role in the activation of B cells and natural killer cells, as well as T cells [150]. Recent work seems to suggest that CARMA9 plays the role of CARMA1 in myeloid cells [157]. Therefore, it would be interesting to analyse the effects of *vulpo* and *zerda* mutations on the frequency of these cells compared to Wt, by staining with appropriate conjugated mAbs followed by flow cytometric analysis.

Finally, we know that *Carma1*$^{vul/vul}$ and *Carma1*$^{zer/zer}$ mutant mice do not develop spontaneous autoimmune disease despite their lack of nTregs and increased frequency of Tconv cells. This

is explained by the generalised activation defect observed in their Tconv cells. With this in mind, it would be interesting to examine the response of *Carma1*$^{vul/vul}$ and *Carma1*$^{zer/zer}$ mutant mice to induced T cell-dependent autoimmune disease. However, selecting a disease model that would allow accurate conclusions to be drawn and enhance our understanding of the role of CARMA1 in immune homeostasis is difficult. Given my renal background, I briefly explored the possibility of using an accelerated nephrotoxic nephritis (NTN) model but the induced kidney inflammation is immune complex-mediated with complement, macrophages and receptors for the Fc portion of IgG playing a key role. Although it is considered a T helper 1 cell-mediated process, it would not allow me to test iTreg or antigen-specific T cell stimulation. The experimental autoimmune encephalomyelitis model is a T-cell mediated inflammatory process and may be a more appropriate disease model to study. Expert guidance is required.

Chapter 4: Materials and Methods

4.1 Materials

Reagent	Formulation
Ethylene diamine tetra-acetate (EDTA)	0.5M EDTA, pH 8.0
Phosphate Buffered Saline (PBS) (10x) pH 7.5	136mM NaCl (80g); 3mM KCl (2g); 8mM Na_2HPO_4 (29g); 1.5mM KH_2PO_4 (2g); make up to 2l with ddH_2O.
FACS buffer (4°C)	0.5% albumin bovine serum (BSA) in PBS
10% sodium dodecyl sulphate (SDS)	10% w/v SDS, pH 7.0
DNA lysis buffer	50mM Tris-HCl, pH8.0; 100mM EDTA; 100mM NaCl; 1% SDS.
TE buffer (Genomic DNA Buffer)	10mM Tris-HCl, pH 8.0; 0.1mM EDTA.
TAE buffer (50x)	242g Tris-base, 57.1ml glacial acetic acid, 18.6g EDTA
MACS buffer (4°C)	0.5% BSA, 2mM EDTA; made up in PBS (1x).
FACS sorting buffer (4°C)	9.6ml HBSS (calcium, magnesium & phenol red free); 200µl 1M HEPES buffer (20mM); 100µl FBS (1%); gentamicin.
FACS collecting buffer (4°C)	8.9ml HBSS, 200µl 1M HEPES buffer (20mM); 1ml FBS (10%); gentamicin.

Table 4.1-1: List of general stock solutions used for this work

Acrylamide gels:	10%	5% stacking
Buffer - lower	8ml	-
Buffer - upper	-	5ml
30% stock acrylamide (4°C)	10.4ml	3ml
ddH_2O	13.4ml	12ml
10% ammonium persulphate (aliquots stored at -20°C)	200µl	100µl
Tetramethyl-ethylenediamine (SIGMA)	50µl	40µl

Table 4.1-2: List of reagents used for SDS-PAGE gels

Solutions	Formulation
Lower buffer	750ml 2M Tris-HCl pH 8.8; 250ml ddH_2O; 4g SDS.
Upper buffer	500ml 1M Tris-HCl pH 6.8; 500ml ddH_2O; 4g SDS.
Laemmli buffer (2x concentrate) (-20°C)	Sigma-Aldrich S23401
Running buffer (4°C)	60.6g Tris Base; 288g Glycine; 20g SDS; make up to 2l with ddH_2O; pH 8.2.
Electro-transfer buffer (EB) (50x)	60.6g Tris Base; 288g Glycine; make up to 2l with ddH_2O.
Electro-transfer buffer (1x)	40ml EB (50x); 400ml methanol; make up to 2l with ddH_2O.
10% Tween/PBS	10ml Tween 20; 90ml PBS (1x).
Wash buffer: 0.1% Tween/PBS	20ml 10% Tween/PBS; 1980ml PBS (1x)
Blocking buffer: 5% milk/0.1% Tween PBS (4°C)	10g *Marvel* skimmed milk powder, 200ml 0.1% Tween/PBS.

Table 4.1-3: Composition of reagents used for SDS-PAGE

Antibody (Ab)	Application	Origin	Distributor
CARD11 (1D12) #4435 (-20°C)	Western blotting ([1:1000] in 5% milk/0.1% Tween PBS).	Rabbit mAb prepared from animals immunised with a synthetic peptide corresponding to residues surrounding threonine 195 of CARD11.	Cell Signaling Technology
Beta-Actin Ab6276 (4°C)	[1:10,000] in 5% milk/0.1% Tween PBS	Mouse mAb to N-terminal of beta isoform of actin	Abcam
Bcl10 (H-197) Sc-5611 (4°C)	Western blotting [1:1000] in 5% milk/0.1% Tween PBS); immunoprecipitation (2µg per 100-500µg of total protein in 1ml cell lysate)	Rabbit polyclonal Ab raised against amino acids 1-197 mapping at the N-terminus of Bcl-10 of human origin.	Santa Cruz Biotechnology

Table 4.1-4: List of primary antibodies used for experiments.

Immunoprecipitation Reagents	Distributor
Protease Inhibitor Cocktail. Used at [1:100] unless otherwise stated. (4°C)	Sigma-Aldrich P8340
RIPA buffer (4°C)	Sigma-Aldrich R0278
Bio-Rad protein assay kit II with BSA standard for total protein quantification	BIO-RAD 500-002
Protein A/G PLUS-Agarose (4°C)	Santa Cruz Biotechnology sc-2003
Protein A-peroxidase (Protein A-HRP). Used as secondary Ab in co-immunoprecipitation experiments for improved western blotting detection to avoid heavy and light chain signals. Used at [1:2500]. (4°C)	Sigma-Aldrich P8651

Table 4.1-5: List of reagents used for immunoprecipitation experiments.

Hybond-ECL 0.45µm	GE Healthcare Amersham
Hyperfilm-ECL 18x24cm	GE Healthcare Amersham
ECL Western Blotting Detection Reagents	GE Healthcare Amersham

Table 4.1-6: Additional materials used for Western Blotting.

Reagent	Application	Distributor
Complete RPMI 1640 medium (4°C)	Cell culture	Invitrogen GIBCO #31870-025
Heat-inactivated fetal bovine serum (-20°C)	Used to supplement RPMI for cell culture	Invitrogen GIBCO #10437028
Penicillin/Streptamycin/Glutamine (P/S/G) (100x) (-20°C)	Used to supplement RPMI for cell culture	Invitrogen GIBCO #10378-016
Hanks' Balanced Salt Solution (HBSS) – calcium, magnesium & phenol red free	Cell preparation for sorting by flow cytometry	Invitrogen GIBCO #14175046
Goat serum (-20°C)	For staining samples for cell sorting by flow cytometry	Invitrogen GIBCO #16210-064
Gentamicin solution (4°C)	Cell preparation for sorting by flow cytometry. Heat and pH stable compared to P/S/G	Sigma-Aldrich #G1272
Anti-mouse CD28	Cell stimulation. Used at 1µg/ml unless otherwise stated.	eBioscience #16-0281-86
Anti-mouse CD3	Cell stimulation. Used at 2µg/ml unless otherwise stated.	eBioscience #16-0032-86

recombinant mouse IL-2 (-80°C)	Cell stimulation. Used at 10units/ml unless otherwise stated.	BD Bioscience #356078
Mouse Transforming Growth Factor β1 (-80°C)	Cell stimulation. Used at 2.5ng/ml unless otherwise stated.	Cell Signaling Technology #5231-LC
Ionomycin, Calcium salt (-20°C)	Cell stimulation. Used at 300ng/ml unless otherwise stated.	Cell Signaling Technology #9995
Phorbol-12-Myristate-13-Acetate (PMA) (-20°C)	Cell stimulation. Used at 200ng/ml unless otherwise stated.	Calbiochem #524400
Mouse CD4 (L3T4) microbeads (4°C)	MACS cell sorting. 10µl per 10^7 cells.	Miltenyi Biotech #130-041-201
MACS separation columns (LS)	MACS cell sorting. Max 10^9 cells per column.	Miltenyi Biotech #130-042-401

Table 4.1-7: List of reagents used for cell culture experiments.

ELISA Reagent	Formulation
Borate Buffered Saline (BBS)	30.92g boric acid [100mM]; 47.68g Na-tetraborate.10H_2O [25mM] = Borax (anhydrous 25.15g); 21.92g NaCl [75mM]; make up to 5l with ddH_2O; pH 8.3-8.5.
PBS 0.5% BSA NaN_3	1g BSA; 400µl NaN_3 10%; make up to 200ml with PBS.
PBS 2% BSA Tween-20 NaN_3	4g BSA; 400µl NaN_3 10%; 1ml Tween-20 10% (2ml Tween-20 + 18ml PBS, add 40 µl NaN_3 for storage); make up to 200ml with PBS.
Substrate: p-Nitrophenyl phosphate tablet sets dissolved in ddH_2O. Used at 50µl/well.	Sigma-Aldrich #N-2770

Table 4.1-8: List of reagents used for Enzyme-linked immunosorbent assay (ELISA).

4.2 Methods

4.2.1 Mice

Mice were bred in Central Biomedical Services (Imperial College London, UK) and kept under specific pathogen-free conditions. All animal work performed as part of this project was authorised by the Home Office under the *Animals (Scientific Procedures) Act 1986*, License PPL 70/6490. Individual mice were identified by numeric ear tagging. The MRL/Mp.*lpr/lpr* mouse serum samples were provided by Professor Marina Botto (Imperial College, London. UK). Homozygous mutants were used for all experiments unless otherwise stated.

4.2.2 *N*-ethyl-*N*-nitrosourea mutagenesis

N-ethyl-*N*-nitrosourea (ENU) mutagenesis was used to generate random mutations in the sperm of C57BL/6J (Charles River sub-strain) male mice, generation (G) 0. G0 mice were bred to C57BL/6J wild-type (Wt) females to obtain G1 mice derived from an ENU-mutated sperm with a unique spectrum of point mutations (~2,500 heterozygous mutations per G1)[177]. The production and maintenance of many thousands of mutant mice demand that a wide variety of screens be applied to the animals; otherwise the cost cannot be justified. Drs Sophie Rutschmann and Onjee Choi set up and executed the ENU mutagenesis and breeding programme in our laboratory, supported by a Medical Research Council grant.

4.2.3 Phenotypic screen

Tail vein blood samples (50µl) were taken from 6-wk old heterozygous, G1 ENU mutant mice and analysed by flow cytometry to identify mutants with abnormal nTreg cell development, defined as a $CD25^{+}FOXP3^{+}/CD4^{+}$ cell population out with 2 SD of the mean.

4.2.4 Cell preparation and flow cytometry

Cells were treated with red blood cell (RBC) lysis buffer (Santa Cruz Biotechnology, SC-296258) and then 25µl of anti-mouse Fcγ-R (CD16/32) antibody (eBioscience, UK) added at a final concentration of 1/20 for 10 minutes at room temperature, to block non-specific antibody binding. Cells were subsequently stained with conjugated monoclonal antibodies for 30 minutes at 4°C. All anti-mouse antibodies were applied to a 1/200 final dilution and from eBioscience, UK, unless stated: PerCP-Cy5.5 conjugated anti-CD4, PB conjugated anti-CD8 (BD Biosciences), PeCy7 conjugated anti-CD25, FITC conjugated anti-B220 (BD Biosciences), APC conjugated anti-CD44, APC conjugated anti-GITR, FITC conjugated anti-CD62L (BD Biosciences), PE conjugated anti-CD69 (PharMingen). Cells were then washed by centrifugation in FACS buffer for 2 minutes at 2100 rpm and 100µl of Cytofix/Cytoperm™ (BD Biosciences) applied for 20 minutes at 4°C, in order to permeabilise the cells prior to intracellular staining with FITC conjugated anti-Foxp3, as per manufacturer's protocol. All samples were acquired on a DAKO Cyan 9 flow cytometer and the data analysed with Summit^{TM} software (DAKO).

4.2.5 Organ dissection

Mice were culled using appropriate methods of humane killing as described in Schedule 1 (revised February 1997) of the Animals (Scientific Procedures) Act 1986. Death was

subsequently confirmed. The animal was then positioned ventral side uppermost on a dissecting board and pinned in a spread-eagle position through the fore-and hind-feet. Using aseptic technique, thymus and spleen were harvested according to the anatomical map described in (***Figure 4.2.5-1***) via a midline, ventral incision and collected in 5ml Complete RMPI medium on ice. Using forceps, organs were ground through nylon mesh to make a single-cell suspension and then centrifuged at 1600 rpm for 5 minutes at 4°C. The medium was poured off and spleen suspensions re-suspended in 2ml RBC lysis buffer for 2 minutes. The reaction was stopped with 8ml RPMI medium and the sample once again centrifuged at 1600 rpm for 5 minutes at 4°C. The medium was poured off and RBC lysis repeated. Finally RBC lysed spleen suspensions and original thymus suspensions were re-suspended in 10ml fresh RPMI medium ready for subsequent experiments. 2µl samples were removed for staining with trypan blue and cell counting (viable and total cell counts) by haemocytometer.

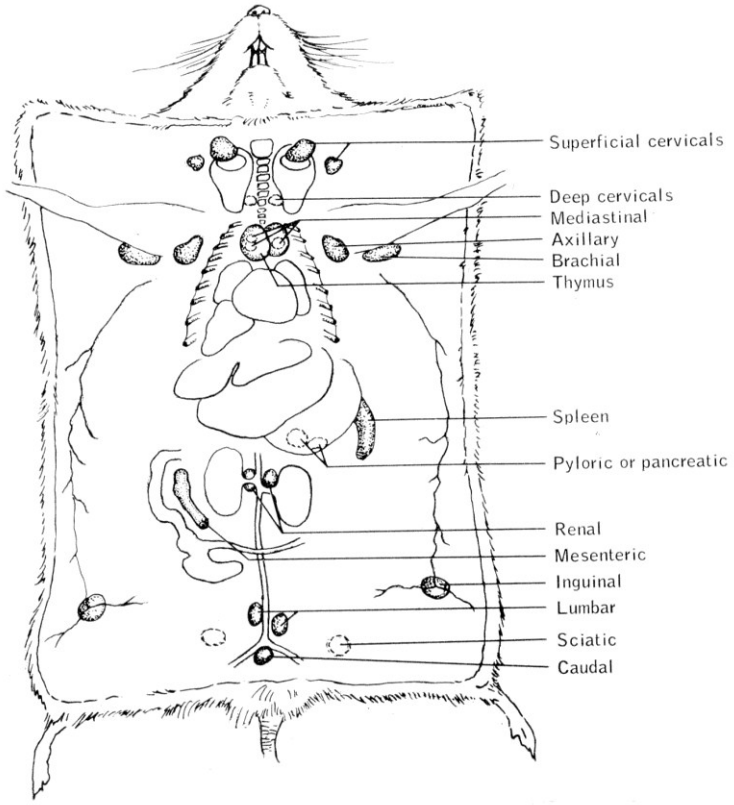


Figure 4.2-1: A general picture of the morphological characteristics of every lymph node and its localization in the normal mouse.

4.2.6 Confirmation of mutation heritability and breeding

Heterozygote G1 phenodeviants with abnormal nTreg development were examined to determine whether the phenotype was heritable: G1 phenodeviants were crossed with Wt mice and the G2 population screened for 50% expression of deviant phenotype. Once transmissibility was confirmed, each nTreg mutation was bred to homozygosity. I was assisted with breeding by my laboratory colleague, Dr Lihui Wang.

4.2.7 Genotyping

To identify the causative genetic mutations underlying these heritable nTreg phenodeviations, I adopted a classical positional cloning strategy (***Figure 4.2-2***). Heterozygote nTreg phenodeviants were outcrossed to phylogenetically-distinct inbred Wt 129Sv1mJ mice (Charles River sub-strain). The resulting hybrid (H) 1 generation mice were screened for abnormal nTreg development, as previously described, and affected H1 mice crossed with the Wt 129Sv1mJ animal again. The H2 offspring were phenotyped and tail DNA prepared from each mouse (***Appendix B***). Samples were sent to LGC Genomics (formerly KBioscience) for genotyping against 358 single nucleotide polymorphisms (SNPs), which differ between C57BL/6 and 129/SvJ mice (***Appendix C***). The meiotic recombination frequency between the SNPs and the mutation was calculated and a Logarithm of Odds (LOD) scored [133]. The LOD score is the log base 10 of the likelihood ratio under the hypotheses of linkage and non-linkage:

$$\textbf{LOD score} = Z = \log_{10}\left[\frac{\theta^{(\#\text{ of recombinants})} \bullet (1-\theta)^{(\#\text{ of nonrecombinants})}}{(0.5)^{(\#\text{ of recombinants})}(0.5)^{(\#\text{ of nonrecombinants})}}\right]$$

A LOD score can be converted into an equivalent chi-squared statistic with the following simple formula:

$$T = 2 \ln (10) Z$$

And so it can be assumed that $Z = 3$, $p = 0.001$

i.e. A LOD score >3 strongly indicates linkage.

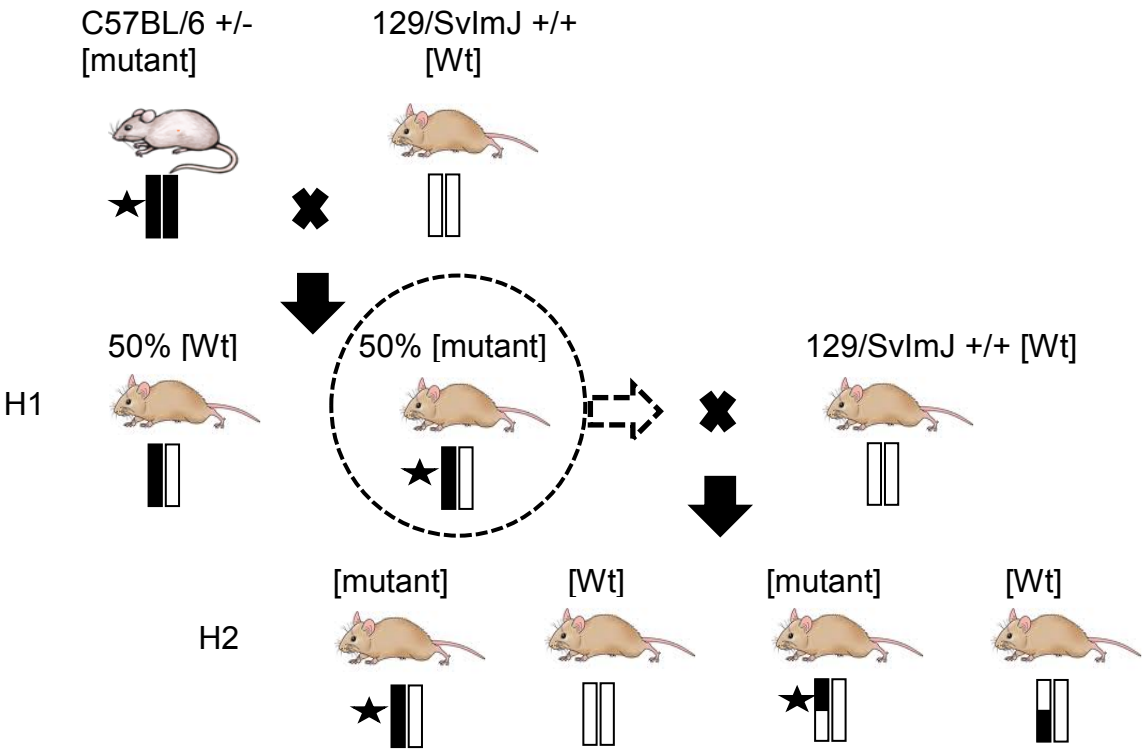


Figure 4.2-2: Diagram illustrating the classical positional cloning strategy adopted to identify causative mutations.

C57BL/6 heterozygote (+/-) nTreg phenodeviants were outcrossed to Wt (+/+) 129Sv1mJ mice. The resulting hybrid (H) 1 generation mice were screened for abnormal nTreg development and affected H1 mice crossed with the Wt 129Sv1mJ animal again. The H2 offspring were phenotyped for abnormal nTreg development. […] = phenotype

4.2.8 *carma1* sequencing

All coding exons from *carma 1* (2-25) were amplified from genomic DNA by polymerase chain reaction (PCR) using JumpStart REDtaq ReadyMix (Sigma). Primers are listed in ***Appendix A***. Typically PCR reactions were set up in 0.5 ml thin walled microcentrifuge tubes to a final volume of 50µl:

25µl JumpStart REDtaq ReadyMix (Sigma)

18µl H_2O

5µl combination primer i.e. 2.5µl forward primer and 2.5µl reverse primer

2µl DNA made up to a concentration of 50ng/µl

DNA amplification was performed using the following program:

Step	Temperature	Time	
1	94°C	2 min	
2a (genomic DNA separation)	94°C	30 seconds	35 cycles
2b (primer annealing)	55°C	30 seconds	
2c (PCR product extension)	72°C	2 minutes	
3	72°C	5 minutes	

Table 4.2-1: Thermal Cycler program used for DNA amplification by PCR.

Southern blotting was used to ensure amplification of a single PCR product: products were electrophoresed through 1% agarose gels at 120 volts for 35 minutes and then exposed to ultraviolet radiation for 90 seconds to confirm the presence of a single band. Where multiple bands were identified, the thermal cycling program was modified to improve PCR product

quality. Once PCR products for all *carma1* exons were optimised, samples were purified by QIAquick PCR Purification Kit (Qiagen), sequenced (MRC CSC Genomics Core Laboratory, Imperial College London) and the data analysed with Sequencher software (Gene Codes Corporation).

4.2.9 *In vitro* $CD4^+$ T cell activation and iTreg differentiation

$CD4^+$T cells were isolated from mouse spleen using magnetic beads (MACS® technology) and activated for 48 hours with plate-bound anti-CD3 (1µg/ml) and anti-CD28 (2µg/ml) in the presence of rIL-2 (30U/ml) (eBioscience). Cells were then stained for CD25, CD62L, CD69 and CD44 in order to assess the upregulation of an activated phenotype, defined as $CD69^+CD44^+CD25^+CD62L^{low}$, by flow cytometry. To measure iTreg differentiation, MACS® purified splenic $CD4^+$ T cells were sorted as naive $CD4^+CD25^-CD44^{lo}$ cells then stimulated with plate-bound anti-CD3 (0-10µg/ml) and anti-CD28 (1µg/ml) for 3 days in the presence of rIL-2 (100U/ml) and rTGF-β1 (2.5ng/ml) (Cell Signaling) and stained for FOXP3 expression.

4.2.10 Immunological assays

4.2.10.1 Enzyme-linked immunosorbent assay (ELISA)

Microtiter plates were coated with 50µl per well of single-stranded DNA in borate buffered saline (BBS) (10 µg/ml) then incubated for 3 hours at 37°C. After washing three times with phosphate buffered saline (PBS) containing 0.05% Tween-20, wells were blocked with 100µl 0.5% bovine serum albumin (BSA) in PBS-Tween/NaN_3 for 1 hour at room temperature. Homozygous Wt, Vulpo and Zerda mouse serum samples from 1 year old mice were prepared to 1/100 concentration in 2% BSA in PBS-Tween/NaN_3. 2% BSA in PBS-Tween/NaN_3 was

used as a negative control. Serum samples derived from an MRL/Mp.*lpr/lpr* mice pool were used as a positive control and prepared for a 12-point standard curve starting at 1/400 concentration diluted in 2% BSA in PBS-Tween/NaN_3. 50µl of each sample was added to each well and plates were incubated overnight at 4°C. The following morning, plates were washed five times in PBS and 50µl Alkaline phosphatase -conjugated goat anti-mouse IgG (γ-chain specific) (Sigma-Aldrich) added to each well at a concentration of 1/3000, diluted in 2% BSA in PBS-Tween/NaN_3. Plates were incubated for a further 4 hours at 4°C, washed five times with PBS and 50µl p-Nitrophenyl phosphate substrate (SIGMA) added to each well. Plates were read by spectrophotometer (Thermo Multiskan Ascent) at 405nm every 15 minutes. Readings taken at 30 minutes provided an ideal standard curve and results were expressed as arbitrary Elisa units (AEU) relative to the standard positive sample derived from the MRL/Mp.*lpr/lpr* mice pool.

4.2.10.2 Western blotting

For Western blots, detergent extracts were resolved by 10% SDS-PAGE and electrophorectically transferred [170]. The primary antibodies used were: rabbit mAb to CARD11 (1D12) (Cell signalling) and mouse mAb to beta ACTIN (Abcam). The secondary antibodies used were: polyclonal goat anti-rabbit immunoglobulin/HRP (Dako) and polyclonal goat anti-mouse immunoglobulin/HRP (Dako). Homozygous Wt, Vulpo and Zerda thymus lysates were run in duplicate. For immunoprecipitations (IP), MACS® purified splenic $CD4^+$ T cells from 3 homozygous mouse spleens were activated in 1.5ml RPMI, phorbol 12-myristate 13-acetate (PMA) (200ng/ml) and ionomycin (300ng/ml) for 6 hours at 37°C. Cells were harvested with PBS and lysed in 1ml RIPA buffer plus protease inhibitor cocktail (Sigma-Aldrich). Polyclonal rabbit anti-mouse Bcl-10 Ab (2µg) (Santa Cruz sc-5611) and protein A/G PLUS-agarose (20µl) (Santa Cruz sc-2003) were added to each 1ml sample (100-

500 µg/ml total protein) followed by rotation at 4°C for 2 hours. Beads were washed 3 times with RIPA buffer, boiled in SDS loading buffer, resolved on 10% SDS-PAGE gels and Western blotted. Primary antibodies used were rabbit mAb to CARD11 (1D12) and polyclonal rabbit anti-mouse Bcl-10 Ab. For improved Western blotting detection to avoid heavy and light chain signals, blots were incubated with 1:5000 dilution of Protein A-HRP (Amersham) prepared in blocking buffer, in place of secondary antibody [174].

4.2.11 Statistical analysis

All results are given as mean values with SD. A nonparametric unpaired *t*-test (two-tailed) was applied: ****p<0.001, **p=0.001–0.01, *p=0.01–0.05, ns=not significant.* All statistical calculations were performed using Prism5 software (GraphPad).

Chapter 5: Appendices

Appendix A: *Carma1* primers used to sequence *Carma1* in mutant and WT genomic DNA.

Exon	Forward Sequence	Reverse Sequence
non-coding	TCATTTCGCATCACAACAAGCACTG	TGGCAACCAGAGGTTTATTTCCAGG
non-coding	AGTGAACACAGAGCCCCAGTATGA	TTCCATCTGGTGATGGCTCCTGA
non-coding	TGCTCAGTTAGAAGAAACAAGGAACCC	CAGGTTCTGCTCAGAATAAAGCAAAAGG
non-coding	TCCAATGGATAAGCACTGCCTCCC	GCGAGGTTGCTTTAGATGCTATCCC
2	CTTATGCCAGGCAAACTGCACTTTC	AGACAGAGACTCACTGCTCAGGAC
non-coding	CCAGAGCACAGTTGGTGACATGAAA	AGAAAACTGACATGATAGTGTGTCCCTTG
3	TGTATGGAACCTCTCACCCACACTC	CCCCAATGACAGGACTTTCCATCTC
4	GGCAGCCCAAGAGTTCAGCA	ACACCATTTAAACCCCTCTGAATGAGAC
5	AGGTCCCCTAACTTTCCATGAGCC	GGGAACTAAGAGTTCAGTAAACGCTGC
6	TGTGCCAACAGCATGGTTTGTAGTC	GGCATTGCATGTGTCAGGAAATGG
6	CTTTTCTCCCAGAGCTAGGGCATTG	AGCTCAAGAATGACATCGAGAACCG
7	ACGGTGGAGATACATCCTTGGTGG	GGCTCAGTGTTCTTGAAGCAGAGAC
8	GAATGCATCTCTGAGCTGGGGAC	CATGAGCTAACTGTAGCCACTAAGCAA
9	AAACAACACAGACACACATACAGACATACA	AGACAGAAACAGGAGGATCATAAGCTCA
10	TCCCTGGGTAGCAACCAAAGTGAC	ACCCTGGAGATGGTATGAGCCAAG
11	AGCATATACATGCGGGCATCACAC	CCTGCCTCTCTGTGCTAATGGAAG
non-coding	GGAAGCCTTGCGTTATACTTCCACC	TTCAGCCACAAACTCCTGGCTC
12	TGTAACAGAAGGCTGGGACCCTAC	ACACAAAAGTTGAGAGCCCCTGAAG
13	CATGTTCAGATGACTCTGAGGCCG	CCAAATCCAAGGTCCTGTTCCATCC
14	GAGAGTGTGTCAGTGTCCCCAATG	GCACCCTTCTGAACAGCTTAGACC
15	AACTGATTTGTGACTGAGACTCTGGC	TGTAGTAAGAGCTGTAGGGTTCTCACC
16	ACCTTGTAATGCAGAGTGATGAGGC	AGAGGACAGGGCGGTAGTTATTCC
17	CTTGTAGCAGACTGGGAAGCATGAC	GCACACAACTCTGAATGGCGATGG
18	GGGCAGGATTGCAAGTTCAATTTTAGAC	ACATTGTGGCTCAGCACAGATGTTAG
19 & 20	ACCTGTCACTGCGGGGATAAAATG	GCTCTCAGCCAATCAGATGGTCAG
21	AGGGCTTCAGTCAATGTGGGCATC	TCTGTGGGAACCTGGATTCTGTACC
22	AACATTACGAGGTGGCCGAGTG	GTTCAGCAGGTTTCTGAGACACCC
23	TTGGGGAGTCACAGCTTGGAAAC	TGGTCTGGCAGAGCAATCATGAAC
24	GGTCAAGGACCACACATGACGG	GTGAGTGTCCATTGCAAGCCCC
25	ACTGTGCTTGATGGAAACACCTGC	TCGAGCCCAAGAATGTAAGAAGCC

Appendix B: DNA isolation

Tail clips were taken from 24 mice (12 from H2 offspring with mutant phenotype and 12 from H2 offspring with Wt phenotype). Clips were digested overnight by rotation at 50°C in 0.7ml lysis buffer and 70µl proteinase K (10mg/ml). Samples were then vortexed and hair/undigested debris precipitated by centrifugation for 15 minutes at 13,000 rpm. The DNA-containing supernatants were transferred to clean tubes and 0.7ml isopropanol added to each sample, followed by mixing by inversion. Tubes were then spun at 13,000 rpm for 10 minutes to precipitate DNA pellets. Supernatants were discarded and DNA pellets washed with 0.5ml ice-cold 70% ethanol. Dry DNA pellets were then re-suspended in 350µl genomic DNA buffer and rotated overnight at 50°C to ensure complete DNA solution. The DNA concentration of samples was calculated using a NanoDrop™ spectrophotometer.

Appendix C: List of single nucleotide polymorphisms (SNPs) used for genotyping Vulpo.

No.	SNP identity						
1	01-034899657-N	**45**	06-122941044-M	**89**	01-159058371-M	**133**	04-068252469-M
2	01-050957023-N	**46**	07-022997618-M	**90**	01-165583809-M	**134**	04-081111774-M
3	01-082250512-N	**47**	07-042943665-M	**91**	01-178701443-M	**135**	04-088959560-M
4	01-089580704-N	**48**	08-093120105-M	**92**	01-185013929-M	**136**	04-097015585-M
5	01-144168459-N	**49**	08-123021323-M	**93**	01-191804699-M	**137**	04-103933951-M
6	01-172554503-N	**50**	09-003938578-M	**94**	02-004006715-M	**138**	04-109025153-M
7	03-065861493-N	**51**	09-053790242-M	**95**	02-012171555-M	**139**	04-116163539-M
8	03-124203459-N	**52**	09-084055613-M	**96**	02-020414303-M	**140**	04-127133018-M
9	03-144955281-N	**53**	10-003233934-M	**97**	02-026654160-M	**141**	04-141084977-M
10	04-014657884-N	**54**	rs3717445	**98**	02-030755750-M	**142**	04-145870512-M
11	04-075245266-N	**55**	10-103158653-M	**99**	02-038092910-M	**143**	04-151168886-M
12	05-065734378-N	**56**	10-123089825-M	**100**	02-043953410-M	**144**	05-009080098-M
13	05-115212503-N	**57**	11-024515722-M	**101**	02-050206336-M	**145**	05-015030133-M
14	06-036210417-N	**58**	11-044333996-M	**102**	02-056933273-M	**146**	05-023890459-M
15	09-033919969-N	**59**	11-054801294-M	**103**	02-064172278-M	**147**	05-030170202-M
16	10-042788082-N	**60**	11-084320332-M	**104**	02-074976198-M	**148**	05-039017415-M
17	11-005661856-N	**61**	12-113315003-M	**105**	02-078062303-M	**149**	05-044010971-M
18	11-063538723-N	**62**	13-023105764-M	**106**	02-101074874-M	**150**	05-050882266-M
19	11-095093300-N	**63**	14-093080383-M	**107**	02-104865091-M	**151**	05-069043957-M
20	13-043995023-N	**64**	17-013493244-M	**108**	02-119931810-M	**152**	05-078151229-M
21	13-052501751-N	**65**	17-073215081-M	**109**	02-124063590-M	**153**	05-084120220-M
22	13-065339791-N	**66**	18-005066417-M	**110**	02-139603599-M	**154**	05-091950247-M
23	14-031978791-N	**67**	18-084751134-M	**111**	02-167943959-M	**155**	05-097007418-M
24	14-042965786-N	**68**	19-025120427-M	**112**	02-175236812-M	**156**	05-100871112-M
25	14-060626617-N	**69**	12-018871120-N	**113**	02-179086475-M	**157**	05-107871207-M
26	14-112205439-N	**70**	12-067692873-N	**114**	03-011350737-M	**158**	05-128944450-M
27	16-064069423-N	**71**	12-107536049-N	**115**	03-026157475-M	**159**	05-136184664-M
28	17-086110517-N	**72**	01-007166135-M	**116**	03-032431792-M	**160**	05-149044358-M
29	17-092673068-N	**73**	01-014123597-M	**117**	03-037152198-M	**161**	06-008104124-M
30	18-063800148-N	**74**	01-022154835-M	**118**	03-053161686-M	**162**	06-015283563-M
31	19-045460279-N	**75**	01-029142332-M	**119**	03-059797081-M	**163**	06-020075608-M
32	01-043168343-M	**76**	01-058997955-M	**120**	03-073214161-M	**164**	06-028759322-M
33	02-113220302-M	**77**	01-065042402-M	**121**	03-081123258-M	**165**	06-045126062-M
34	02-133158154-M	**78**	01-069924080-M	**122**	03-098415492-M	**166**	06-050967077-M
35	02-152934935-M	**79**	01-077241287-M	**123**	03-110268748-M	**167**	06-058199906-M
36	03-104386660-M	**80**	01-086182722-M	**124**	03-138370314-M	**168**	06-076285738-M
37	04-022875524-M	**81**	01-094081544-M	**125**	03-152200034-M	**169**	06-090142535-M
38	04-043070534-M	**82**	01-102073421-M	**126**	03-158497808-M	**170**	06-095139289-M
39	04-122948823-M	**83**	01-110152038-M	**127**	04-008229128-M	**171**	06-101960309-M
40	04-132955150-M	**84**	01-116988763-M	**128**	04-030080285-M	**172**	06-115164803-M
41	05-003188964-M	**85**	01-124147455-M	**129**	04-037053163-M	**173**	06-128926170-M
42	05-143026004-M	**86**	01-132126870-M	**130**	04-046972984-M	**174**	06-136943848-M
43	06-062599520-M	**87**	01-137189321-M	**131**	04-053894587-M	**175**	06-146079591-M
44	06-083216741-M	**88**	01-152031524-M	**132**	04-061409675-M	**176**	07-006208019-M

177	07-009057918-M	**221**	09-111881261-M	**265**	13-077818021-M	**309**	18-043868444-M	**353**	rs13480578
178	07-018939701-M	**222**	09-118995402-M	**266**	13-084819885-M	**310**	18-078158450-M	**354**	rs13478808
179	07-028240185-M	**223**	09-125082704-M	**267**	13-091042598-M	**311**	18-090060367-M	**355**	rs29347820
180	07-029991530-M	**224**	10-014021037-M	**268**	13-101929792-M	**312**	19-018239318-M	**356**	rs29365622
181	07-036014647-M	**225**	10-019253812-M	**269**	13-107993079-M	**313**	19-031186563-M	**357**	rs3165748
182	07-048028246-M	**226**	10-027070647-M	**270**	13-113945175-M	**314**	19-038092479-M	**358**	rs4211507
183	07-057062790-M	**227**	10-045078228-M	**271**	14-004082624-M	**315**	19-051918908-M		
184	07-064095712-M	**228**	10-053898997-M	**272**	14-011059049-M	**316**	19-058179075-M		
185	07-071043704-M	**229**	10-092128703-M	**273**	14-016913520-M	**317**	X-008280846-M		
186	07-078044642-M	**230**	10-094049193-M	**274**	14-024063411-M	**318**	X-036314320-M		
187	07-085095955-M	**231**	10-107333522-M	**275**	14-029078879-M	**319**	X-054638016-M		
188	07-092021090-M	**232**	10-115062433-M	**276**	14-046108187-M	**320**	X-068494838-M		
189	07-099391547-M	**233**	10-129117100-M	**277**	14-054014360-M	**321**	X-088983890-M		
190	07-106153798-M	**234**	11-011378766-M	**278**	14-067021276-M	**322**	X-111633440-M		
191	07-114576068-M	**235**	11-019956728-M	**279**	14-074468555-M	**323**	16-005053446-C		
192	07-118127386-M	**236**	11-039194893-M	**280**	14-077156430-M	**324**	16-012092571-C		
193	07-124090029-M	**237**	11-047224208-M	**281**	14-099172131-M	**325**	16-019621494-C		
194	07-129989877-M	**238**	11-070331570-M	**282**	14-108203728-M	**326**	16-025179119-C		
195	08-004138223-M	**239**	11-077198334-M	**283**	15-004024569-M	**327**	16-031026287-C		
196	08-011103791-M	**240**	11-091287860-M	**284**	15-010120073-M	**328**	16-037994236-C		
197	08-017931675-M	**241**	11-108428031-M	**285**	15-017113859-M	**329**	16-045078790-C		
198	08-022074356-M	**242**	11-115546745-M	**286**	15-022235389-M	**330**	16-049079612-C		
199	08-028926710-M	**243**	11-122195777-M	**287**	15-030334445-M	**331**	16-056118825-C		
200	08-035000451-M	**244**	12-009581325-M	**288**	15-038029796-M	**332**	16-066862514-C		
201	08-041947937-M	**245**	12-016244499-M	**289**	15-044071932-M	**333**	16-075684315-C		
202	08-047239384-M	**246**	12-026312484-M	**290**	15-051946000-M	**334**	16-090091107-C		
203	08-054093936-M	**247**	12-029244061-M	**291**	15-057561875-M	**335**	16-096070057-C		
204	08-075249544-M	**248**	12-034563785-M	**292**	15-074039561-M	**336**	X-123551831-M		
205	08-088042210-M	**249**	12-041270227-M	**293**	15-081163423-M	**337**	02-145828186-N		
206	08-098901421-M	**250**	12-048364436-M	**294**	15-088202966-M	**338**	02-160869410-N		
207	08-107088585-M	**251**	12-054303300-M	**295**	15-094178941-M	**339**	02-069853291-N		
208	08-114059240-M	**252**	12-061271925-M	**296**	17-007230139-M	**340**	03-131286062-N		
209	09-008979920-M	**253**	12-074494300-M	**297**	17-027262193-M	**341**	03-017511270-N		
210	09-016198772-M	**254**	12-081758527-M	**298**	17-035364626-M	**342**	03-088155864-N		
211	09-020768402-M	**255**	12-084289638-M	**299**	17-042164456-M	**343**	05-120623301-N		
212	09-027092605-M	**256**	12-092440423-M	**300**	17-048262313-M	**344**	06-107618320-N		
213	09-040838924-M	**257**	12-099072867-M	**301**	17-056073815-M	**345**	07-014548611-N		
214	09-048062033-M	**258**	13-009820324-M	**302**	17-065545592-M	**346**	08-069496369-N		
215	09-061026505-M	**259**	13-015609597-M	**303**	17-080241937-M	**347**	08-080610993-N		
216	09-067826343-M	**260**	13-030913320-M	**304**	18-013036555-M	**348**	11-102928307-N		
217	09-076920055-M	**261**	13-037832161-M	**305**	18-019171445-M	**349**	15-101356293-N		
218	09-089891382-M	**262**	13-047833889-M	**306**	18-022777507-M	**350**	17-022861830-N		
219	09-097984353-M	**263**	13-060129254-M	**307**	18-030864114-M	**351**	18-049391366-N		
220	09-105828528-M	**264**	13-071928027-M	**308**	18-037875535-M	**352**	18-070565016-N		

Chapter 6: References

1. Burnet FM. Biology and medicine. *The Medical journal of Australia* 1957; **44**(13): 406-10.

2. Grakoui A, Bromley SK, Sumen C, et al. The immunological synapse: a molecular machine controlling T cell activation. *Science* 1999; **285**(5425): 221-7.

3. Bromley SK, Burack WR, Johnson KG, et al. The immunological synapse. *Annu Rev Immunol* 2001; **19**: 375-96.

4. Huppa JB, Davis MM. T-cell-antigen recognition and the immunological synapse. *Nat Rev Immunol* 2003; **3**(12): 973-83.

5. Kappler JW, Roehm N, Marrack P. T cell tolerance by clonal elimination in the thymus. *Cell* 1987; **49**(2): 273-80.

6. Kisielow P, Bluthmann H, Staerz UD, Steinmetz M, von Boehmer H. Tolerance in T-cell-receptor transgenic mice involves deletion of nonmature CD4+8+ thymocytes. *Nature* 1988; **333**(6175): 742-6.

7. Kyewski B, Klein L. A central role for central tolerance. *Annu Rev Immunol* 2006; **24**: 571-606.

8. Peterson P, Org T, Rebane A. Transcriptional regulation by AIRE: molecular mechanisms of central tolerance. *Nat Rev Immunol* 2008; **8**(12): 948-57.

9. Mathis D, Benoist C. Aire. *Annu Rev Immunol* 2009; **27**: 287-312.

10. Nagamine K, Peterson P, Scott HS, et al. Positional cloning of the APECED gene. *Nat Genet* 1997; **17**(4): 393-8.

11. Wirnsberger G, Hinterberger M, Klein L. Regulatory T-cell differentiation versus clonal deletion of autoreactive thymocytes. *Immunology and cell biology* 2011; **89**(1): 45-53.

12. Picca CC, Oh S, Panarey L, Aitken M, Basehoar A, Caton AJ. Thymocyte deletion can bias Treg formation toward low-abundance self-peptide. *Eur J Immunol* 2009; **39**(12): 3301-6.

13. Simons DM, Picca CC, Oh S, et al. How specificity for self-peptides shapes the development and function of regulatory T cells. *J Leukoc Biol* 2010; **88**(6): 1099-107.

14. Germain RN. T-cell development and the CD4-CD8 lineage decision. *Nat Rev Immunol* 2002; **2**(5): 309-22.

15. Zinkernagel RM. Immunology taught by viruses. *Science* 1996; **271**(5246): 173-8.

16. Alferink J, Tafuri A, Vestweber D, Hallmann R, Hammerling GJ, Arnold B. Control of neonatal tolerance to tissue antigens by peripheral T cell trafficking. *Science* 1998; **282**(5392): 1338-41.

17. Kurts C, Miller JF, Subramaniam RM, Carbone FR, Heath WR. Major histocompatibility complex class I-restricted cross-presentation is biased towards high dose antigens and those released during cellular destruction. *J Exp Med* 1998; **188**(2): 409-14.

18. Jenkins MK, Schwartz RH. Antigen presentation by chemically modified splenocytes induces antigen-specific T cell unresponsiveness in vitro and in vivo. *J Exp Med* 1987; **165**(2): 302-19.

19. Walker LS, Abbas AK. The enemy within: keeping self-reactive T cells at bay in the periphery. *Nat Rev Immunol* 2002; **2**(1): 11-9.

20. Watanabe-Fukunaga R, Brannan CI, Copeland NG, Jenkins NA, Nagata S. Lymphoproliferation disorder in mice explained by defects in Fas antigen that mediates apoptosis. *Nature* 1992; **356**(6367): 314-7.

21. Sobel ES, Kakkanaiah VN, Cohen PL, Eisenberg RA. Correction of gld autoimmunity by co-infusion of normal bone marrow suggests that gld is a mutation of the Fas ligand gene. *Int Immunol* 1993; **5**(10): 1275-8.

22. Suda T, Takahashi T, Golstein P, Nagata S. Molecular cloning and expression of the Fas ligand, a novel member of the tumor necrosis factor family. *Cell* 1993; **75**(6): 1169-78.

23. Fisher GH, Rosenberg FJ, Straus SE, et al. Dominant interfering Fas gene mutations impair apoptosis in a human autoimmune lymphoproliferative syndrome. *Cell* 1995; **81**(6): 935-46.

24. Sakaguchi S, Ono M, Setoguchi R, et al. Foxp3+ CD25+ CD4+ natural regulatory T cells in dominant self-tolerance and autoimmune disease. *Immunol Rev* 2006; **212**: 8-27.

25. Sakaguchi S, Yamaguchi T, Nomura T, Ono M. Regulatory T cells and immune tolerance. *Cell* 2008; **133**(5): 775-87.

26. Belkaid Y, Tarbell K. Regulatory T cells in the control of host-microorganism interactions (*). *Annu Rev Immunol* 2009; **27**: 551-89.

27. Wood KJ, Sakaguchi S. Regulatory T cells in transplantation tolerance. *Nat Rev Immunol* 2003; **3**(3): 199-210.

28. Yamaguchi T, Sakaguchi S. Regulatory T cells in immune surveillance and treatment of cancer. *Semin Cancer Biol* 2006; **16**(2): 115-23.

29. Feuerer M, Hill JA, Mathis D, Benoist C. Foxp3+ regulatory T cells: differentiation, specification, subphenotypes. *Nat Immunol* 2009; **10**(7): 689-95.

30. Fontenot JD, Dooley JL, Farr AG, Rudensky AY. Developmental regulation of Foxp3 expression during ontogeny. *J Exp Med* 2005; **202**(7): 901-6.

31. Huehn J, Siegmund K, Lehmann JC, et al. Developmental stage, phenotype, and migration distinguish naive- and effector/memory-like CD4+ regulatory T cells. *J Exp Med* 2004; **199**(3): 303-13.

32. Herman AE, Freeman GJ, Mathis D, Benoist C. CD4+CD25+ T regulatory cells dependent on ICOS promote regulation of effector cells in the prediabetic lesion. *J Exp Med* 2004; **199**(11): 1479-89.

33. Sugimoto N, Oida T, Hirota K, et al. Foxp3-dependent and -independent molecules specific for CD25+CD4+ natural regulatory T cells revealed by DNA microarray analysis. *Int Immunol* 2006; **18**(8): 1197-209.

34. Lin W, Haribhai D, Relland LM, et al. Regulatory T cell development in the absence of functional Foxp3. *Nat Immunol* 2007; **8**(4): 359-68.

35. Hill JA, Feuerer M, Tash K, et al. Foxp3 transcription-factor-dependent and -independent regulation of the regulatory T cell transcriptional signature. *Immunity* 2007; **27**(5): 786-800.

36. Molinero LL, Yang J, Gajewski T, Abraham C, Farrar MA, Alegre ML. CARMA1 controls an early checkpoint in the thymic development of FoxP3+ regulatory T cells. *J Immunol* 2009; **182**(11): 6736-43.

37. Caton AJ, Cozzo C, Larkin J, 3rd, Lerman MA, Boesteanu A, Jordan MS. CD4(+) CD25(+) regulatory T cell selection. *Ann N Y Acad Sci* 2004; **1029**: 101-14.

38. Zheng SG, Gray JD, Ohtsuka K, Yamagiwa S, Horwitz DA. Generation ex vivo of TGF-beta-producing regulatory T cells from CD4+CD25- precursors. *J Immunol* 2002; **169**(8): 4183-9.

39. Isomura I, Palmer S, Grumont RJ, et al. c-Rel is required for the development of thymic Foxp3(+) CD4 regulatory T cells. *Journal of Experimental Medicine* 2009; **206**(13): 3001-14.

40. Chen W, Jin W, Hardegen N, et al. Conversion of peripheral CD4+CD25- naive T cells to CD4+CD25+ regulatory T cells by TGF-beta induction of transcription factor Foxp3. *J Exp Med* 2003; **198**(12): 1875-86.

41. Williams Z. Inducing tolerance to pregnancy. *N Engl J Med* 2012; **367**(12): 1159-61.

42. Wildin RS, Ramsdell F, Peake J, et al. X-linked neonatal diabetes mellitus, enteropathy and endocrinopathy syndrome is the human equivalent of mouse scurfy. *Nat Genet* 2001; **27**(1): 18-20.

43. Somerset DA, Zheng Y, Kilby MD, Sansom DM, Drayson MT. Normal human pregnancy is associated with an elevation in the immune suppressive CD25+ CD4+ regulatory T-cell subset. *Immunology* 2004; **112**(1): 38-43.

44. Samstein RM, Josefowicz SZ, Arvey A, Treuting PM, Rudensky AY. Extrathymic generation of regulatory T cells in placental mammals mitigates maternal-fetal conflict. *Cell* 2012; **150**(1): 29-38.

45. Scarpellini F, Sbracia M. Use of granulocyte colony-stimulating factor for the treatment of unexplained recurrent miscarriage: a randomised controlled trial. *Hum Reprod* 2009; **24**(11): 2703-8.

46. Buckner JH. Mechanisms of impaired regulation by CD4(+)CD25(+)FOXP3(+) regulatory T cells in human autoimmune diseases. *Nat Rev Immunol* 2010; **10**(12): 849-59.

47. Vignali DA, Collison LW, Workman CJ. How regulatory T cells work. *Nat Rev Immunol* 2008; **8**(7): 523-32.

48. Valencia X, Stephens G, Goldbach-Mansky R, Wilson M, Shevach EM, Lipsky PE. TNF downmodulates the function of human CD4+CD25hi T-regulatory cells. *Blood* 2006; **108**(1): 253-61.

49. Thornton AM, Donovan EE, Piccirillo CA, Shevach EM. Cutting edge: IL-2 is critically required for the in vitro activation of CD4+CD25+ T cell suppressor function. *J Immunol* 2004; **172**(11): 6519-23.

50. Korn T, Reddy J, Gao W, et al. Myelin-specific regulatory T cells accumulate in the CNS but fail to control autoimmune inflammation. *Nat Med* 2007; **13**(4): 423-31.

51. King IL, Segal BM. Cutting edge: IL-12 induces CD4+CD25- T cell activation in the presence of T regulatory cells. *J Immunol* 2005; **175**(2): 641-5.

52. Ben Ahmed M, Belhadj Hmida N, Moes N, et al. IL-15 renders conventional lymphocytes resistant to suppressive functions of regulatory T cells through activation of the phosphatidylinositol 3-kinase pathway. *J Immunol* 2009; **182**(11): 6763-70.

53. Clough LE, Wang CJ, Schmidt EM, et al. Release from regulatory T cell-mediated suppression during the onset of tissue-specific autoimmunity is associated with elevated IL-21. *J Immunol* 2008; **180**(8): 5393-401.

54. Walker LS. Regulatory T cells overturned: the effectors fight back. *Immunology* 2009; **126**(4): 466-74.

55. Yang J, Brook MO, Carvalho-Gaspar M, et al. Allograft rejection mediated by memory T cells is resistant to regulation. *Proc Natl Acad Sci U S A* 2007; **104**(50): 19954-9.

56. Yates J, Rovis F, Mitchell P, et al. The maintenance of human CD4+ CD25+ regulatory T cell function: IL-2, IL-4, IL-7 and IL-15 preserve optimal suppressive potency in vitro. *Int Immunol* 2007; **19**(6): 785-99.

57. Takeda I, Ine S, Killeen N, et al. Distinct roles for the OX40-OX40 ligand interaction in regulatory and nonregulatory T cells. *J Immunol* 2004; **172**(6): 3580-9.

58. Choi BK, Bae JS, Choi EM, et al. 4-1BB-dependent inhibition of immunosuppression by activated CD4+CD25+ T cells. *J Leukoc Biol* 2004; **75**(5): 785-91.

59. Sakaguchi S, Miyara M, Costantino CM, Hafler DA. FOXP3+ regulatory T cells in the human immune system. *Nat Rev Immunol* 2010; **10**(7): 490-500.

60. Floess S, Freyer J, Siewert C, et al. Epigenetic control of the foxp3 locus in regulatory T cells. *PLoS Biol* 2007; **5**(2): e38.

61. Workman CJ, Szymczak-Workman AL, Collison LW, Pillai MR, Vignali DA. The development and function of regulatory T cells. *Cell Mol Life Sci* 2009; **66**(16): 2603-22.

62. Gregori S, Giarratana N, Smiroldo S, Adorini L. Dynamics of pathogenic and suppressor T cells in autoimmune diabetes development. *J Immunol* 2003; **171**(8): 4040-7.

63. D'Alise AM, Auyeung V, Feuerer M, et al. The defect in T-cell regulation in NOD mice is an effect on the T-cell effectors. *Proc Natl Acad Sci U S A* 2008; **105**(50): 19857-62.

64. Kohm AP, Carpentier PA, Anger HA, Miller SD. Cutting edge: CD4+CD25+ regulatory T cells suppress antigen-specific autoreactive immune responses and central nervous system inflammation during active experimental autoimmune encephalomyelitis. *J Immunol* 2002; **169**(9): 4712-6.

65. Monk CR, Spachidou M, Rovis F, et al. MRL/Mp CD4+,CD25- T cells show reduced sensitivity to suppression by CD4+,CD25+ regulatory T cells in vitro: a novel defect of T cell regulation in systemic lupus erythematosus. *Arthritis Rheum* 2005; **52**(4): 1180-4.

66. Brusko T, Wasserfall C, McGrail K, et al. No alterations in the frequency of FOXP3+ regulatory T-cells in type 1 diabetes. *Diabetes* 2007; **56**(3): 604-12.

67. Long SA, Cerosaletti K, Bollyky PL, et al. Defects in IL-2R signalling contribute to diminished maintenance of FOXP3 expression in CD4(+)CD25(+) regulatory T-cells of type 1 diabetic subjects. *Diabetes* 2010; **59**(2): 407-15.

68. Willcox A, Richardson SJ, Bone AJ, Foulis AK, Morgan NG. Analysis of islet inflammation in human type 1 diabetes. *Clin Exp Immunol* 2009; **155**(2): 173-81.

69. Tree TI, Roep BO, Peakman M. A mini meta-analysis of studies on CD4+CD25+ T cells in human type 1 diabetes: report of the Immunology of Diabetes Society T Cell Workshop. *Ann N Y Acad Sci* 2006; **1079**: 9-18.

70. Schneider A, Rieck M, Sanda S, Pihoker C, Greenbaum C, Buckner JH. The effector T cells of diabetic subjects are resistant to regulation via CD4+ FOXP3+ regulatory T cells. *J Immunol* 2008; **181**(10): 7350-5.

71. Lawson JM, Tremble J, Dayan C, et al. Increased resistance to CD4+CD25hi regulatory T cell-mediated suppression in patients with type 1 diabetes. *Clin Exp Immunol* 2008; **154**(3): 353-9.

72. McFarland HF, Martin R. Multiple sclerosis: a complicated picture of autoimmunity. *Nat Immunol* 2007; **8**(9): 913-9.

73. Michel L, Berthelot L, Pettre S, et al. Patients with relapsing-remitting multiple sclerosis have normal Treg function when cells expressing IL-7 receptor alpha-chain are excluded from the analysis. *J Clin Invest* 2008; **118**(10): 3411-9.

74. Huan J, Culbertson N, Spencer L, et al. Decreased FOXP3 levels in multiple sclerosis patients. *J Neurosci Res* 2005; **81**(1): 45-52.

75. Venigalla RK, Tretter T, Krienke S, et al. Reduced CD4+,CD25- T cell sensitivity to the suppressive function of CD4+,CD25high,CD127 -/low regulatory T cells in patients with active systemic lupus erythematosus. *Arthritis Rheum* 2008; **58**(7): 2120-30.

76. Gerli R, Nocentini G, Alunno A, et al. Identification of regulatory T cells in systemic lupus erythematosus. *Autoimmun Rev* 2009; **8**(5): 426-30.

77. Suarez A, Lopez P, Gomez J, Gutierrez C. Enrichment of CD4+ CD25high T cell population in patients with systemic lupus erythematosus treated with glucocorticoids. *Ann Rheum Dis* 2006; **65**(11): 1512-7.

78. Zhang B, Zhang X, Tang F, Zhu L, Liu Y. Reduction of forkhead box P3 levels in CD4+CD25high T cells in patients with new-onset systemic lupus erythematosus. *Clin Exp Immunol* 2008; **153**(2): 182-7.

79. Alvarado-Sanchez B, Hernandez-Castro B, Portales-Perez D, et al. Regulatory T cells in patients with systemic lupus erythematosus. *J Autoimmun* 2006; **27**(2): 110-8.

80. Valencia X, Yarboro C, Illei G, Lipsky PE. Deficient CD4+CD25high T regulatory cell function in patients with active systemic lupus erythematosus. *J Immunol* 2007; **178**(4): 2579-88.

81. Vargas-Rojas MI, Crispin JC, Richaud-Patin Y, Alcocer-Varela J. Quantitative and qualitative normal regulatory T cells are not capable of inducing suppression in SLE patients due to T-cell resistance. *Lupus* 2008; **17**(4): 289-94.

82. Morgan ME, Sutmuller RP, Witteveen HJ, et al. CD25+ cell depletion hastens the onset of severe disease in collagen-induced arthritis. *Arthritis Rheum* 2003; **48**(5): 1452-60.

83. Mottonen M, Heikkinen J, Mustonen L, Isomaki P, Luukkainen R, Lassila O. CD4+ CD25+ T cells with the phenotypic and functional characteristics of regulatory T cells are enriched in the synovial fluid of patients with rheumatoid arthritis. *Clin Exp Immunol* 2005; **140**(2): 360-7.

84. Lawson CA, Brown AK, Bejarano V, et al. Early rheumatoid arthritis is associated with a deficit in the CD4+CD25high regulatory T cell population in peripheral blood. *Rheumatology (Oxford)* 2006; **45**(10): 1210-7.

85. Cao D, Malmstrom V, Baecher-Allan C, Hafler D, Klareskog L, Trollmo C. Isolation and functional characterization of regulatory CD25brightCD4+ T cells from the target organ of patients with rheumatoid arthritis. *Eur J Immunol* 2003; **33**(1): 215-23.

86. Ehrenstein MR, Evans JG, Singh A, et al. Compromised function of regulatory T cells in rheumatoid arthritis and reversal by anti-TNFalpha therapy. *J Exp Med* 2004; **200**(3): 277-85.

87. Izcue A, Powrie F. Special regulatory T-cell review: Regulatory T cells and the intestinal tract--patrolling the frontier. *Immunology* 2008; **123**(1): 6-10.

88. Saruta M, Yu QT, Fleshner PR, et al. Characterization of FOXP3+CD4+ regulatory T cells in Crohn's disease. *Clin Immunol* 2007; **125**(3): 281-90.

89. Takahashi M, Nakamura K, Honda K, et al. An inverse correlation of human peripheral blood regulatory T cell frequency with the disease activity of ulcerative colitis. *Dig Dis Sci* 2006; **51**(4): 677-86.

90. Maul J, Loddenkemper C, Mundt P, et al. Peripheral and intestinal regulatory CD4+ CD25(high) T cells in inflammatory bowel disease. *Gastroenterology* 2005; **128**(7): 1868-78.

91. Hvas CL, Kelsen J, Agnholt J, Dige A, Christensen LA, Dahlerup JF. Discrete changes in circulating regulatory T cells during infliximab treatment of Crohn's disease. *Autoimmunity* 2010; **43**(4): 325-33.

92. Ricciardelli I, Lindley KJ, Londei M, Quaratino S. Anti tumour necrosis-alpha therapy increases the number of FOXP3 regulatory T cells in children affected by Crohn's disease. *Immunology* 2008; **125**(2): 178-83.

93. Kelsen J, Agnholt J, Hoffmann HJ, Romer JL, Hvas CL, Dahlerup JF. FoxP3(+)CD4(+)CD25(+) T cells with regulatory properties can be cultured from colonic mucosa of patients with Crohn's disease. *Clin Exp Immunol* 2005; **141**(3): 549-57.

94. Whiteside TL, Schuler P, Schilling B. Induced and natural regulatory T cells in human cancer. *Expert Opin Biol Ther* 2012; **12**(10): 1383-97.

95. Roncarolo MG, Bacchetta R, Bordignon C, Narula S, Levings MK. Type 1 T regulatory cells. *Immunol Rev* 2001; **182**: 68-79.

96. Whiteside TL. Disarming suppressor cells to improve immunotherapy. *Cancer Immunol Immunother* 2012; **61**(2): 283-8.

97. Afzali B, Lechler RI, Hernandez-Fuentes MP. Allorecognition and the alloresponse: clinical implications. *Tissue Antigens* 2007; **69**(6): 545-56.

98. Turka LA, Lechler RI. Towards the identification of biomarkers of transplantation tolerance. *Nature reviews Immunology* 2009; **9**(7): 521-6.

99. Francis RS, Feng G, Tha-In T, Lyons IS, Wood KJ, Bushell A. Induction of transplantation tolerance converts potential effector T cells into graft-protective regulatory T cells. *Eur J Immunol* 2011; **41**(3): 726-38.

100. Wood KJ, Bushell A, Jones ND. Immunologic unresponsiveness to alloantigen in vivo: a role for regulatory T cells. *Immunol Rev* 2011; **241**(1): 119-32.

101. Graca L, Thompson S, Lin CY, Adams E, Cobbold SP, Waldmann H. Both CD4(+)CD25(+) and CD4(+)CD25(-) regulatory cells mediate dominant transplantation tolerance. *J Immunol* 2002; **168**(11): 5558-65.

102. Feng G, Nadig SN, Backdahl L, et al. Functional regulatory T cells produced by inhibiting cyclic nucleotide phosphodiesterase type 3 prevent allograft rejection. *Sci Transl Med* 2011; **3**(83): 83ra40.

103. Feng G, Wood KJ, Bushell A. Interferon-gamma conditioning ex vivo generates CD25+CD62L+Foxp3+ regulatory T cells that prevent allograft rejection: potential avenues for cellular therapy. *Transplantation* 2008; **86**(4): 578-89.

104. Joffre O, Santolaria T, Calise D, et al. Prevention of acute and chronic allograft rejection with CD4+CD25+Foxp3+ regulatory T lymphocytes. *Nat Med* 2008; **14**(1): 88-92.

105. Golshayan D, Jiang S, Tsang J, Garin MI, Mottet C, Lechler RI. In vitro-expanded donor alloantigen-specific CD4+CD25+ regulatory T cells promote experimental transplantation tolerance. *Blood* 2007; **109**(2): 827-35.

106. Tsang JY, Tanriver Y, Jiang S, et al. Indefinite mouse heart allograft survival in recipient treated with CD4(+)CD25(+) regulatory T cells with indirect allospecificity and short term immunosuppression. *Transpl Immunol* 2009; **21**(4): 203-9.

107. Sagoo P, Ali N, Garg G, Nestle FO, Lechler RI, Lombardi G. Human regulatory T cells with alloantigen specificity are more potent inhibitors of alloimmune skin graft damage than polyclonal regulatory T cells. *Sci Transl Med* 2011; **3**(83): 83ra42.

108. Brunstein CG, Miller JS, Cao Q, et al. Infusion of ex vivo expanded T regulatory cells in adults transplanted with umbilical cord blood: safety profile and detection kinetics. *Blood* 2011; **117**(3): 1061-70.

109. Edinger M, Hoffmann P. Regulatory T cells in stem cell transplantation: strategies and first clinical experiences. *Curr Opin Immunol* 2011; **23**(5): 679-84.

110. Di Ianni M, Falzetti F, Carotti A, et al. Tregs prevent GVHD and promote immune reconstitution in HLA-haploidentical transplantation. *Blood* 2011; **117**(14): 3921-8.

111. Salomon B, Lenschow DJ, Rhee L, et al. B7/CD28 costimulation is essential for the homeostasis of the CD4+CD25+ immunoregulatory T cells that control autoimmune diabetes. *Immunity* 2000; **12**(4): 431-40.

112. Tang Q, Henriksen KJ, Boden EK, et al. Cutting edge: CD28 controls peripheral homeostasis of CD4+CD25+ regulatory T cells. *J Immunol* 2003; **171**(7): 3348-52.

113. Tai X, Cowan M, Feigenbaum L, Singer A. CD28 costimulation of developing thymocytes induces Foxp3 expression and regulatory T cell differentiation independently of interleukin 2. *Nat Immunol* 2005; **6**(2): 152-62.

114. Fontenot JD, Rasmussen JP, Gavin MA, Rudensky AY. A function for interleukin 2 in Foxp3-expressing regulatory T cells. *Nat Immunol* 2005; **6**(11): 1142-51.

115. D'Cruz LM, Klein L. Development and function of agonist-induced CD25+Foxp3+ regulatory T cells in the absence of interleukin 2 signalling. *Nat Immunol* 2005; **6**(11): 1152-9.

116. Burchill MA, Yang J, Vogtenhuber C, Blazar BR, Farrar MA. IL-2 receptor beta-dependent STAT5 activation is required for the development of Foxp3+ regulatory T cells. *J Immunol* 2007; **178**(1): 280-90.

117. Malek TR, Yu A, Vincek V, Scibelli P, Kong L. CD4 regulatory T cells prevent lethal autoimmunity in IL-2Rbeta-deficient mice. Implications for the nonredundant function of IL-2. *Immunity* 2002; **17**(2): 167-78.

118. Burchill MA, Yang J, Vang KB, et al. Linked T cell receptor and cytokine signalling govern the development of the regulatory T cell repertoire. *Immunity* 2008; **28**(1): 112-21.

119. Soper DM, Kasprowicz DJ, Ziegler SF. IL-2Rbeta links IL-2R signalling with Foxp3 expression. *Eur J Immunol* 2007; **37**(7): 1817-26.

120. Vang KB, Yang J, Mahmud SA, Burchill MA, Vegoe AL, Farrar MA. IL-2, -7, and -15, but not thymic stromal lymphopoeitin, redundantly govern CD4+Foxp3+ regulatory T cell development. *J Immunol* 2008; **181**(5): 3285-90.

121. Yao Z, Kanno Y, Kerenyi M, et al. Nonredundant roles for Stat5a/b in directly regulating Foxp3. *Blood* 2007; **109**(10): 4368-75.

122. Bayer AL, Yu A, Adeegbe D, Malek TR. Essential role for interleukin-2 for CD4(+)CD25(+) T regulatory cell development during the neonatal period. *J Exp Med* 2005; **201**(5): 769-77.

123. Antov A, Yang L, Vig M, Baltimore D, Van Parijs L. Essential role for STAT5 signalling in CD25+CD4+ regulatory T cell homeostasis and the maintenance of self-tolerance. *J Immunol* 2003; **171**(7): 3435-41.

124. Burchill MA, Goetz CA, Prlic M, et al. Distinct effects of STAT5 activation on CD4+ and CD8+ T cell homeostasis: development of CD4+CD25+ regulatory T cells versus CD8+ memory T cells. *J Immunol* 2003; **171**(11): 5853-64.

125. Liston A, Nutsch KM, Farr AG, et al. Differentiation of regulatory Foxp3+ T cells in the thymic cortex. *Proc Natl Acad Sci U S A* 2008; **105**(33): 11903-8.

126. Lio CW, Hsieh CS. A two-step process for thymic regulatory T cell development. *Immunity* 2008; **28**(1): 100-11.

127. Gaide O, Martinon F, Micheau O, Bonnet D, Thome M, Tschopp J. Carma1, a CARD-containing binding partner of Bcl10, induces Bcl10 phosphorylation and NF-kappaB activation. *FEBS Lett* 2001; **496**(2-3): 121-7.

128. Pomerantz JL, Denny EM, Baltimore D. CARD11 mediates factor-specific activation of NF-kappaB by the T cell receptor complex. *EMBO J* 2002; **21**(19): 5184-94.

129. Beutler B, Du X, Hoebe K. From phenomenon to phenotype and from phenotype to gene: Forward genetics and the problem of sepsis. *J Infect Dis* 2003; **187**: S321-S6.

130. Appleby MW, Ramsdell F. A forward-genetic approach for analysis of the immune system. *Nature Reviews Immunology* 2003; **3**(6): 463-71.

131. Waterston RH, Lindblad-Toh K, Birney E, et al. Initial sequencing and comparative analysis of the mouse genome. *Nature* 2002; **420**(6915): 520-62.

132. Kile BT, Hilton DJ. The art and design of genetic screens: Mouse. *Nat Rev Genet* 2005; **6**(7): 557-67.

133. Choi O, Rutschmann S. Dissecting immunity by germline mutagenesis. *Immunology* 2012; **137**(2): 124-30.

134. Su LK, Kinzler KW, Vogelstein B, et al. Multiple intestinal neoplasia caused by a mutation in the murine homolog of the APC gene. *Science* 1992; **256**(5057): 668-70.

135. King DP, Zhao Y, Sangoram AM, et al. Positional cloning of the mouse circadian clock gene. *Cell* 1997; **89**(4): 641-53.

136. Beutler B, Crozat K, Koziol JA, Georgel P. Genetic dissection of innate immunity to infection: the mouse cytomegalovirus model. *Curr Opin Immunol* 2005; **17**(1): 36-43.

137. Tabeta K, Hoebe K, Janssen EM, et al. The Unc93b1 mutation 3d disrupts exogenous antigen presentation and signalling via Toll-like receptors 3, 7 and 9. *Nat Immunol* 2006; **7**(2): 156-64.

138. Casrouge A, Zhang SY, Eidenschenk C, et al. Herpes simplex virus encephalitis in human UNC-93B deficiency. *Science* 2006; **314**(5797): 308-12.

139. Curotto de Lafaille MA, Lafaille JJ. Natural and adaptive foxp3+ regulatory T cells: more of the same or a division of labor? *Immunity* 2009; **30**(5): 626-35.

140. Molinero LL, Miller ML, Evaristo C, Alegre ML. High TCR stimuli prevent induced regulatory T cell differentiation in a NF-kappaB-dependent manner. *J Immunol* 2011; **186**(8): 4609-17.

141. Turner MS, Kane LP, Morel PA. Dominant role of antigen dose in CD4+Foxp3+ regulatory T cell induction and expansion. *J Immunol* 2009; **183**(8): 4895-903.

142. Su B, Jacinto E, Hibi M, Kallunki T, Karin M, Ben-Neriah Y. JNK is involved in signal integration during costimulation of T lymphocytes. *Cell* 1994; **77**(5): 727-36.

143. Medoff BD, Sandall BP, Landry A, et al. Differential requirement for CARMA1 in agonist-selected T-cell development. *Eur J Immunol* 2009; **39**(1): 78-84.

144. Barnes MJ, Krebs P, Harris N, et al. Commitment to the regulatory T cell lineage requires CARMA1 in the thymus but not in the periphery. *PLoS Biol* 2009; **7**(3): e51.

145. Che T, You Y, Wang D, Tanner MJ, Dixit VM, Lin X. MALT1/paracaspase is a signalling component downstream of CARMA1 and mediates T cell receptor-induced NF-kappaB activation. *J Biol Chem* 2004; **279**(16): 15870-6.

146. Thome M. CARMA1, BCL-10 and MALT1 in lymphocyte development and activation. *Nat Rev Immunol* 2004; **4**(5): 348-59.

147. Cannons JL, Yu LJ, Hill B, et al. SAP regulates T(H)2 differentiation and PKC-theta-mediated activation of NF-kappaB1. *Immunity* 2004; **21**(5): 693-706.

148. Wegener E, Oeckinghaus A, Papadopoulou N, et al. Essential role for IkappaB kinase beta in remodeling Carma1-Bcl10-Malt1 complexes upon T cell activation. *Mol Cell* 2006; **23**(1): 13-23.

149. Dimitratos SD, Woods DF, Stathakis DG, Bryant PJ. Signalling pathways are focused at specialized regions of the plasma membrane by scaffolding proteins of the MAGUK family. *Bioessays* 1999; **21**(11): 912-21.

150. Jiang C, Lin X. Regulation of NF-kappaB by the CARD proteins. *Immunol Rev* 2012; **246**(1): 141-53.

151. Wang L, Guo Y, Huang WJ, et al. Card10 is a novel caspase recruitment domain/membrane-associated guanylate kinase family member that interacts with BCL10 and activates NF-kappa B. *J Biol Chem* 2001; **276**(24): 21405-9.

152. McAllister-Lucas LM, Inohara N, Lucas PC, et al. Bimp1, a MAGUK family member linking protein kinase C activation to Bcl10-mediated NF-kappaB induction. *J Biol Chem* 2001; **276**(33): 30589-97.

153. Blonska M, Lin X. CARMA1-mediated NF-kappaB and JNK activation in lymphocytes. *Immunol Rev* 2009; **228**(1): 199-211.

154. Matsumoto R, Wang D, Blonska M, et al. Phosphorylation of CARMA1 plays a critical role in T Cell receptor-mediated NF-kappaB activation. *Immunity* 2005; **23**(6): 575-85.

155. Schmidt-Supprian M, Tian J, Grant EP, et al. Differential dependence of CD4+CD25+ regulatory and natural killer-like T cells on signals leading to NF-kappaB activation. *Proc Natl Acad Sci U S A* 2004; **101**(13): 4566-71.

156. Lee AJ, Wu X, Cheng H, Zhou X, Cheng X, Sun SC. CARMA1 regulation of regulatory T cell development involves modulation of interleukin-2 receptor signalling. *J Biol Chem* 2010; **285**(21): 15696-703.

157. Hara H, Saito T. CARD9 versus CARMA1 in innate and adaptive immunity. *Trends Immunol* 2009; **30**(5): 234-42.

158. Li S, Yang X, Shao J, Shen Y. Structural insights into the assembly of CARMA1 and BCL10. *PLoS One* 2012; **7**(8): e42775.

159. Sommer K, Guo B, Pomerantz JL, et al. Phosphorylation of the CARMA1 linker controls NF-kappaB activation. *Immunity* 2005; **23**(6): 561-74.

160. Tanner MJ, Hanel W, Gaffen SL, Lin X. CARMA1 coiled-coil domain is involved in the oligomerization and subcellular localization of CARMA1 and is required for T cell receptor-induced NF-kappaB activation. *J Biol Chem* 2007; **282**(23): 17141-7.

161. Gaide O, Favier B, Legler DF, et al. CARMA1 is a critical lipid raft-associated regulator of TCR-induced NF-kappa B activation. *Nat Immunol* 2002; **3**(9): 836-43.

162. Wang S, Li Y, Hu YH, et al. STUB1 is essential for T-cell activation by ubiquitinating CARMA1. *Eur J Immunol* 2013; **43**(4): 1034-41.

163. Zheng Y, Josefowicz S, Chaudhry A, Peng XP, Forbush K, Rudensky AY. Role of conserved non-coding DNA elements in the Foxp3 gene in regulatory T-cell fate. *Nature* 2010; **463**(7282): 808-12.

164. Ruan Q, Kameswaran V, Tone Y, et al. Development of Foxp3(+) regulatory t cells is driven by the c-Rel enhanceosome. *Immunity* 2009; **31**(6): 932-40.

165. Blonska M, Pappu BP, Matsumoto R, et al. The CARMA1-Bcl10 signalling complex selectively regulates JNK2 kinase in the T cell receptor-signalling pathway. *Immunity* 2007; **26**(1): 55-66.

166. Moreno-Garcia ME, Sommer K, Rincon-Arano H, et al. Kinase-independent feedback of the TAK1/TAB1 complex on BCL10 turnover and NF-kappaB activation. *Mol Cell Biol* 2013; **33**(6): 1149-63.

167. Chen L, Wu J, Ren W, Yang X, Shen Z. c-Jun N-terminal kinase (JNK)-phospho-c-JUN (ser63/73) pathway is essential for FOXP3 nuclear translocation in psoriasis. *Journal of dermatological science* 2013; **69**(2): 114-21.

168. Liu Y, Wang Y, Li W, Zheng P, Liu Y. Activating transcription factor 2 and c-Jun-mediated induction of FoxP3 for experimental therapy of mammary tumor in the mouse. *Cancer Res* 2009; **69**(14): 5954-60.

169. Bertin J, Wang L, Guo Y, et al. CARD11 and CARD14 are novel caspase recruitment domain (CARD)/membrane-associated guanylate kinase (MAGUK) family members that interact with BCL10 and activate NF-kappa B. *J Biol Chem* 2001; **276**(15): 11877-82.

170. Newton K, Dixit VM. Mice lacking the CARD of CARMA1 exhibit defective B lymphocyte development and impaired proliferation of their B and T lymphocytes. *Curr Biol* 2003; **13**(14): 1247-51.

171. Egawa T, Albrecht B, Favier B, et al. Requirement for CARMA1 in antigen receptor-induced NF-kappa B activation and lymphocyte proliferation. *Curr Biol* 2003; **13**(14): 1252-8.

172. Hara H, Wada T, Bakal C, et al. The MAGUK family protein CARD11 is essential for lymphocyte activation. *Immunity* 2003; **18**(6): 763-75.

173. Jun JE, Wilson LE, Vinuesa CG, et al. Identifying the MAGUK protein Carma-1 as a central regulator of humoral immune responses and atopy by genome-wide mouse mutagenesis. *Immunity* 2003; **18**(6): 751-62.

174. Lal A, Haynes SR, Gorospe M. Clean Western blot signals from immunoprecipitated samples. *Molecular and cellular probes* 2005; **19**(6): 385-8.

175. Liu Y, Song R, Gao Y, et al. Protein kinase C-delta negatively regulates T cell receptor-induced NF-kappaB activation by inhibiting the assembly of CARMA1 signalosome. *J Biol Chem* 2012; **287**(24): 20081-7.

176. Park JH, Park HH. Crystallization and preliminary X-ray crystallographic studies of the CARD domain of human CARMA1. *Acta crystallographica Section F, Structural biology and crystallization communications* 2013; **69**(Pt 4): 435-7.

177. Concepcion D, Seburn KL, Wen G, Frankel WN, Hamilton BA. Mutation rate and predicted phenotypic target sizes in ethylnitrosourea-treated mice. *Genetics* 2004; **168**(2): 953-9.